Statistical Analysis of Trends in Red River Water Quality Over a 45-Year Period

by

Carrie Beth Paquette

A Practicum submitted to
the Faculty of Graduate Studies
In Partial Fulfillment of the Requirements for the Degree of

MASTER OF SCIENCE

Department of Statistics
University of Manitoba
Winnipeg, Manitoba

Statistical Analysis of Trends in Red River Water Quality Over a 45-Year Period

By

Carrie Beth Paquette

A Thesis/Practicum submitted to the Faculty of Graduate Studies of The University of Manitoba in partial fulfillment of the requirement of the degree

Of

Master of Science

Abstract

Trend analysis of water quality indicators is important in assessing the impact of changes in the landscape and land usage as well as the impact of precipitation within watersheds. I perform a statistical evaluation of trends in dissolved ion concentrations namely: calcium, sodium, potassium, magnesium, chloride as well as trends in total dissolved solids and specific conductance for the Red River within Manitoba over a 45-year period ranging from 1960 until 2007. The analysis is done using two different methods, a nonparametric method namely the Mann-Kendall test for trend, and a parametric flow-weighted method (developed by Aldo Vecchia, USGS). Both methods were used to analyze the water quality constituents and yielded fairly similar conclusions. While the parametric method adjusts for streamflow, there are still significant increasing trends in both methods, it can be concluded that some part of the increasing trends may be due to factors other than flow.

Acknowledgments

There have been many contributions by various individuals that led to the completion of this practicum. I would like to acknowledge with deep gratitude my advisor, Dr. Brad Johnson, who skillfully guided me through this practicum. Thank you to my committee members, Dr. John Brewster and Dr. Gordon Goldsborough, for having taken the time and interest to participate in this practicum and Dr. Liquin Wang for serving as a member of the contract advisory committee. Also, a special thank you to the International Watersheds Initiative program of the International Joint Commission for financial support, and the International Red River Board for their support.

A very special and sincere thank you to Dr. David Donald and Dr. Brian Parker of Environment Canada for all of their assistance and to Nicole Armstrong of the Manitoba Water Stewardship for all her help with the provincial data. I would also like to acknowledge Aldo Vecchia of the United States Geological Survey for all his invaluable support and assistance.

To my amazing family and friends that have supported this endeavour and have lived through it right along side me, I appreciate every one of you. To my amazing children Jakob and Sadie Paquette watching you two grow everyday inspires me beyond words and it is because of that, mom knew she could do it!

Dedication

This practicum is dedicated to my Zaida Jakob Giter, for all the memories he has left me, and his spirit that continually guides me through life.

Contents

List of Tables

List of Figures

Chapter 1

Introduction

The Red River of the North is formed by the confluence of the Bois de Sioux and Otter Tail Rivers in the United States. It flows northward through the Red River Valley and forms the border between the states of Minnesota and North Dakota before continuing into Manitoba, Canada, and finally discharging into Lake Winnipeg (Figure 1.1). Along its path, the Red River flows through Greater Grand Forks and Fargo, in the United States, and through Winnipeg in Canada. The Canadian portion of the Red River is about 249 km long, while the US portion is approximately 636 kilometers in length. The river falls 70 meters on its trip to Lake Winnipeg where it spreads into the vast deltaic wetland known as Netley -Libau Marsh. The entire Red River Basin encompasses 287,500 square kilometers of rich agricultural lands, forests, wetlands, and prairies and contains numerous lakes.

Statistical evaluation of trends in water quality data over the 45-year period of record, from 1960 through until 2007, is useful for assessing effects of the variation in precipitation in the Red River and the impact that landscape runoff has on water quality. Changes in the Red River water quality have a direct bearing on Lake Winnipeg into which it discharges; the eutrophication of Lake Winnipeg is a research priority for Environment Canada and the Manitoba Water Stewardship.

This practicum focuses on three water quality monitoring stations along the Red River and presents results of trend analysis using non-parametric methods

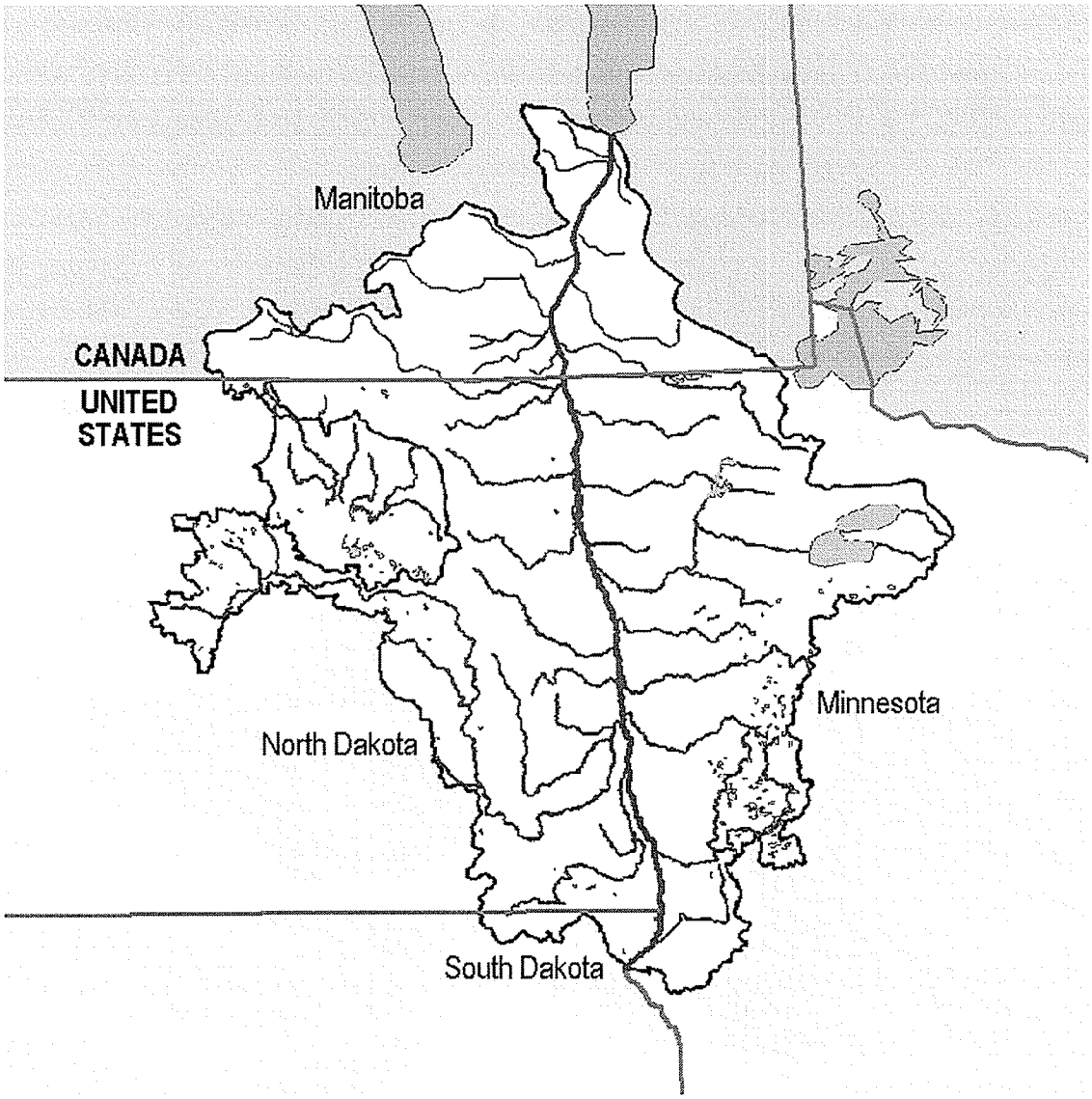

Figure 1.1: The Red River Basin

such as those used by Nancy Glozier (Environment Canada)(Glozier et. al. 2004) and parametric methods developed by Aldo Vecchia (United States Geological Survey)(Vecchia 2000, 2003, 2005). Comparisons between methods are made and recommendations are presented. The results presented are based on streamflow data from January 1960 through to December 2007 and on concentration data from January 1960 to December 2007. The constituents for the report include six dissolved major ions (calcium, sodium, potassium, magnesium, sulphate, and chloride), total dissolved solids and specific conductance. The constituents were evaluated for three monitoring stations along the Red River: the Red River at Emerson station; the south gate of the floodway near St. Norbert; and the Selkirk water quality monitoring station. Constituents were evaluated on the basis of availability. The streamflow data were obtained from the Water Survey of Canada-Archived Hydrometric Data website (http://www.wsc.ec.gc.ca/hydat/H2O), federal concentration data were obtained through Environment Canada and provincial concentration data were obtained from Manitoba Water Stewardship, Province of Manitoba. Nitrogen and phosphorus are the basis for eutrophication of Lake Winnipeg; an assumption can be made that if ion concentrations show temporal trends reflecting climatic cycles and/or landscape change, so too will nitrogen and phosphorus.

1.1 Description of the Red River

From about 12,500 years ago to 7,500 years ago, pro-glacial Lake Agassiz covered much of what is known today as western Minnesota, eastern North Dakota, southern Manitoba, and southwestern Ontario. As a result of deglaciation Lake Agassiz virtually disappeared, leaving few remnants, one of which is Lake Winnipeg. Lake Agassiz left behind a fertile, flat plain that ultimately drains to the Hudson Bay. The Red River meanders north along this plain to Lake Winnipeg. A difference in elevation occurs along route, at its starting point the elevation is 287 meters above mean sea level while the elevation at Lake Winnipeg is 218 meters above mean sea level. The Red River, being located in a flat plain, also has a shallow river channel

meandering northward 636 km to the Canadian border. Due to the northerly flow of the river, the flatness of the basin, the shallow river channel and the timing of the spring thaw and snowmelt, severe flooding can occur. Four major floods have occurred since Europeans settled in the area, in 1826, 1950, 1997, and 2009 but it is believed there have been many other floods of equal or larger size prior to European settlement. The climate of the Red River of the North basin is continental and ranges from dry sub-humid in the western part of the basin to sub-humid in the eastern part (Stoner, et al., 1993). Mean annual precipitation for the Red River basin ranges from about 43 centimeters in the extreme western part of the basin to about 66 cm in the extreme eastern part of the basin. Precipitation across the basin generally increases from southwest to northeast (Stoner, et al., 1993). Actual evapotranspiration from the basin also generally increases from southwest to northeast but at a lesser rate than precipitation. Thus, mean annual runoff from the basin also increases in that direction. The Red River of the North receives 75 percent of its annual flow from eastern tributaries. Concentrations of dissolved chemical constituents in surface waters are normally low during spring runoff and after thunderstorms. The Red River of the North generally has a dissolved solids concentration less than 600 milligrams per litre with mean values near 406 milligrams per litre at the Canadian border near Emerson, Manitoba. Calcium and magnesium are the principal cations and bicarbonate is the principal anion along most of the reach of the Red River of the North. Cations are atoms that have lost an electron to become positively charged while anions are atoms or groups of atoms that have gained electrons resulting in a negative charge. Ion concentrations are important to water quality to protect aquatic life and human health. Dissolved solids concentrations generally are lower in the eastern tributaries than in the tributaries draining the western part of the basin. As the river flows further downstream, dissolved solids concentration increases, and magnesium and sulphate are predominant ions. Nitrogen and phosphorous in surface runoff from cropland fertilizers, manure and domestic sewage can contribute nutrients to lakes, reservoirs, and streams.

Chapter 2

Streamflow Data and Concentration Data Used for Water-Quality Trend Analysis

The three water quality monitoring stations selected for this analysis are depicted in Figure 2.1. Selected station characteristics are given in Table 2.1. Contributing drainage areas for the stations range from 287,000 square kilometers at the Selkirk monitoring station, to 102,000 square kilometers at the Emerson monitoring station. For the Red River at Emerson, Manitoba, monitoring station, the data that were used for analysis was collected by the Government of Canada. At the remaining two stations, South entrance of the floodway near St. Norbert and Selkirk, data were collected by the provincial government. Not only are sample and collection methods different between provincial and federal governments, but the sample analysis methods differ too. The constituents used for analysis are given in Table 2.2 and analysis of constituents are based on availability and sample size which are outlined in Table 2.3.

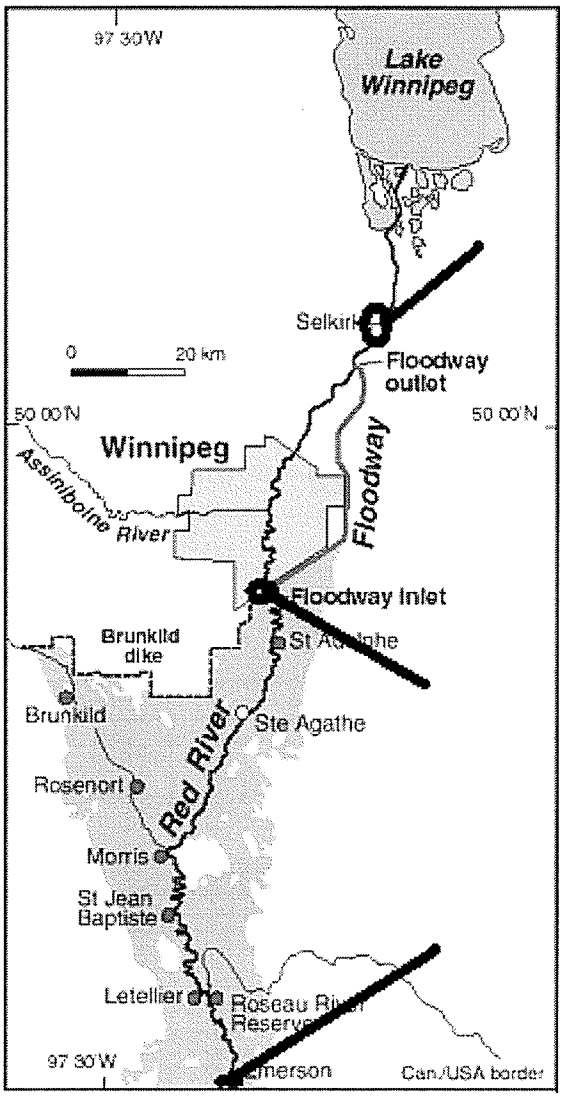

Figure 2.1: Map of the Red River and the central portion of the Red River Valley, Manitoba, depicting the monitoring station locations: (heading upstream) Emerson Station, South Floodway at St. Norbert Stations and Selkirk Station

Table 2.1: Selected characteristics of water quality monitoring stations for trend analysis.

Station #	Name (Station ID)	Drainage Area (sq. km)	Latitude	Longitude
1.	Red River of the North at Emerson, Manitoba (05OC001)	102,000	49° 0′ 18″ N	97° 12′ 54″ W
2.	Red River of the North Floodway near St. Norbert (05OC017)	119,450	49° 45′ 24″ N	97° 7′ 36″ W
3.	Red River of the North at Selkirk (05OJ005)	287,000	50° 8′ 30″ N	96° 52′ 5″ W

Source: www.wsc.ec.gc.ca/hydat/H2O

Table 2.2: Major ions & dissolved solids used for water quality trend analysis.

Constituent	Chemical Symbol	Units
Calcium, dissolved	Ca^{2+}	Milligrams per litre (mg/l)
Sodium, dissolved	Na^{+}	Milligrams per litre (mg/l)
Potassium, dissolved	K^{+}	Milligrams per litre (mg/l)
Magnesium, dissolved	Mg^{2+}	Milligrams per litre (mg/l)
Sulphate, dissolved	SO_4^{2-}	Milligrams per litre (mg/l)
Chloride, dissolved	Cl^{-}	Milligrams per litre (mg/l)
Total dissolved solids	n/a	Milligrams per litre (mg/l)
Specific Conductance	n/a	Microsiemens/centimeter (μS/cm)

2.1 Methodologies

Characteristics that complicate the statistical analysis of water quality time series are non-normal distributions, seasonality, flow effects, missing values, values falling below detection levels, and serial correlation (Hirsch, et al., 1982). Three techniques have been used in order to deal with the above complications. The first technique is a non-parametric test for trend known as the Seasonal Mann-Kendall test, the second procedure introduces an estimator of trend magnitude known as the Sen slope estimator and the third procedure tests for changes over time with constituent concentrations being corrected for flow. This avoids the problem of identifying the trends in water quality that are due to droughts or floods for example, however, neither of these are considered an exact test in the presence of serial correlation. Much research has been conducted in order to study the trends in water quality. Most of these studies employed various parametric and non-parametric analytical techniques. The Strymon River in Greece was the subject of such a study (Antonopoulus et al., 2001); the objective of this study was to provide a system-wide synopsis of water quality, monitor long-range trends in selected parameters, detect actual or potential water quality problems and to enforce standards. Previous studies proved that water quality data do not usually follow convenient probability distributions and that streamflow data exhibit hydrological persistence and seasonal variation. There are suggestions that, for water quality variables that are highly dependent on streamflow, the confounding effects of discharge variations be removed by analyzing the residuals from the discharge-concentration relationship for trend rather than the raw data. In a technical report about the Red River a lattice model was constructed (Fritz and Zhang, 2006) and correlation was analyzed to determine the strength of interactions between the nearest neighbour nodes. A scaling hypothesis that acts as a modifier to the Mann-Kendall test was introduced by Hamed (2008). The basic hypothesis of scaling is that the data exhibit invariance at any scale greater than annual, so if the results of the Mann-Kendall test show an observed trend is significant, we proceed to check the effect of scaling. Nonparametric methods (Glozier et al., 2004), consist of testing for seasonality. If it yields a significant result, the Sea-

sonal Mann-Kendall test is applied, otherwise the Mann-Kendall test is conducted. Parametric methods can model both flow and concentration data jointly (Vecchia, 2000) and are good not only for exploratory analysis but explanatory analyses as well.

2.2 Analysis Techniques

The Government of Canada and the Province of Manitoba used different sampling protocols. For samples collected at the Emerson stations a 2 litre low density polyethylene bottle is mounted onto a stainless steel sampling iron. This method is used to prevent contamination of the water samples with metals. The bottle is then lowered into the river, partially filled and rinsed two times in order to remove possible contaminants from inside the bottle. On the third drop the sampling iron and bottle are lowered to the bottom of the river and retrieved. This collects an integrated sample of water from the water column. The reason this is done is because water chemistry can vary widely within different levels of the river. Upon retrieval a subsample is removed and sent to the National Laboratory for Environmental Testing (NLET) in Burlington, Ontario for cation and anion analysis. A portion of this sample is then filtered to remove such particulates as algae, bacteria and sediments. Analysis is conducted on the dissolved constituents because extractable ions are difficult to analyze. Filtering methods differ between the provincial and the federal governments. The Government of Canada filters shortly after collection, while the province filters on return to the lab. This can be approximately 8-10 hours or more after the sample is collected. Filtering of the water sample is important because it removes all of the bacteria and algae from the samples. If the samples are not filtered, then cells can grow, take nutrients out of the water and excrete waste products. This may affect analytical results especially for dissolved nutrients. In order to minimize the growth of cells samples are kept just above freezing.

The provincial water samples collected at the St. Norbert and Selkirk stations are collected using either a 2.0 litre Nalgene bottle with 30 m of rope or a 1.0 litre

opaque laboratory bottle on the end of a 3 m reaching pole. Both the Nalgene and laboratory bottles are rinsed three times prior to filling, and are used to transfer water to the sample bottles. Sample bottles are filled and then submitted to Cantest Laboratories for analysis of nutrients, metals, conductivity, total dissolved solids, pesticides, dissolved oxygen, major ions and pH. Prior to April 2001, all water samples were submitted to EnviroTest Laboratories for analysis of these parameters (Hughes C., 2009). All data analyses were done as per standard methods for the examination of water (Eaton et al., 2005). Currently the provincial water quality section does not assess dissolved calcium, dissolved sodium, dissolved potassium or dissolved magnesium.

Table 2.3: Sample size of stations and constituents used for water quality trend analysis

Station #	1960–2007	1960–1965	1966–1970	1971–1975	1976–1980	1981–1985	1986–1990	1991–1995	1996–2000	2001–2007
Calcium, dissolved (mg/l)										
1.	912	232	146	68	70	51	70	61	72	142
2.	4	0	0	0	0	0	0	0	4	0
3.	9	0	0	0	0	0	0	0	9	0
Sodium, dissolved (mg/l)										
1.	900	232	143	68	71	41	70	61	72	142
2.	4	0	0	0	0	0	0	0	4	0
3.	9	0	0	0	0	0	0	0	9	0
Potassium, dissolved (mg/l)										
1.	900	224	141	68	71	51	70	61	72	142
2.	4	0	0	0	0	0	0	0	4	0
3.	9	0	0	0	0	0	0	0	9	0
Magnesium, dissolved (mg/l)										
1.	727	222	27	12	71	50	70	61	72	142
2.	4	0	0	0	0	0	0	0	4	0
3.	9	0	0	0	0	0	0	0	9	0
Sulphate, dissolved (mg/l)										
1.	899	224	135	67	71	58	70	60	72	142
2.	42	0	0	0	0	0	0	0	15	27
3.	140	0	0	0	0	0	0	0	55	85
Chloride, dissolved (mg/l)										
1.	919	239	146	67	66	57	70	60	72	142
2.	42	0	0	0	0	0	0	1	14	27
3.	140	0	0	0	0	0	0	7	48	85
Total dissolved solids (mg/l)										
1.	376	0	0	0	12	33	71	62	64	134
2.	74	0	0	0	0	2	60	12	0	0
3.	159	0	6	54	24	2	60	13	0	0
Specific Conductance (μS/cm)										
1.	959	234	146	68	70	54	71	92	80	144
2.	247	0	0	0	33	36	56	62	57	3
3.	270	0	0	0	33	36	56	63	79	3

Chapter 3

Non-Parametric Methods used for Water Quality Trend Analysis

A modified form of Kendall's τ (Kendall, 1938, 1975) is used as a test for trend (Hirsch, et al., 1982). This modification is called the seasonal Mann-Kendall test for trend. It is robust in comparison to the parametric alternatives, since non-parametric methods do not rely on known probability distributions. It may also be less powerful when the assumptions of the parametric methods are met. An estimate of trend magnitude that is closely related to the seasonal Kendall test procedure is known as the seasonal Kendall slope estimator or Sen's slope estimator (Sen, 1968). In cases where concentrations of 'less than detection limit' were reported by the laboratories, values equal to half the detection limit are used for statistical calculation and graphical representation (Gilbert, 1987). Key questions in water quality monitoring are: Does the water chemistry change over time?; Can the observed changes be attributed to natural patterns?; And, could the observed changes in water chemistry impact the biological integrity of the aquatic ecosystem? Seasonal patterns, which occur yearly regardless of longer term trends, are normally examined as an aid to understanding the natural patterns of chemical concentrations. Seasons are defined by reviewing monthly frequency graphs for chemical patterns (Figure 3.1). The time periods of the seasons may be unequal in length

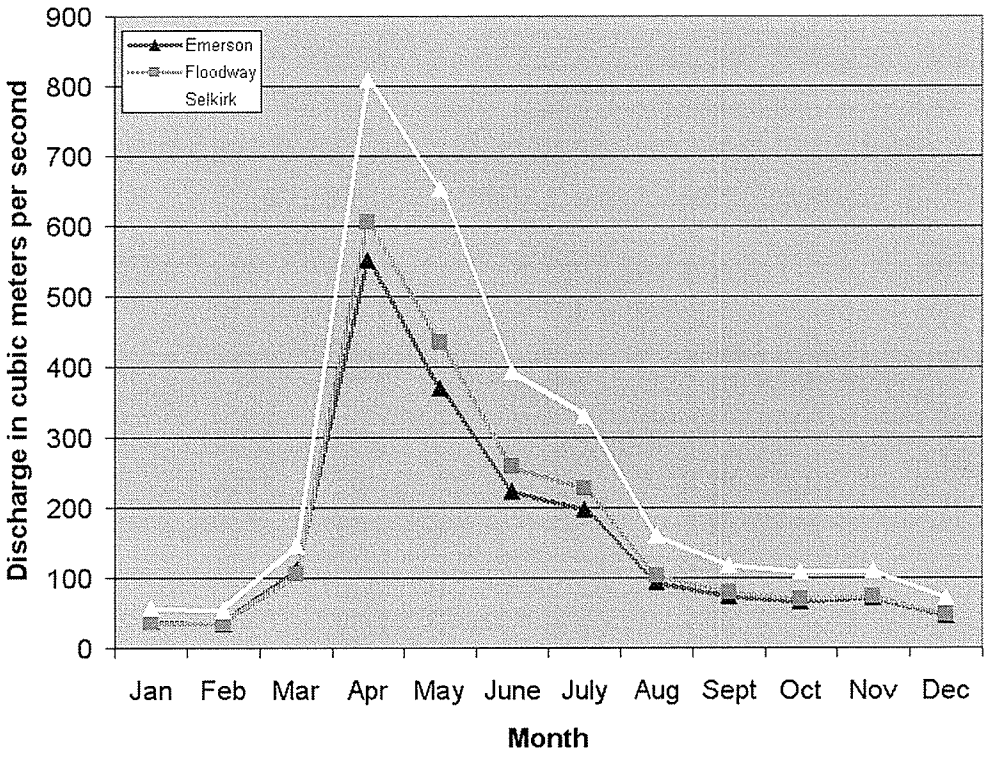

Figure 3.1: Mean monthly streamflow (1960-2007) at each monitoring station in order to define hydrologic seasons

but they represent distinct hydrological periods. Hydrologic seasons define similar periods in some characteristics, but do not correspond to equally length seasons, like "summer" or "winter" do for climate, but rather directional tendencies (Glozier, et al., 2004). The yearly streamflow patterns were similar within the three stations with all sites exhibiting peak discharge between March and June. Based on these patterns, Table 3.1 represents the seasons defined for the analysis of seasonality. Clearly these time periods are dissimilar in length but represent periods which are distinct hydrologically.

In order to get a graphical representation of the data for each constituent we can examine boxplots of the concentrations. Concentrations of dissolved calcium (Figure 3.2) are quite similar between the three stations however data were sparse

Table 3.1: Defined Seasons.

Season	Months	Description
Spring	February - March	rising limb of hydrograph
Summer	April - May	peak streamflow
Fall	June - August	falling limb of hydrograph
Winter	September - January	low flow, ice-cover period

at the south floodway near St. Norbert and the Selkirk monitoring stations. At the Emerson monitoring station the boxplot is symmetric and takes the appearance of an approximately normal distribution. Concentrations of dissolved sodium (see appendix Figure A.2) appear to be extremely skewed to the right with a few outlying observations with a maximum value at 305.0 mg/l and high values of dissolved sodium occurring from November 1988 through January 1989. The median values of the concentrations of dissolved potassium and magnesium (see appendix Figures A.3 and A.4) are similar between stations and follow an approximately normal distribution at the Emerson station. There was more data for the analysis of the concentrations of dissolved sulphate at the south floodway near St. Norbert and Selkirk monitoring stations (see appendix Figure A.5) than the previous constituents. For both stations the distributions seem approximately normal. The Emerson station exhibits the greatest degree of variability amongst the three stations, possessing values from 4.0 mg/l to 1050.0 mg./l of dissolved sulphate and has a strong skew to the right. Dissolved chloride is right skewed for all three stations possessing a high degree of variability at the Emerson station. Total dissolved solids and specific conductance also exhibit an approximately normal distribution at all three stations.

Concentrations of dissolved calcium have median concentrations between 56.3 mg/l and 73.0 mg/l and range from 4.60 mg/l to 130.0 mg/l with few evident outliers. The median and mean concentration of dissolved sodium are similar amongst the stations, however the Emerson station exhibit values ranging from 1.70 mg/l to 305.0 mg/l, this can be indicative of seasonal change and change in flow rate. The

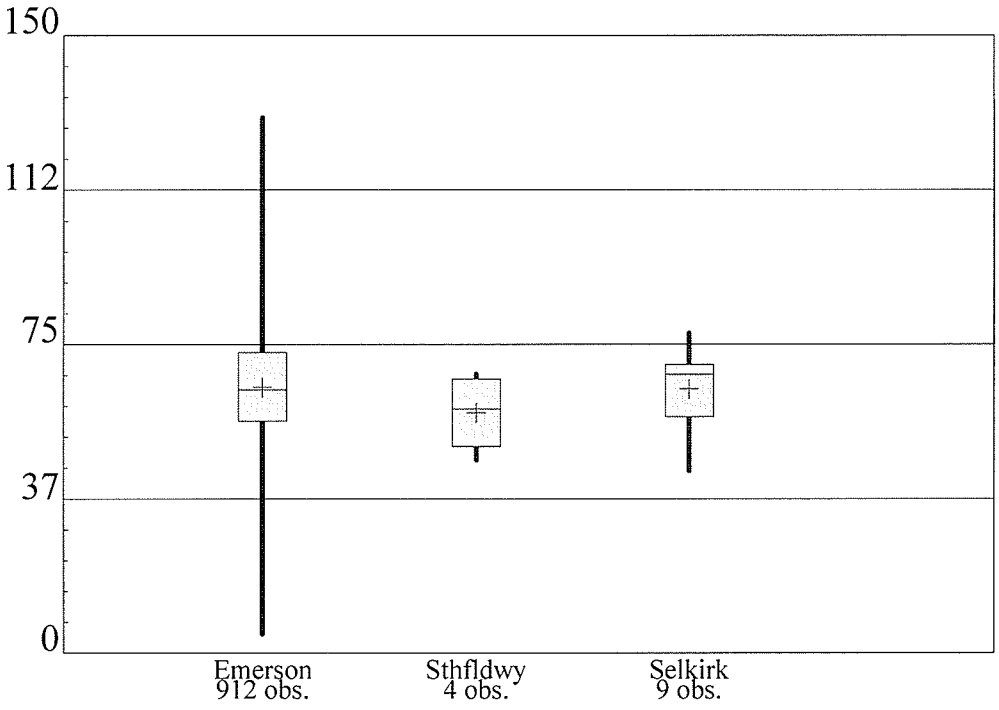

Figure 3.2: Boxplot of dissolved calcium (mg/l) depicting the five number summary of the constituent

Table 3.2: Five Number Summaries for Selected Constituents

Station #	Min.	First Quartile	Median	Third Quartile	Max.	Mean	Std. Dev.
			Calcium, dissolved (mg/l)				
1.	4.60	56.30	63.90	72.98	130.00	64.48	13.53
2.	46.90	48.53	59.25	67.13	67.80	58.30	9.84
3.	44.30	57.35	67.70	70.00	77.70	64.09	9.85
			Sodium, dissolved (mg/l)				
1.	1.70	25.00	34.00	47.00	305.00	42.43	32.64
2.	20.40	23.78	34.10	34.75	34.90	30.88	7.00
3.	20.10	21.75	45.40	53.25	57.20	39.72	15.04
			Potassium, dissolved (mg/l)				
1.	0.38	5.48	6.40	7.54	18.40	6.59	1.82
2.	4.70	4.85	5.55	6.48	6.70	5.63	0.85
3.	6.80	7.15	7.60	8.75	8.90	7.90	0.84
			Magnesium, dissolved (mg/l)				
1.	3.30	27.00	31.25	36.68	61.00	31.90	8.56
2.	19.40	21.08	27.50	32.65	33.90	27.08	6.05
3.	18.60	27.95	31.50	35.85	40.40	31.30	6.44
			Sulphate, dissolved (mg/l)				
1.	4.00	69.60	92.20	119.00	1050.00	99.04	55.78
2.	40.00	76.13	94.50	118.50	220.00	98.86	37.67
3.	32.00	100.00	128.50	160.00	240.00	127.81	44.71
			Chloride, dissolved (mg/l)				
1.	0.10	21.70	31.00	50.00	473.00	46.33	51.09
2.	8.40	16.75	25.10	36.30	160.00	32.99	28.98
3.	6.10	20.00	32.20	42.40	120.00	35.39	22.08
			Total Dissolved Solids (mg/l)				
1.	0.00	375.00	447.50	527.40	1289.00	459.46	140.10
2.	210.00	425.00	550.00	670.00	1140.00	564.66	200.74
3.	240.00	450.00	510.00	600.00	1500.00	535.44	152.03
			Specific Conductance (μS/cm)				
1.	278.00	585.00	676.00	806.00	2253.00	716.79	230.49
2.	7.70	592.00	700.00	821.00	1875.00	741.06	261.86
3.	157.00	621.80	756.50	867.00	1497.00	757.30	223.68

medians and means for the concentrations of dissolved sulphate are much higher at the Selkirk monitoring station compared with the Emerson and south floodway near St. Norbert stations. Total dissolved solids, which are calculated by summing the concentrations of major anions and cations, have similar means; however, the south floodway at St. Norbert station exhibits a high degree of variability. A comparison of specific conductance shows virtually identical spatial patterns. Specific conductance increases slightly from the Emerson to Selkirk water monitoring stations and has a very high degree of variability. Specific conductance measures the amount of dissolved ions in the water, when there is an increase of base flow relative to run off, the specific conductance increases. Specific conductivity is lowest in the spring season when the snow melts and measurements were taken on the samples done in the field samples as opposed to laboratory samples. The summary statistics for constituents are shown in Table 3.2.

When testing for seasonality, the existence of seasonal patterns in water chemistry were analyzed using the non-parametric Kruskal-Wallis test (cf. Conover, 1999). The null hypothesis for this test was that the populations for each season have the same median; versus the alternative hypothesis that not all medians are the same. In order to test for trends in water quality parameters, the Mann-Kendall test for trend and Sen's slope (Hirsch, et al.,1982) was implemented to help evaluate the correlation of selected constituent concentrations with time. This test does not depend on the assumption of a particular parametric form for the underlying distribution and hence is a "non-parametric" method. WQSTAT PLUS v.1.56, (NIC Environmental Division developed with assistance from Colorado State University faculty)©1998-2007 by Sanitas Technologies, is the program used for the non-parametric methods and there are certain data requirements for this program:

1. The application of the Kruskal-Wallis test for seasonality requires a minimum sample size of four data points in each "hydrologic season"

2. For the trend analysis statistics, (Sen's Slope and the Mann-Kendall Test)if there are fewer than 41 data points an *exact test procedure* is performed

3. If 41 or more data points are available, the normal approximation test is used by this program (equivalently a χ^2 test)

4. If the Seasonal Mann-Kendall test is required, that test requires a minimum sample size of four data points in each "hydrologic season"

The Kruskal-Wallis test statistic, H is;

$$H = \left[\frac{12}{N(N+1)} \sum_{i=1}^{n} \frac{R_i^2}{N_i} \right] - 3(N+1),$$

where the k seasons are first ordered and assigned ranks (R_i) and

R_i is the sum of the ranks of the ith station;

N_i is the number of observations in the ith station;

N is the total number of observations; and

k is the number of seasons;

This test statistic has an approximate χ^2 distribution on $k-1$ degrees of freedom.

Using the seasons defined in Table 3.1, the following table indicates the constituents exhibiting seasonality at the 5% level of significance. A significant result indicates at least one season has a significantly different median concentration than one or more other seasons. The p-value is approximately the probability of a χ^2 random variable with $k-1$ degrees of freedom exceeding the observed value of H. At certain stations, there was insufficient data for some constituents and that is denoted by "n/a".

Seasonality is evident in all water quality parameters tested (shown in Table 3.3) and most parameters demonstrate similar seasonal patterns across all sites. Two basic seasonality patterns emerged; dissolved calcium, sodium, magnesium, total dissolved solids and specific conductance exhibit peak concentrations in the winter months. This follows an inverse pattern to the hydrograph, so that maximum

Table 3.3: Kruskal-Wallis test for seasonality results.

Station	Seasonality	p-value	Seasonality	p-value
	Calcium, Dissolved (mg/l)		Sulphate, Dissolved (mg/l)	
1.	yes	$< \underline{\underline{0.005}}$	yes	$< \underline{\underline{0.005}}$
2.	n/a		n/a	
3.	n/a		yes	$< \underline{\underline{0.005}}$
	Sodium, Dissolved (mg/l)		Chloride, Dissolved (mg/l)	
1.	yes	$< \underline{\underline{0.005}}$	yes	$< \underline{\underline{0.005}}$
2.	n/a		n/a	
3.	n/a		yes	$< \underline{\underline{0.005}}$
	Potassium, Dissolved (mg/l)		Total Dissolved Solids (mg/l)	
1.	yes	$< \underline{\underline{0.005}}$	yes	$< \underline{\underline{0.005}}$
2.	n/a		yes	$< \underline{\underline{0.005}}$
3.	n/a		yes	$< \underline{\underline{0.005}}$
	Magnesium, Dissolved (mg/l)		Specific Conductance (μS/cm)	
1.	yes	$< \underline{\underline{0.005}}$	yes	$< \underline{\underline{0.005}}$
2.	n/a		yes	$< \underline{\underline{0.005}}$
3.	n/a		yes	$< \underline{\underline{0.005}}$

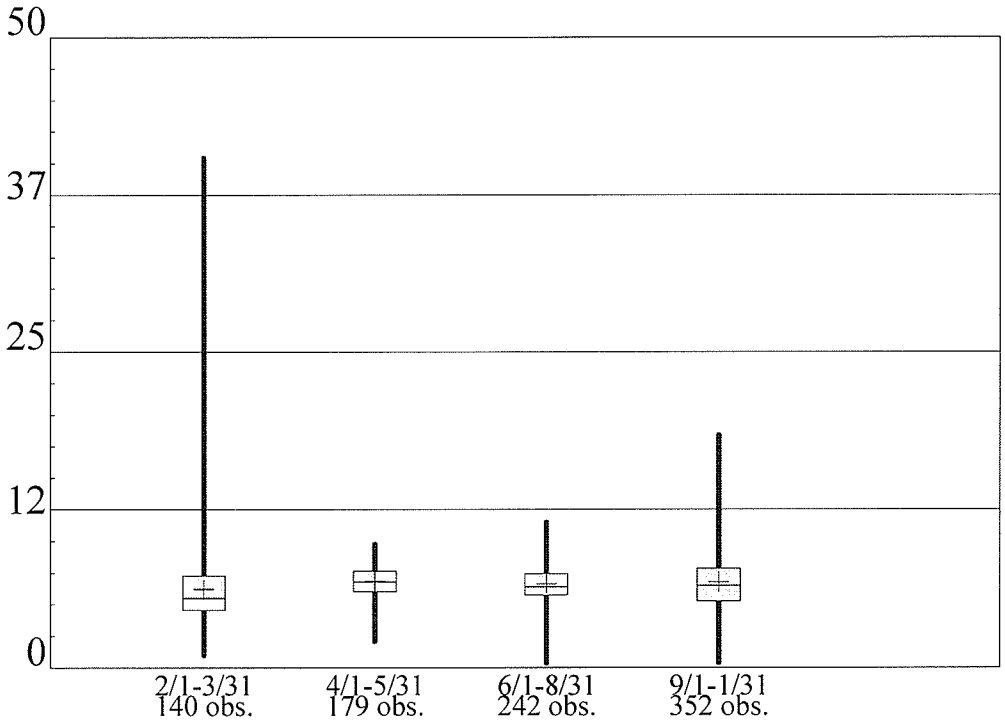

Figure 3.3: Boxplots of Dissolved Potassium (mg/l) depicting the seasonal pattern of the constituent amongst all three monitoring stations

concentrations occur during the low flow winter months. Major ions derived from geological weathering and ground water become more concentrated as flows decrease in winter and ground water comprises a higher proportion of flow (Glozier, et al., 2004). Parameters exhibiting this winter pattern tend to be correlated positively with each other and inversely with discharge. The second typical seasonal pattern observed had maximum concentrations occurring in conjunction with high summer/fall discharge levels. The parameter demonstrating this pattern is dissolved sulphate. Significant seasonality was detected for dissolved potassium, it is low in Feb/Mar but slightly higher in other seasons (Figure 3.3). The seasonality patterns of the remaining constituents can be seen in appendix Figures A.9 to A.16.

In order to test for trend the seasonal Mann-Kendall test and Sen's slope was used for the stations that exhibited seasonality. The null hypothesis for this test is that no temporal trend exists versus the alternate hypothesis that a significant

upward (or downward) temporal trend exists. The direction of the alternative hypothesis (upward/downward) is specified and hence this is a one-sided test. Sen's slope estimator procedure is a simple nonparametric procedure developed by Sen (1968) and presented in Gilbert (1987) to estimate true slope.

The $N^{'} = \binom{n}{2}$ individual slope estimates, $Q_{i,i'}$, are computed for each time period:

$$Q_{i,i'} = \frac{x_i^{'} - x_i}{i^{'} - i},$$

where

$x_i^{'}$ and x_i are the data values at time $i^{'}$ and i (in days), respectively, $i^{'} > i$ and;

$N^{'}$ is the number data pairs for which $i^{'} > i$

Sen's slope estimator is then calculated by choosing the middle-ranked slope as follows;

$$\begin{cases} Q_{[N'=n(n-1)/2]} & \text{if } N^{'} \text{ is odd} \\ \frac{1}{2}\left(Q_{\frac{N'}{2}} + Q_{\frac{N'=n(n+2)}{2}}\right) & \text{if } N^{'} \text{ is even;} \end{cases}$$

where n is the number of time periods;this value is multiplied by 365 to give the yearly slope value.

The seasonal Mann-Kendall test is an extension of the Mann-Kendall test for trend that removes seasonal cycles. To compute the seasonal Mann-Kendall statistic, S_i, for each season there must be a minimum sample size of four data points in each season.

$$S_i = \sum_{k=1}^{n_i-1} \sum_{l=k+1}^{n_i} \text{sgn}(x_{il} - x_{ik})$$

where S_i is the statistic for the ith season and

$$\text{sgn}(x) = \begin{cases} -1, & \text{if } x < 0; \\ 0, & \text{if } x = 0; \\ 1, & \text{if } x > 0. \end{cases}$$

With use of the normal approximation (i.e.: greater than 41 observations) the Mann-Kendall test statistic, S is calculated. When there are no tied values, the variance of S is computed;

$$\text{Var(S)} = \frac{n(n-1)(2n+5)}{18}$$

and the test statistic Z, is as follows;

$$Z = \begin{cases} \dfrac{S-1}{[\text{Var(S)}]^{1/2}}, & \text{if } S > 0; \\ 0, & \text{if } S = 0; \\ \dfrac{S+1}{[\text{Var(S)}]^{1/2}}, & \text{if } S < 0. \end{cases}$$

When there are tied values,

$$\text{Var(S)} = \frac{1}{18}\left[n(n-1)(2n+5) - \sum_{p=1}^{g} t_p(t_p-1)(2t_p+5)\right],$$

where g is the number of tied groups and t_p is the number of observations in the pth group

Once $\text{Var}(S_i)$ is computed, we pool across the K seasons,

$$S' = \sum_{i=1}^{k} S_i$$

and our test statistic Z is computed. If the result of the test statistic for a one sided test is greater than 1.645 we reject our null hypothesis that no trend exists at the 5% level of significance.

The seasonal Mann-Kendall slope estimator procedure is as follows;

First we compute individual N_i slope estimates for the ith season:

$$Q_i = \frac{x_{il} - x_{ik}}{l - k},$$

where x_{il} the data for the i'th season of the l'th year and x_{ik} the data for the i'th season of the k'th year $(l > k)$.

This process is computed for each of the K seasons. Then rank the $N'1 + N'2 + \ldots + N'K = N'$ individual slope estimates and find their median. This median is the seasonal Mann-Kendall slope estimator.

As most parameters consistently exhibited significant seasonality, the Seasonal Mann-Kendall test was used for trend analysis. For certain constituents the requirement that there be a minimum per season sample size of four was not met. The analysis is summarized in Table 3.4, "n/a" implies the size requirements were not met, a positive slope is indicative of an increasing trend. If the p-value of the statistic is less than our 5% significance level we reject the null hypothesis of there being no trend. In order to calculate Sen's slope the data was read in as the median of each season because the program is not equipped to calculate Sen's slope for copious amounts of data.

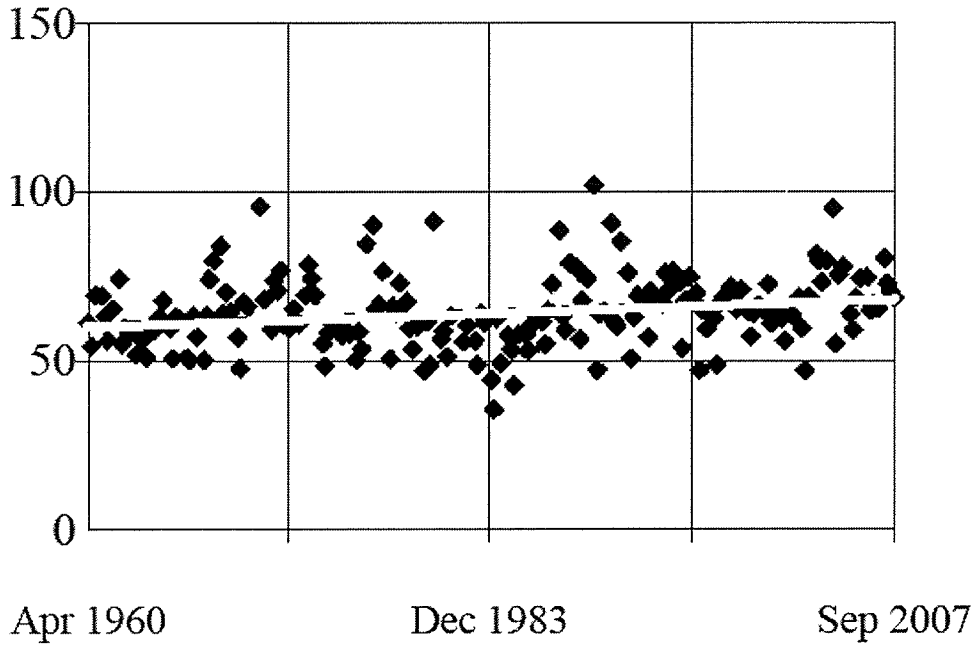

Figure 3.4: Long term temporal trend of Dissolved Calcium (mg/l) at the Emerson monitoring station

Concentrations in dissolved calcium presented an increasing significant trend at the Emerson monitoring station (Figure 3.4). There was insufficient data at the south floodway near St. Norbert monitoring station as well as the Selkirk station (remaining constituents can be seen in the appendix). Dissolved sodium has a significant increasing trend at the Emerson water quality monitoring station with insufficient data again at the other two water quality monitoring station. The dissolved potassium constituent has a significant slightly increasing slope at the Emerson monitoring station with the minimum sample size not being met at the south floodway near St. Norbert station and Selkirk monitoring station. Dissolved sulphate have increasing significant slopes at both the Emerson and Selkirk water quality monitoring stations, and minimum sample size was not met at the south floodway station. The slope of dissolved chloride at the Emerson station has an insignificant slopes at the 5% level of significance, while there was insufficient data at the south floodway station. Total dissolved solids produced significant increas-

Table 3.4: Seasonal Mann-Kendall Test for Trend Results.

Station	Slope (units/year)	p-value	Slope (units/year)	p-value
	Calcium, dissolved (mg/l)		Sulphate, dissolved (mg/l)	
1.	0.1665	$< \underline{0.001}$	1.190	$< \underline{0.001}$
2.	n/a	n/a	n/a	n/a
3.	n/a	n/a	4.860	$< \underline{0.001}$
	Sodium, dissolved (mg/l)		Chloride, dissolved (mg/l)	
1.	0.1957	$< \underline{0.001}$	0.113	0.330
2.	n/a	n/a	n/a	n/a
3.	n/a	n/a	1.246	$< \underline{0.001}$
	Potassium, dissolved (mg/l)		Total Dissolved Solids (mg/l)	
1.	0.0428	$< \underline{0.001}$	4.356	$< \underline{0.001}$
2.	n/a	n/a	29.55	$\underline{0.005}$
3.	n/a	n/a	3.479	$\underline{0.003}$
	Magnesium, dissolved (mg/l)		Specific Conductance (μS/cm)	
1.	0.2372	$< \underline{0.001}$	2.973	$< \underline{0.001}$
2.	n/a	n/a	0.702	0.337
3.	n/a	n/a	0.587	0.424

ing slopes at all three monitoring stations and an extremely large slope at the south floodway monitoring station and specific conductivity produced an increasing significant slope at the Emerson station and insignificant slopes at the south floodway and Selkirk monitoring stations. Certain constituents were also weighted for flow and trends re-examined using this non-parametric method. Flow adjusting data allows one to relate streamflow to various constituents and to remove flow effects prior to statistical analysis. For water quality constituents, which are closely related to flow, an apparent trend in quality could be caused by the change in flow. WQSTAT uses linear regression to estimate the slope and intercept of $\log(concentration) = a + b\log(flow)$. Then from each log concentration, the corresponding prediction based on flow, $a + b\log(flow)$, is subtracted, producing a series of residuals with a mean of zero. To each residual, the mean of the original log concentration is added, producing a flow-adjusted series of log concentrations, which has the same mean as the original. Finally, the antilogs of the log concentrations are found, and a final correction is made so that the resulting series, in original concentration units, will have the same mean as the original series of observations. Slopes from the four constituents selected increased slightly and remained significant after the removal of flow, this can imply part of the increasing trends may be due to factors other than streamflow. The question is how one would handle such increases; if the slope is only increasing slightly relative to others with large increases the latter should be looked at and evaluated first. Although the slopes are significant, the p-values given in Table 3.4 and Table 3.5 are that of Kendall's τ.

Table 3.5: Flow Adjusted Seasonal Mann-Kendall Test for Trend Results.

Station	Slope (units/year)	p-value
	Calcium, dissolved (mg/l)	
1.	0.1710	$< \underline{0.001}$
2.	n/a	n/a
3.	n/a	n/a
	Sodium, dissolved (mg/l)	
1.	0.2580	$< \underline{0.001}$
2.	n/a	n/a
3.	n/a	n/a
	Potassium, dissolved (mg/l)	
1.	0.0460	$< \underline{0.001}$
2.	n/a	n/a
3.	n/a	n/a
	Magnesium, dissolved (mg/l)	
1.	0.3567	$< \underline{0.001}$
2.	n/a	n/a
3.	n/a	n/a

Chapter 4

Parametric Methods used for Water Quality Trend Analysis

In the previous section, a non-parametric method of water quality trend analysis was examined, namely the seasonal Mann-Kendall test. The advantages to such methods are that they are easy to compute, require few assumptions, are robust to outliers and can handle numerous data from many stations. A weakness of the seasonal Mann-Kendall test is that it assumes monotonic trend and seasons must be defined. Some advantages of parametric methods are: they can be used to model complex trends; and are good for explanatory and not just exploratory analysis. Introducing ancillary data such as livestock or farming data can help better explain certain trends. These methods use the full power and flexibility of maximum likelihood theory, and flow and concentration are modeled jointly (Vecchia, 2004). However, disadvantages of parametric methods are: they require specification of a parametric model; usually are computationally intensive; require care in fitting the model and verifying assumptions and may require more data than non-parametric methods do. QWTREND, developed by Aldo Vecchia (USGS), was used to analyze trends in water quality. There are specific data requirements for this program:

1. Record length at least 15 years (not necessarily consecutive)

2. Average of at least 4 samples per year (sampling frequency may vary from year-to-year)

3. At least 10 samples during each 3-month "season" (Jan-Mar, Feb-Apr, Mar-May, ..., Dec-Feb)

4. Less than 10 percent of values can fall below detection limit (may be more, but extra care required to interpret results)

5. Full record of daily streamflow from 5 years before the first water quality sample through the end of the record

Streamflow variation exists on many time scales (annual, seasonal, daily, etc.), and the variation can affect concentrations in complex and diverse ways (Vecchia, 2004). Seasonal and annual variability in streamflow in the Red River Basin is high. Generally, high flows occur during spring and early summer (primarily from snowmelt or rainfall runoff from spring storms) and low flows occur during late fall and winter (primarily from ground-water or reservoir discharges). Streamflow data were complete for the Emerson station from 1955 to 2007. Flow data for the Red River at St. Norbert was insufficient for the trend analysis program, therefore, flows for the analysis of that station were calculated by summing the flow data from the Red River at Ste. Agathe hydrometric station with those from the Rat River at Otterburne hydrometric station (Jones and Armstrong, 2001). Selkirk station data ranged from 1950 to 1969, so flow data for the trend analysis at the Selkirk station was obtained from the hydrometric station located approximately 9 km upstream at Lockport.

The general time series structure defined by Vecchia (2000) expresses the **streamflow** data as:

$$\log(Q) = M_Q + ANN_Q + SEAS_Q + HFV_Q,$$

where

log denotes the base-10 logarithm;

Q is the streamflow, in cubic feet per second;

M_Q is the long-term mean of the log-transformed streamflow;

ANN_Q is the annual streamflow anomaly (dimensionless);

$SEAS_Q$ is the season streamflow anomaly (dimensionless); and

HFV_Q is the high-frequency variability of the streamflow.

The **concentrations** data is expressed as:

$$\log(C) = M_C + ANN_C + SEAS_C + TREND_C + HFV_C,$$

where

C is the concentration, in milligrams or micrograms per litre;

M_C is the long-term mean of the log-transformed concentration;

ANN_C is the annual concentration anomaly (dimensionless);

$SEAS_C$ is the seasonal concentration anomaly (dimensionless);

$TREND_C$ is the concentration trend; and

HFV_C is the high-frequency variability of the concentration (dimensionless).

All of the terms in the above model except the trend, are assumed to represent "natural" variability. The high frequency variability is the variability that remains after the removal of seasonal and annual anomalies. Day-to-day changes in meteorological conditions may cause high-frequency variability in both streamflow and concentration. It may also be caused by the inability to exactly determine a concentration at any given time.

The different scales of variation of streamflow are expressed as:

$$\log(Q) - M_Q = ANN_Q + SEAS_Q + HFV_Q,$$

where ANN_Q, $SEAS_Q$, HFV_Q are defined above.

For a particular time (t, in decimal years);

$ANN_Q = A5YR + A1YR$ "annual streamflow anomaly";

A5YR is the average of $\log Q - M_Q$ for five years up to and including time t ("5 year streamflow anomaly");

A1YR is the average of $\log Q - M_Q - A5YR$ for one year up to and including time t ("1 year streamflow anomaly");

$SEAS_Q = A3M + APER$;

$A3M$ is the average of $\log Q - M_Q - ANN_Q$ for 3 months up to and including time t ("3 month streamflow anomaly");

$APER$ = Periodic function of t with period 1-year.

The top graph in Figure 4.1 depicts the daily streamflow at the Emerson monitoring station while the bottom one depicts the streamflow by month. The values at the bottom of the graphs indicate the values included, for streamflow all 36 values per year (3 per month) are included. The two plots of dissolved calcium (Figure 4.2) show that sampling started in 1960 and ended in 2007, there are 47 years with at least 1 sample and an average of 16 samples per year, thereby indicating there is enough data for time series analysis. Further plots for the remaining constituents are in the appendix.

QWTREND employs a periodic auto-regressive moving average model (PARMA model) (cf. Box and Jenkins, 1976) to remove the "non-random" structure in the high-frequency variability of the streamflow:

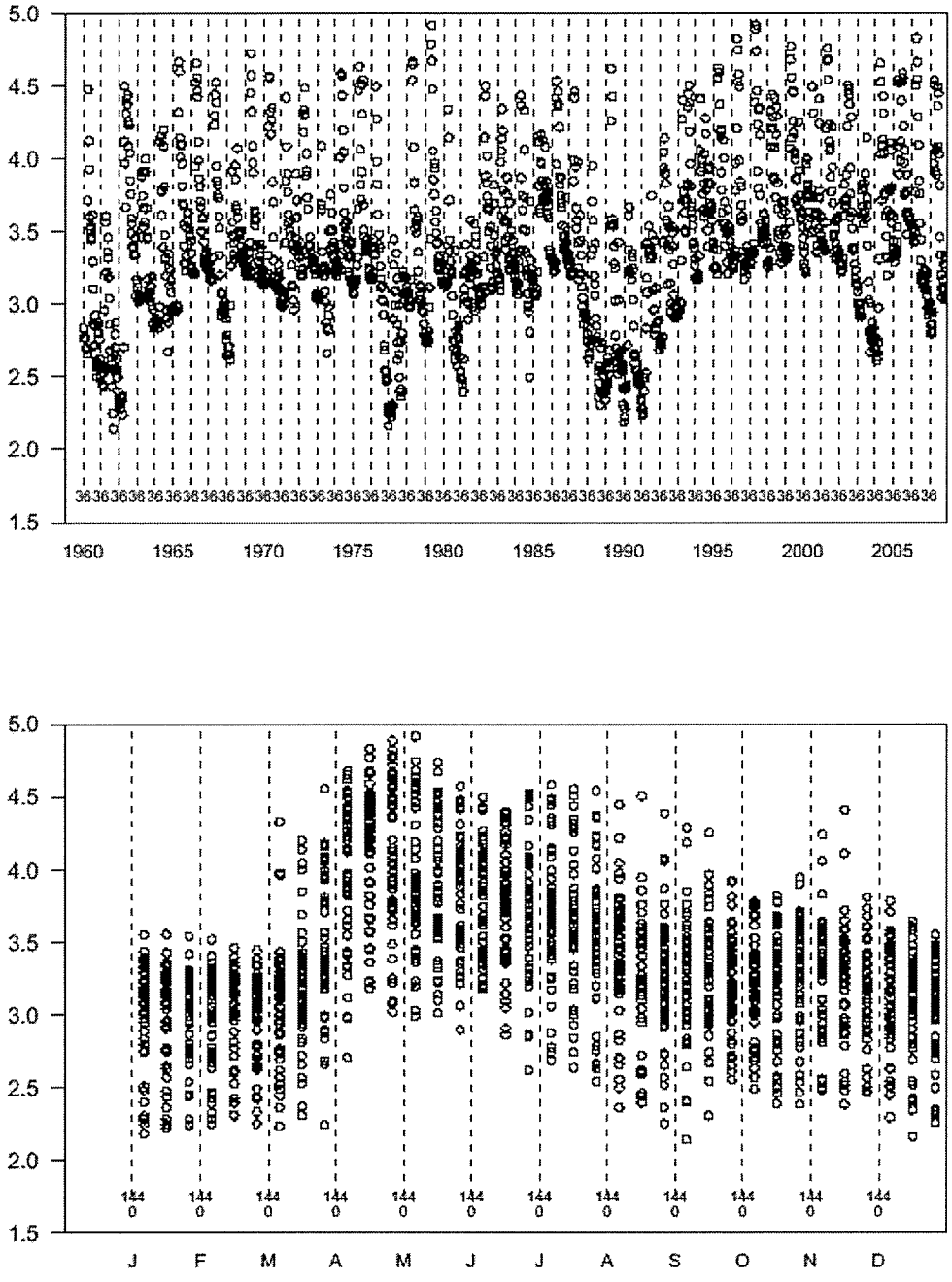

Figure 4.1: Daily Streamflow at Emerson ($\log_{10}$ m^3/s)

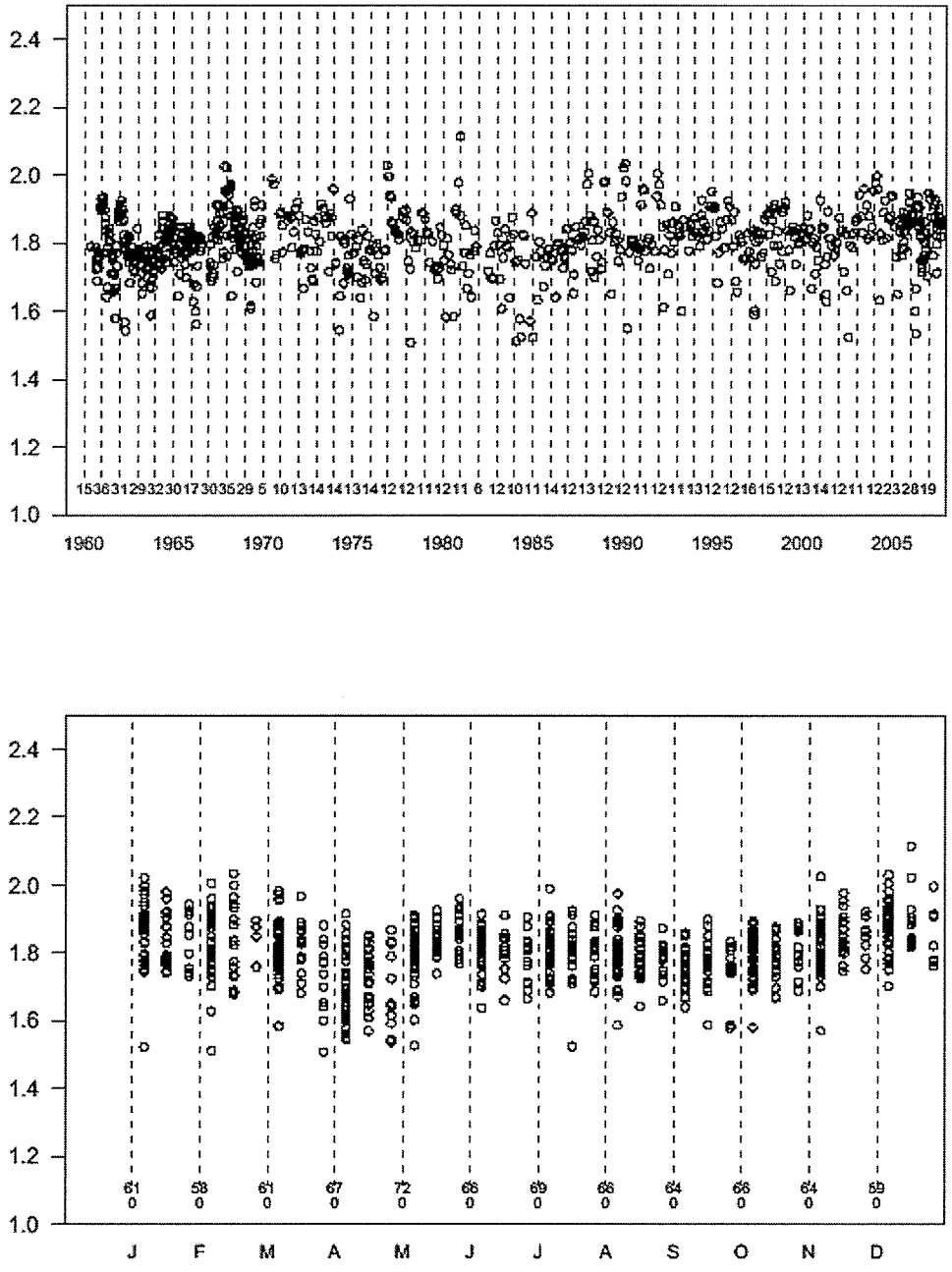

Figure 4.2: Dissolved Calcium at Emerson ($\log_{10}$ mg/l)

$$[B_i, H(t)] = b_{i0} + b_{i1}\cos(2\pi t) + b_{i2}\sin(2\pi t) + b_{i3}\cos(4\pi t) + b_{i4}\sin(4\pi t)$$

where;

$B_i = [b_{i0}, b_{i1}, b_{i2}, b_{i3}, b_{i4}]$ are the parameters to be estimated,

$H(t) = [1, \cos(2\pi t), \sin(2\pi t), \cos(4\pi t), \sin(4\pi t)]$ and

Therefore, the PARMA model for streamflow is:

$$HFV_Q(t) = PAR(t)HFV_Q(t-d) + PMA(t)\epsilon_1(t-d) + \epsilon_1(t)$$

where;

$PAR(t) = [B_1, H(t)]$ is a periodic autoregressive coefficient

$PMA(t) = [B_2, H(t)]$ is a periodic moving average coefficient

$\epsilon_1(t)$ is the PARMA model noise with the assumption that E[$\epsilon_1(t)$]=0, Var[$\epsilon_1(t)$]=σ_1^2(t) and Corr[$\epsilon_1(t)$,ϵ_1(t-kd)]=0

$\sigma_1(t) = [B_3, H(t)]$ is the periodic standard deviation of the noise.

There is also a periodic auto-regressive moving average model (PARMA model) to remove the "non-random" structure in the high-frequency variability of concentration, notation is as follows:

$$HFV_C(t) = PAR_0(t)HFV_Q(t) + PAR_1(t)HFV_C(t-d) + PMA_0(t)\epsilon_1(t) + \epsilon_2(t)$$

where;

$PAR_0(t) = [B_4, H(t)]$ is a periodic autoregressive coefficient,

$PAR_1(t) = [B_5, H(t)]$ is a periodic autoregressive coefficient,

$PMA_0(t) = [B_6, H(t)]$ is a periodic moving average coefficient, and

$\epsilon_1(t)$ is the PARMA model noise for streamflow and $\epsilon_2(t)$ is the PARMA model noise for concentration.

There are two complementary approaches for fitting trends (Vecchia, 2004), exploratory trend analysis will provide the best statistical fit to the data using generalized likelihood ratio tests or an explanatory trend analysis which will use ancillary time-series data such as livestock data, to explain the trends in concentration.

Figures 4.3–4.8 depict the recorded data of dissolved calcium at the Emerson monitoring station, seasonally adjusted and de-trended data, the seasonally adjusted and flow-adjusted data and the PARMA model residuals and a line showing the lowess smooth. Lowess, locally weighted scatterplot smoothing is an outlier resistant method based on local polynomial fits (Cleveland, 1979). These smoothers make no assumptions about the form of the relationship, and allows the form to be discovered using the data itself. The plots of the remaining constituents and stations can be seen in the appendix.

4.1 Generalized Likelihood Ratio

To compute the overall significance of the fitted trend model we are testing the null hypothesis that there is no trend versus the alternate hypothesis that at least one trend coefficient is non-zero. $L(0)$ is the value of -2 ln L , L is the likelihood function, for the model with no trend and $L(k)$ is the value of -2 ln L for the model with k trend functions. If all the trend coefficients equal zero, implying no trend exists, $\Gamma(k)$=$L(0) - L(k)$ has χ^2 distribution on k degrees of freedom, thus the p-value is 1-P($\chi^2_{\Gamma(k),k}$).

The no trend model was initially fitted for the Emerson station constituents, a single linear trend was then fitted for all constituents and upon closer examination

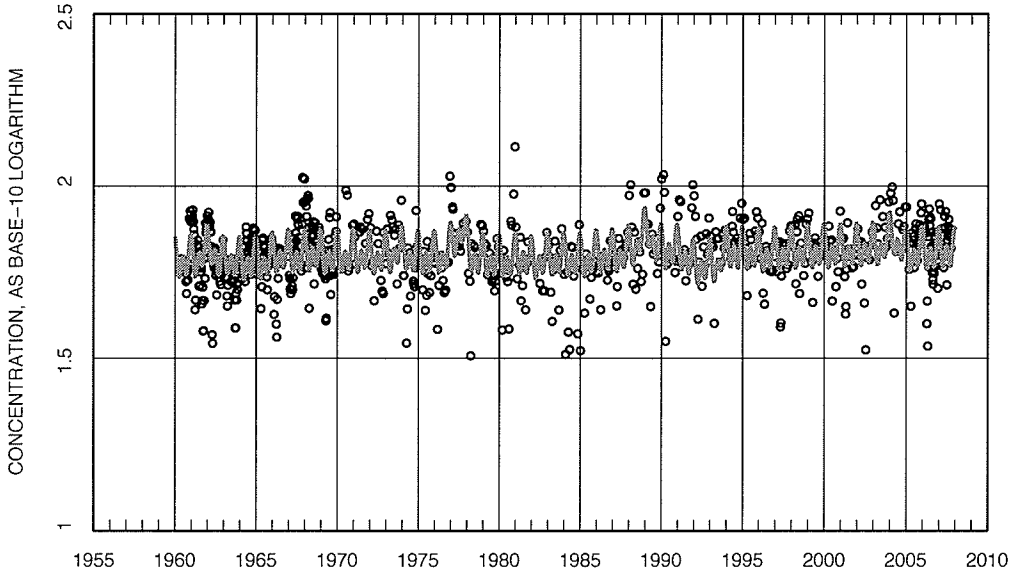

Figure 4.3: Emerson: Dissolved Calcium concentrations (points) and streamflow related anomaly + trend (line)

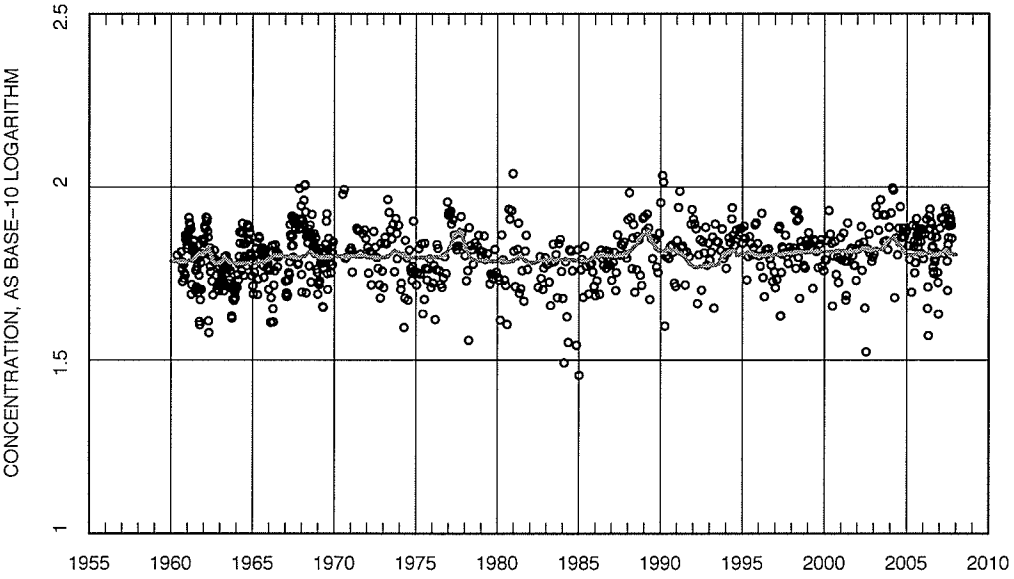

Figure 4.4: Emerson: Dissolved Calcium Flow Adjustments — Seasonally adjusted and de-trended data (points) and annual streamflow-related anomaly (line).

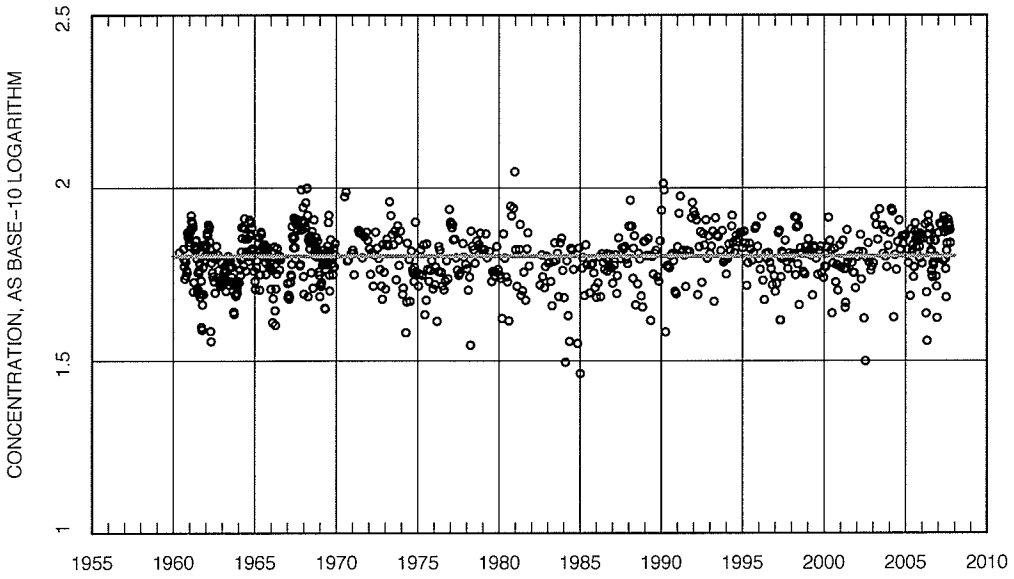

Figure 4.5: Emerson: Dissolved Calcium Flow Adjustments — Seasonally adjusted and flow adjusted data (points) and no-trend (line).

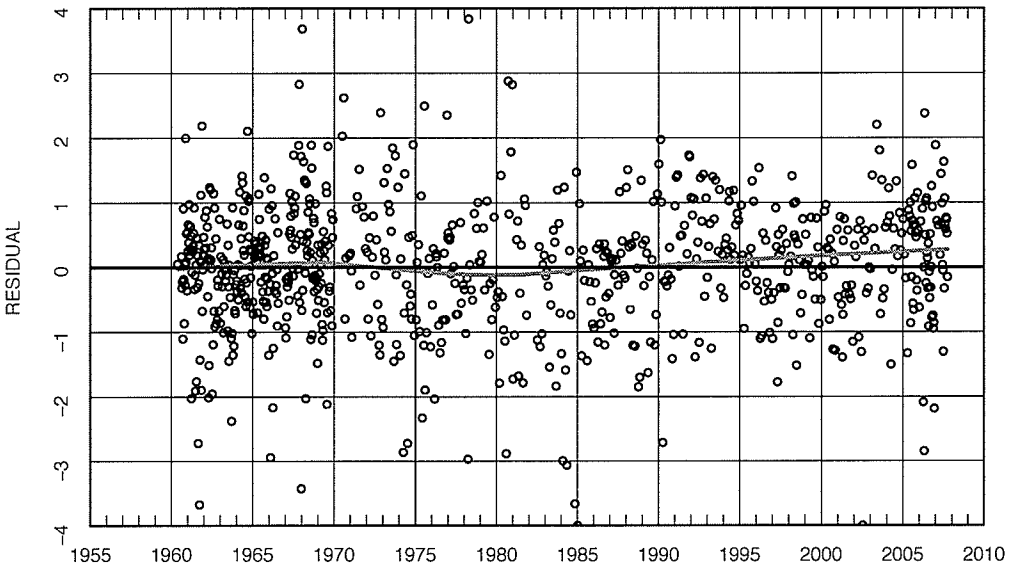

Figure 4.6: Emerson: Dissolved Calcium Flow Adjustments — Parametric no-trend model residuals (points) and lowess smooth line with $F = 0.5$.

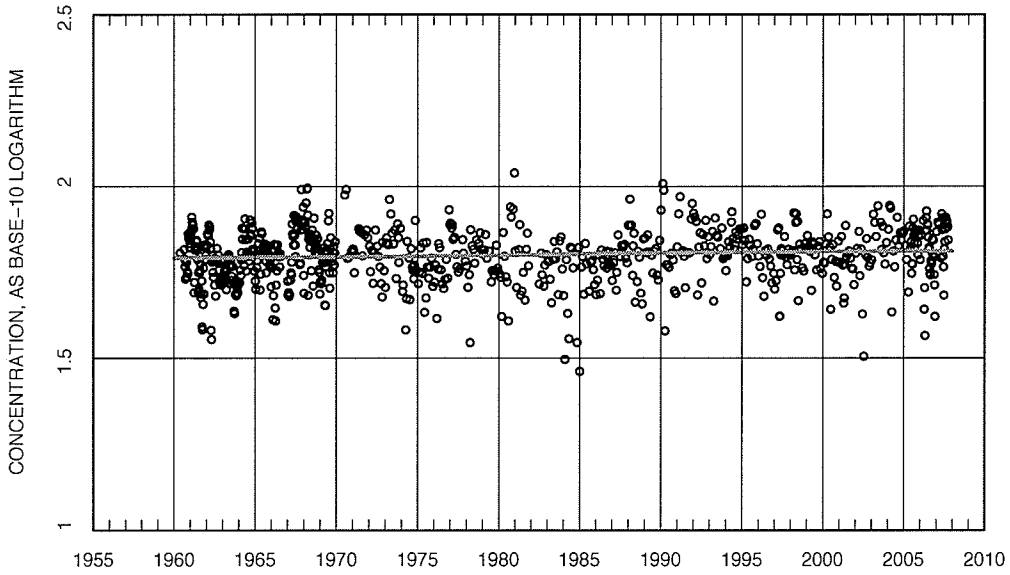

Figure 4.7: Emerson: Dissolved Calcium Flow Adjustments — Seasonally adjusted and flow adjusted data (points) and single trend (line).

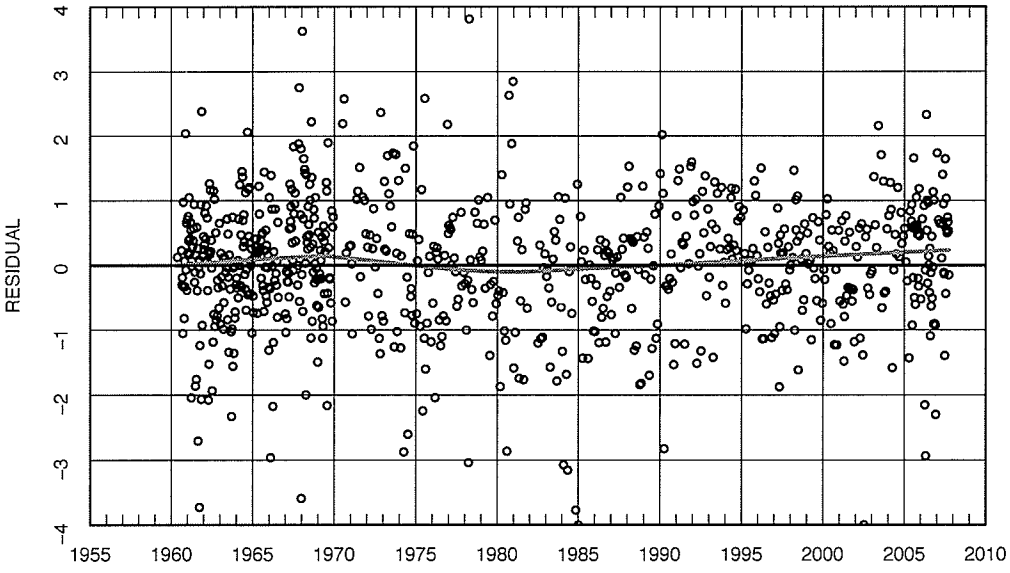

Figure 4.8: Emerson: Dissolved Calcium Flow Adjustments — Parametric single trend model residuals (points) and lowess smooth line with $F = 0.5$.

of the residuals it can be seen that not all constituents are best modeled with a single linear trend. Also given is the percent change in the median of the flow-adjusted concentration trend line over the period of reporting.

Table 4.1 shows the results of fitting a single linear trend model to the data from the Emerson monitoring station. For each of the eight constituents considered, the percent change is calculated as $(10^x - 1) * 100$, where x is the estimated coefficient. For the Emerson station, the value of the log likelihood of dissolved calcium and sulphate is slightly greater than that of the no-trend model so the significance of this trend can not be computed. Dissolved sodium and dissolved potassium constituents yielded an estimated 47.9% with concentrations from 28.44 mg/l to 41.98 mg/l and an estimated 32.7% respective significant increase of 5.36 mg/l and 7.12 mg/l from 1960-2007. Dissolved magnesium did not meet the all the requirements of QWTREND, there is a period of time where no data was collected as seen in the top graph of Figure A.33 thus the trend was fitted on the data from 1975 to 2007 which yielded an estimated significant 21.1% increase from 26.49 mg/l to 32.06 mg/l. Total dissolved solids significantly increased 43.2% with concentrations ranging from 349.14 mg/l to 501.19 mg/l from 1985-2007. Dissolved chloride and specific conductance both had significant increasing trends from 1960-2007 with estimates of 39.0% and 28.8% respectively with concentrations ranging from 28.64 mg/l to 39.81 mg/l for dissolved chloride and from 588.84 μS/cm to 756.83 μS/cm. Dissolved sulphate also had an estimated 52.4% increase in median concentration ranging from 66.68 mg/l to 101.62 mg/l between 1960 and 2007, however, a single linear trend is not an appropriate measure for this constituent. The remaining comparisons for all constituents and stations is summarized in Table 5.2.

One method to further explore other possible monotonic trends is to analyze the residual plots of the no trend models. Dissolved calcium seems to exhibit three monotonic trends; an increase from 1960-1970 a slight decline until 1983 and then increase again to 2007. Dissolved potassium and specific conductance are other constituents exhibiting two different monotonic trends a slight decrease from 1960 to 1974 and increase until to 2007. The trend for magnesium was examined from

Table 4.1: Fitted Single Linear Trends at the Emerson Station

Constituent	est. % change	est. coef.	std. error	p-value	time period
Dissolved Calcium	4.7	0.020	1.632	can't determine	1960-2007
Dissolved Sodium	47.9	0.170	6.401	$< \underline{0.001}$	1960-2007
Dissolved Potassium	32.7	0.123	7.279	$< \underline{0.001}$	1960-2007
Dissolved Magnesium	21.1	0.083	4.190	$< \underline{0.001}$	1975-2007
Dissolved Sulphate	52.5	0.183	6.363	can't determine	1960-2007
Dissolved Chloride	39.0	0.143	3.439	0.001	1960-2007
Total Dissolved Solids	43.2	0.183	6.363	$< \underline{0.001}$	1985-2007
Specific Conductance	28.8	0.110	6.974	0.001	1960-2007

Table 4.2: Three Monotonic Trends found from exploring no-trend model residuals

Constituent	% change	% change	% change	p-value
Dissolved Calcium	24.5	-15.9	26.2	$< \underline{0.001}$
Total Dissolved Solids	10.7	-19.1	11.4	$< \underline{0.001}$

1975 and shows a decrease until 1983 and then proceeds to increase through to 2007. Total dissolved solids also show three different monotonic trends, an increase from 1982-1992 then a slight decrease until 1999 and then increase again until 2007. Dissolved sulphate appears to have two monotonic trends, a decrease from 1960 until 1977 and then increase until 2007, while dissolved chloride seems best modeled with a single linear trend. This is outlined in Table 4.2 and Table 4.3.

Initially dissolved sodium was fitted with two monotonic trends: a suspected decrease from 1960 until 1970 and an increase until 2007. The estimated coefficients of the model were all positive making it difficult to fit a proper model by just looking at the residual plots. Since this method does not give us accurate "cut-offs" the following section offers an alternate method of fitting trend functions for the constituents at the Emerson monitoring station.

Table 4.3: Two Monotonic Trends found from exploring no-trend model residuals

Constituent	% change	% change	p-value
Dissolved Potassium	-3.3	38.4	$< \underline{0.001}$
Dissolved Magnesium	-5.6	43.5	$< \underline{0.001}$
Dissolved Sulphate	-24.8	84.1	$< \underline{0.001}$
Specific Conductance	-9.2	36.8	$< \underline{0.001}$

For the constituents at the South Floodway monitoring station, a no trend model was fitted for three constituents, dissolved sulphate, dissolved chloride and specific conductance. However, since QWTREND has quite specific requirements as stated earlier, for the South Floodway at St. Norbert and Selkirk monitoring stations the only constituent with enough data for trend analysis is specific conductance. There was found to be a 33.7% significant increase in specific conductance from 1976-2007 with a p-value < 0.001 as seen in Figure A.86–A.89 and for the Selkirk monitoring station there was a 28.8% significant increase in the median specific conductance from 1978-2001 with a p-value of < 0.001 as seen in Figure A.92–A.95. Both of these results contradicted the insignificant results obtained by using the non-parametric methods.

4.1.1 Generalized Likelihood Ratio Tests for Comparing Models

To compare models: L(k) is the value of -2 ln L for the model with k equally spaced trend functions and L(k+j) is the value of -2 ln L for a model with j additional trend functions. If all the additional coefficients equal zero, implying no trend exists, $\Gamma(j)$=L(k) − L(k+j) has χ^2 distribution with j degrees of freedom, thus the p-value is 1-P($\chi^2_{\Gamma(j),j}$). The model which yields the lowest p-value computed by the generalized likelihood ratio test is the best model to use.

In the previous section, all constituents were modeled with a single linear trend

and from exploring the residual plots of the no trend model, several different monotonic trends may emerge, that method is a form of "data-peeking." We are running variations on regression models prior to running the final model and this is highly susceptible to generating spurious results.

To facilitate comparisons between the fitted trends for the different constituents, the same initial model was fitted in each case and then simplified to obtain the fitted trend for each individual constituent. The initial model consisted of ten trend functions with midpoints 1960, 1965, 1970, 1975, 1980, 1985, 1990, 1995, 2000, 2005 and a half-width of 2.5 for all midpoints. The model was then simplified by using the algebraic signs of the coefficients to combine adjacent trends. For example if the fitted coefficients for the trend functions with midpoints of 1965 and 1970 were both positive, the two functions were combined into a single function with a midpoint of 1967.5 and a half-width of 5. Table 4.4 shows the number of monotonic trend functions for each constituent using the above described method. The significance of dissolved calcium could not be determined by a single linear trend and after combining adjacent coefficients the four trend model yielded the lowest p-value and showed a 17% decrease from 1960 to 1962.5, a 23% increase from 1962.5 to 1967.5, another 15% decrease from 1967.5 to 1977.5 and finally a 21% increase through to 2007. Dissolved sodium exhibited a 57.2% decrease from 1960 to 1962.5, a 37.4% increase from 1962.5 to 1967.5, another 7.3% decrease from 1967.5 to 1982.5 and an increase of 63.7% through to 2007. Dissolved potassium was best fitted with six monotonic trends a 43.1% decrease from 1960 to 1962.5, a 15.1% increase from 1962.5 to 1967.5, a decrease of 10.5% from 1967.5 to 1977.5 another 35.8% increase until 1997.5 a small decrease of 5.8% until 2002.5 and finally an increase of 16.9% through to 2007. Dissolved magnesium having been analyzed with data from 1975 showed a decrease of 13.9% until 1978 and an increase of 48.3% until 2007. Dissolved sulphate yielded a 28.4% decrease until 1979 and a 78.2% increase through until 2007 using this method which can compare to the results in the previous section. Dissolved chloride was fitted with four monotonic trends and showed a 74.6% decrease in concentration from 1960 to 1962.5 then an increase of 41.6% until 1967.5 another 23.1% decrease till 1985 and finally a large

Table 4.4: Best Fitted Model for each Constituent

Constituent	number of trends	p-value
Dissolved Calcium	4	< 0.001
Dissolved Sodium	4	< 0.001
Dissolved Potassium	6	< 0.001
Dissolved Magnesium	2	< 0.001
Dissolved Sulphate	2	< 0.001
Dissolved Chloride	4	< 0.001
Total Dissolved Solids	1	< 0.001
Specific Conductance	4	< 0.001

increase of 102.3% to 2007. Using this method a single linear trend was the most appropriate model for total dissolved solids and showed a 43.5% increase until 2007 which corresponds to the earlier method of fitting the trend. Specific conductance is modeled with four monotonic trends; decrease of 44.5% from 1960 to 1962.5, a 5.4% increase until 1967.5 another 3.2% decrease and finally a 36.4% increase until 2007.

Now since these methods only explore fitted trends one may still wish to know reasonable causes for such trends. Without a detailed chemical source and transport model, definitive causes for trends are difficult to determine however, ancillary time series variables can be used to determine if changes in the variables are consistent with the approximate timing and direction of the trends.

Chapter 5

Comparison of Non-Parametric and Parametric Results and Future Recommendations

5.1 Comparisons

The non-parametric method is simpler to employ and can be used with less data than the parametric methods employed in QWTREND. Small sample size and short period of record, coupled with the high variability in data make the detection of statistically significant trends using the parametric approach quite difficult. However, QWTREND allows one to fit trends using an exploratory approach that indicate the approximate times and directions of changes in concentrations. In order to explain the change, this also allows the introduction of ancillary data to see if the changes are a result of human causes (i.e., changes in land use, agricultural practices, sewage treatment, etc.) (Vecchia, 2004).

Both methods exhibited similarities with significant trend results amongst dissolved sodium, dissolved potassium and dissolved magnesium. The significance of the trend for dissolved calcium could not be computed using the parametric method.

Table 5.1: Comparison Results with respective p-values

Station #	Constituent	Non-Parametric	Parametric
1.	Dissolved Calcium	$< \underline{0.001}$	n/a
1.	Dissolved Sodium	$< \underline{0.001}$	$< \underline{0.001}$
1.	Dissolved Potassium	$< \underline{0.001}$	$< \underline{0.001}$
1.	Dissolved Magnesium	$< \underline{0.001}$	$< \underline{0.001}$
1.	Dissolved Sulphate	$< \underline{0.001}$	n/a
3.	Dissolved Sulphate	$< \underline{0.001}$	n/a
1.	Dissolved Chloride	0.330	0.001
3.	Dissolved Chloride	$< \underline{0.001}$	n/a
1.	Total Dissolved Solids	$< \underline{0.001}$	$< \underline{0.001}$
2.	Total Dissolved Solids	0.005	n/a
3.	Total Dissolved Solids	0.003	n/a
1.	Specific Conductance	$< \underline{0.001}$	0.001
2.	Specific Conductance	0.337	$< \underline{0.001}$
3.	Specific Conductance	0.424	$< \underline{0.001}$

Total dissolved solids exhibited a significant trend at the Emerson station using both methods and at the remaining two stations using the non-parametric methods, however data from the South Floodway and Selkirk stations were too sparse to employ the parametric method. There are also some obvious differences. For example, using non-parametric techniques, dissolved chloride concentrations at the Emerson monitoring station did not exhibit a significant trend but they did with the parametric methods. However, using parametric techniques, specific conductance at both stations showed significant increases while the non-parametric method yielded insignificant results. Table 5.1 summarizes the comparisons of each method with their respective p-values.

The estimated percent change for dissolved calcium was relatively similar between the non-parametric and flow adjusted non-parametric methods as can be seen in Table 5.2 however, there is a notable difference between these results and

Table 5.2: Changes in Concentrations with each Method

			Non Parametric			Non-Parametric (Flow Adj.)			Parametric		
Station #	Constituent	Dates	From	To	% Change	From	To	% Change	From	To	% Change
1.	Dissolved Calcium	1960–2007	60.53	68.43	13.0%	60.30	68.42	13.4%	60.95	63.83	4.7%*
1.	Dissolved Sodium	1960–2007	37.78	47.08	24.6%	33.58	45.84	36.5%	28.44	41.98	47.9%
1.	Dissolved Potassium	1960–2007	5.57	7.61	36.5%	5.46	7.64	40.2%	5.36	7.12	32.7%
1.	Dissolved Magnesium	1975–2007	26.27	37.53	42.9%	23.24	40.18	72.9%	26.49	32.06	21.1%
1.	Dissolved Sulphate	1960–2007	70.78	127.30	79.8%				66.68	101.62	52.5%*
1.	Dissolved Chloride	1960–2007	not significant						28.64	39.81	39.0%
1.	Total Dissolved Solids	1985–2007	403.19	515.73	27.9%				349.14	501.19	43.2%
1.	Specific Conductance	1960–2007	646.18	787.40	21.9%				588.84	756.83	28.8%
2.	Total Dissolved Solids	1985–1991	461.35	638.65	38.4%				insufficient data		
2.	Specific Conductance	1976–2007	not significant						578.10	772.68	33.7%
3.	Dissolved Sulphate	1997–2007	100.94	156.06	54.6%				insufficient data		
3.	Dissolved Chloride	1997–2007	25.14	39.26	56.2%				insufficient data		
3.	Total Dissolved Solids	1970–1991	470.86	549.14	16.6%				insufficient data		
3.	Specific Conductance	1978–2001	not significant						645.65	831.76	28.8%

* significance could not be determined, see Section 4.1

the parametric method. The estimated percent change in dissolved sodium is increasing amongst all three methods, while dissolved sulphate yielded an estimated 79.8% change with the non-parametric method, but only an estimated 52.5% change using parametric methods (although the significance of this trend could not be computed). It is difficult to compare these two methods because they both use entirely different models. The parametric model includes numerous streamflow anomalies and allows fitting more than a single linear trend, while the non-parametric model does not. Using the parametric flow adjusted models show that increases in ion concentration may not be entirely related to flow. Variation in precipitation as well as landscape changes can be other contributing factors. Even though there are statistically significant increasing trends occurring in most of the constituents, there is still a need to test different models and correlations between stations. The sparse data from the South floodway at St. Norbert and Selkirk stations, different lab methods and the different time periods of record make it difficult to compare between stations.

5.1.1 Advantages and Disadvantages

Non-parametric and parametric time series come with their own sets of advantages and disadvantages and these are only two of those methods that have been employed, there are further non-parametric methods that can be used and serial correlation needs to be addressed and with the non-parametric and parametric time series models there should be considerations in coming up with an automatic model selection process that can best describe the trends.

Advantages of Non-Parametric Methods using WQSTAT:

- Easy to compute
- Requires few assumptions
- Robust to outliers

Disadvantages of Non-Parametric Methods using WQSTAT:

- May not be as powerful (when parametric assumptions are met)
- "Hydrologic" seasons must be clearly defined
- Assumes monotonic trend
- No flexibility for defining trend lengths

Advantages of Parametric Methods using QWTREND:

- Can model complex trends
- Good for explanatory and exploratory analysis
- Uses full power of the maximum likelihood theory
- Flow and concentration are modeled jointly
- Fitted trends indicate approximate times and direction of the changes in concentrations

Disadvantages of Parametric Methods using QWTREND:

- Requires specification of a parametric model
- Certain data requirements must be met
- Requires care in fitting the model and verifying assumptions
- Computationally intensive

5.2 Future Recommendations and Conclusions

First and foremost there should be a **sampling design** employed for monitoring concentration trends in order to make a complete data set for future water quality monitoring projects. If all stations are continually monitored then this design should be uniform throughout. QWTREND computes effective sampling designs for monitoring trends in order for parametric trend results to be as accurate as possible. Designs can be variable or fixed to be the same year after year. Variable sampling frequencies should be considered only if one can specify the starting time and duration of the trend. Since this is quite difficult a fixed sampling design is a more efficient method. Fixed sampling designs can be compared by two characteristics, their sensitivity and efficiency. An efficient design is one that maximizes the likelihood of detecting a trend for a fixed cost. After fitting the time series model for analyzing historical trends, the model can be used to compute the characteristic trend for any specified design using QWTREND. The characteristic trend is the increase (or decrease) in concentration, in percent, that has an 80% chance of being detected after 5 years of sampling. Trends larger than this characteristic trend will have more than an 80% chance of being detected, while trends smaller will have less than an 80% chance of being detected, if they exist. For future studies this would be useful to establish.

If a comparison is to be made between concentration data and concentration data weighted for flow, then that should be done using the non-parametric method as well. Vecchia's method deals with flow-adjusted models and, as such, are dealing with the log of streamflows and concentrations, when comparing the non-parametric methods the data is not transformed in the same manner. QWTREND merges the streamflow and concentration data sets quite easily whereas WQSTAT allows for a **flow-adjusting** procedure to be applied to the raw data. The streamflow data is given on a daily basis while concentration of the constituents are not and WQSTAT makes it difficult to merge the streamflow and concentration.

Ancillary data could also be used in order to better explain the trends in concentrations and whether or not they are ecologically significant. Cropland and

livestock data for the Red River are reported by the National Agricultural Statistics Service, this available data can be incorporated into QWTREND and allows one to have more of an explanation as to why certain fitted trends make sense. For example, if there has been an increase in the amount of cattle in an area surrounding the Red River, does that explain a certain percent increase in ion concentration? Or, with more roads near the Red River will there be an increase in sodium and chloride ions due to road salt usage?

Without more research, it is hard to say which of these two methods should be used in any given situation. In addition, more complex models should also be considered — especially ones that can incorporate not only the serial correlation, but also spatial components and the correlation between ion concentrations. These may be parametric, non-parametric or semi-parametric in nature. A Bayesian approach may prove advantageous in handling these more complicated models.

Chapter 6

Bibliography

Antonopoulus, Vassilis; Papamichail, Dimitris M.; and Mitsiou, Konstantina; 2001 "Statistical and Trend Analysis of Water Quality and Quantity Data for the Strymon River in Greece", *Hydrology and Earth System Sciences*,5(4) 679-691.

Box, George; and Jenkins, Gwilym, *"Time Series Analysis: Forecasting and Control,"* rev. ed; Oakland, California: Holden-Day, 1976.

Cleveland, W.S., 1979, Robust Locally Weighted Regression and Smoothing Scatterplots, *Journal of the American Statistical Association*, 74(368), pages 829-836.

Conover, W.J., *"Practical Nonparametric Statistics-Third Edition,"* John Wiley & Sons, 1999.

Eaton, Andrew D.; Lenore, Clescrei S.; Rice, Eugene W.; and Greenberg, Arnold E., 2005 Centennial Edition. "Prepared and published jointly by the American Public Health Association, the American Water Works Association, and the Water Environment Federation.

Fritz, Charles; and Zhang, Haimeng., 2006, Red River of the North Water Quality: Nutrient and Ion Study Emerson - Fargo. International Joint Commission Contract

Gilbert, R.O., *Statistical Methods for Environmental Pollution Monitoring.* Van Nostrand Reinhold Company, New York, NY. 320pp.

Glozier, Nancy; Crosley, Robert; Mottle, Larry; and Donald, David., 2004 *Water Quality Characteristics and Trends for Banff and Jasper National Parks: 1973-2002* Environmental Conservation Branch, Environment Canada.

Hamed, Khaled.,; 2008, Trend Detection in Hydrologic Data: The Mann-Kendall Trend Test Under the Scaling Hypothesis. *Journal of Hydrology*, 349, 350-363.

Helsel, D.R., 2005, *Nondetects and data analysis* Hoboken, New Jersey, John Wiley & Sons, Inc.

Helsel, D.R., and Hirsch, R.M., 1992, *Statistical Methods in Water Resources* Elsevier, Amsterdam.

Hirsch, Robert; Slack, James; and Smith, Richard., 1982, Techniques of Trend Analysis for Monthly Water Quality Data, *Water Resources Research*, Vol. 18, No. 1, pages 107-121.

Hughes, C., 2009, *An assessment of twenty-nine southern Manitoba rivers and streams using benthic macroinvertebrates and water chemistry (1995 to 2005).* Water Science and Management Branch, Manitoba Water Stewardship, Winnipeg, MB.

Jones, G. and Armstrong, N., 2001, *Long-term trends in total nitrogen and total phosphorus concentrations in Manitoba streams*, Water Quality Management Section, Water Branch, Manitoba Conservation, Report No. 2001-07, 154p.

Kendall, M. G., 1938, A new measure of rank correlation, *Biometrika*, 30, 81–93.

Kendall, M. G., 1975, *Rank Correlation Methods*, Charles Griffin, London.

Ryberg, Karen R.; and Vecchia, Aldo., 2006, *Water-Quality Trend Analysis and Sampling Design for the Devils Lake Basin, North Dakota, January 1965*

through September 2003,U.S. Geological Survey Water Resources Investigations Report 2006-5238.

Sen, P. K., 1968, Estimates of the Regression Coefficient Based on Kendall's Tau, *Journal of the American Statistical Association*, 63, 1379-1389.

Stoner, J.D.;, Lorenz, D.L.; Wiche, G.J.; and Goldstein, R.M., 1993, Red River of the North Basin, Minnesota, North Dakota and South Dakota, *Water Resources Bulletin, v. 29, no.4, p. 575-615.*

Vecchia, A.V., 2000, *Water-quality trend analysis and sampling design for the Souris River, Saskatchewan, North Dakota, and Manitoba, U.S. Geological Survey Water Resources Investigations Report 2000-4019*, 77 p.

Vecchia, Aldo., 2003, *Water-Quality Trend Analysis and Sampling Design for Streams in North Dakota, 1971-2000*, U.S. Geological Survey Water Resources Investigations Report 2003-4094.

Vecchia, Aldo., 2004, *Presentation on using time series analysis to analyze trends in concentration, Statistical techniques for trend and load estimation*, personal communication, Oct. 18-22.

Vecchia, Aldo., 2005, *Water-Quality Trend Analysis and Sampling Design for Streams in the Red River of the North Basin, Minnesota, North Dakota and South Dakota, 1970-2001*, U.S. Geological Survey Water Resources Investigations Report 2005-5224.

Appendix A

Figures

A.1 Boxplots of Constituents

The following figures are the boxplots of the selected constituents at all three monitoring stations: Emerson, South Floodway and Selkirk. These boxplots show the five-number summaries of the data. The tails extend to the maximum and minimum value of our data, while the box encompasses the middle 50% of our data.

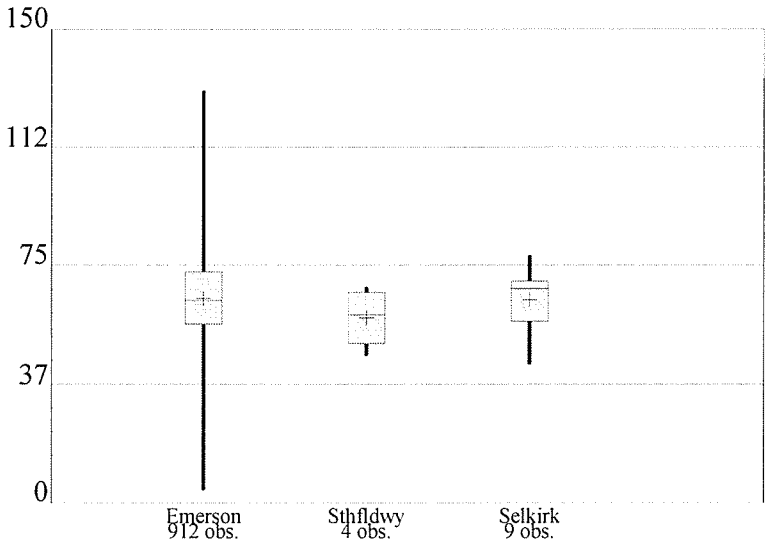

Figure A.1: Boxplot of dissolved Calcium (mg/l) depicting the five number summary of the constituent

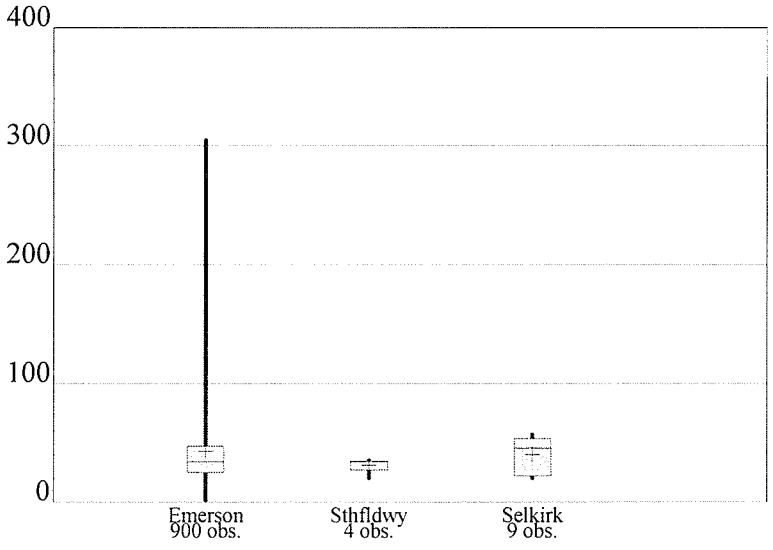

Figure A.2: Boxplot of Dissolved Sodium (mg/l) depicting the five number summary of the constituent

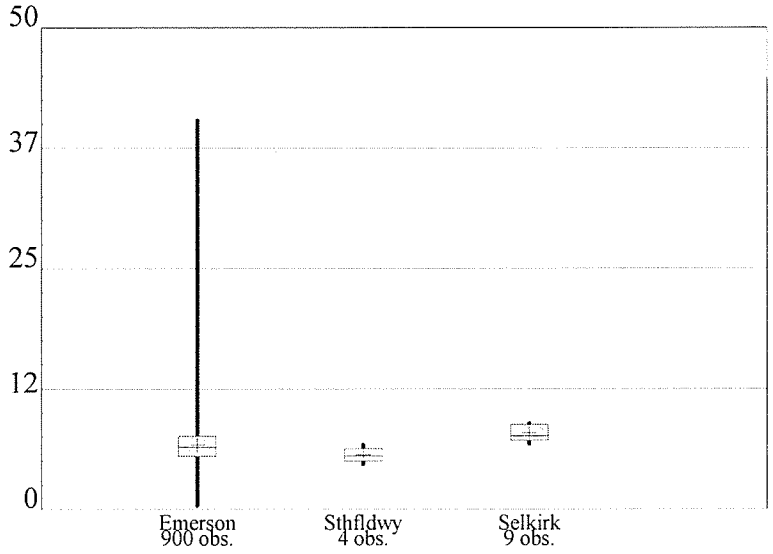

Figure A.3: Boxplot of Dissolved Potassium (mg/l) depicting the five number summary of the constituent

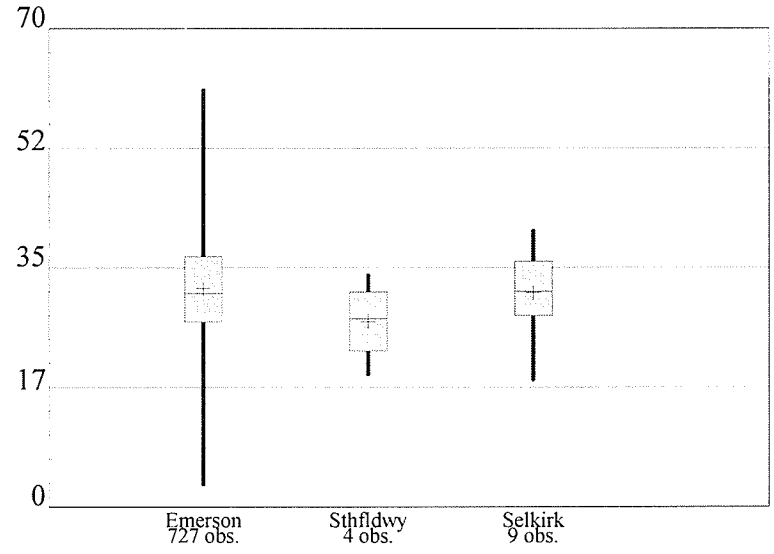

Figure A.4: Boxplot of Dissolved Magnesium (mg/l) depicting the five number summary of the constituent

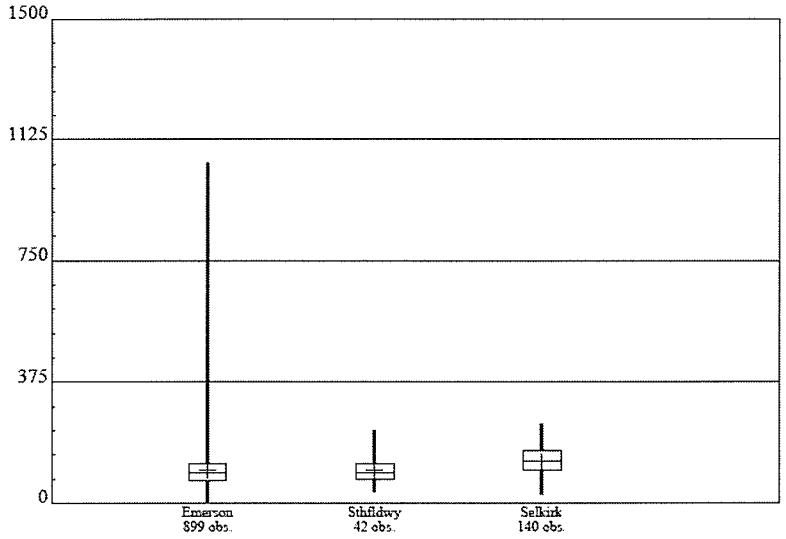

Figure A.5: Boxplot of Dissolved Sulphate (mg/l) depicting the five number summary of the constituent

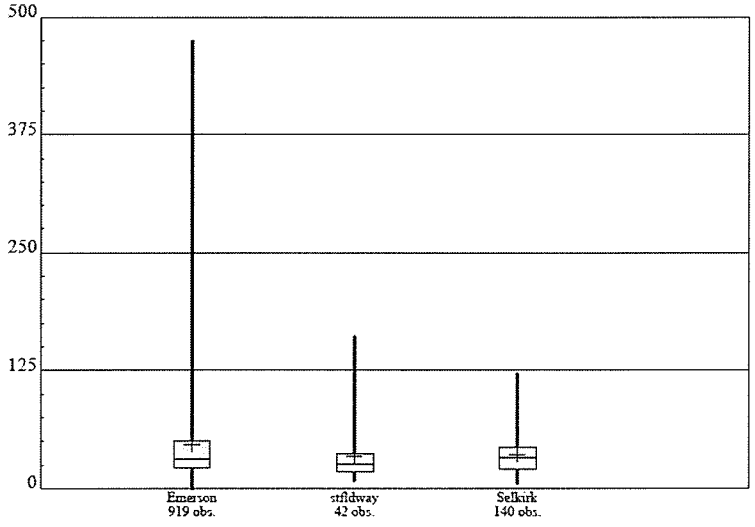

Figure A.6: Boxplot of Dissolved Chloride (mg/l) depicting the five number summary of the constituent

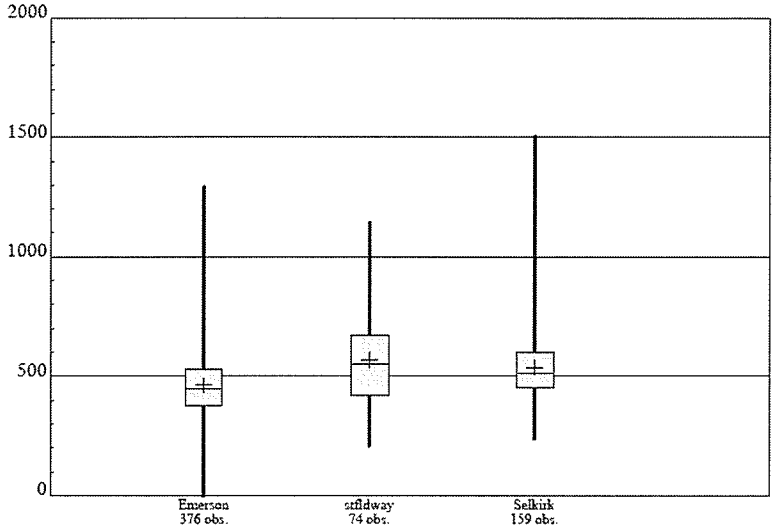

Figure A.7: Boxplot of Total Dissolved Solids (mg/l) depicting the five number summary of the constituent

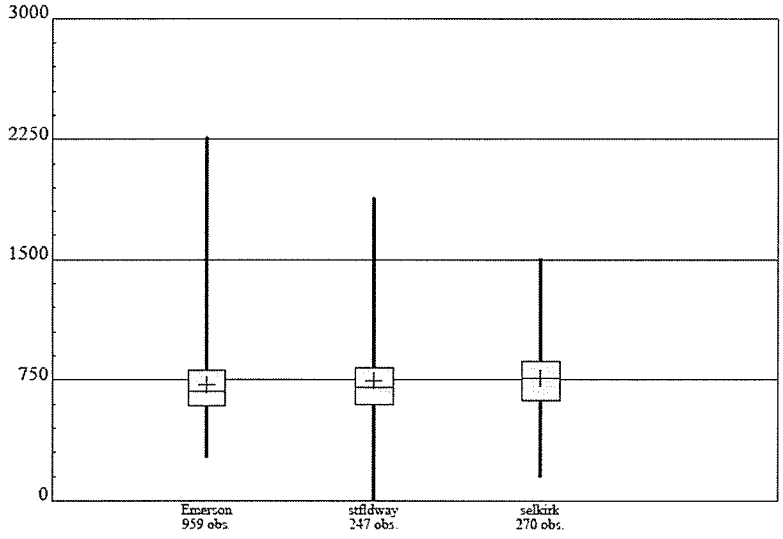

Figure A.8: Boxplot of Specific Conductance (μS/cm) depicting the five number summary of the constituent

A.2 Seasonal Boxplots

The following figures are the seasonal boxplots of the selected constituents at all three monitoring stations: Emerson, South Floodway and Selkirk. These boxplots show the seasonal patterns of the constituents defined by their "hydrologic seasons."

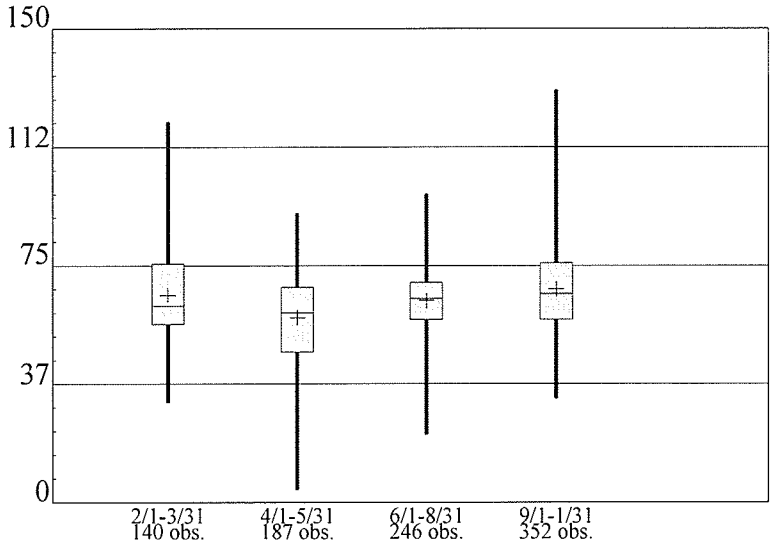

Figure A.9: Seasonality pattern of Dissolved Calcium (mg/l) depicting the seasonal pattern of the constituent amongst all three monitoring stations

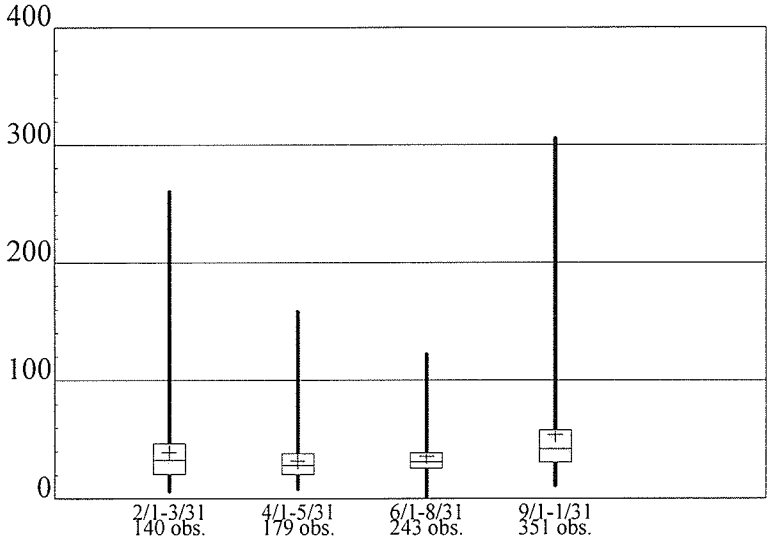

Figure A.10: Seasonality pattern of Dissolved Sodium (mg/l) depicting the seasonal pattern of the constituent amongst all three monitoring stations

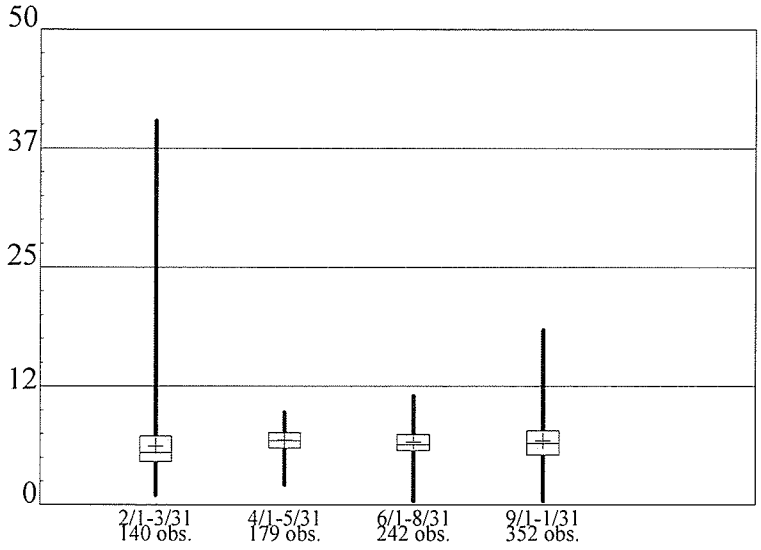

Figure A.11: Boxplots of Dissolved Potassium (mg/l) depicting the seasonal pattern of the constituent amongst all three monitoring stations

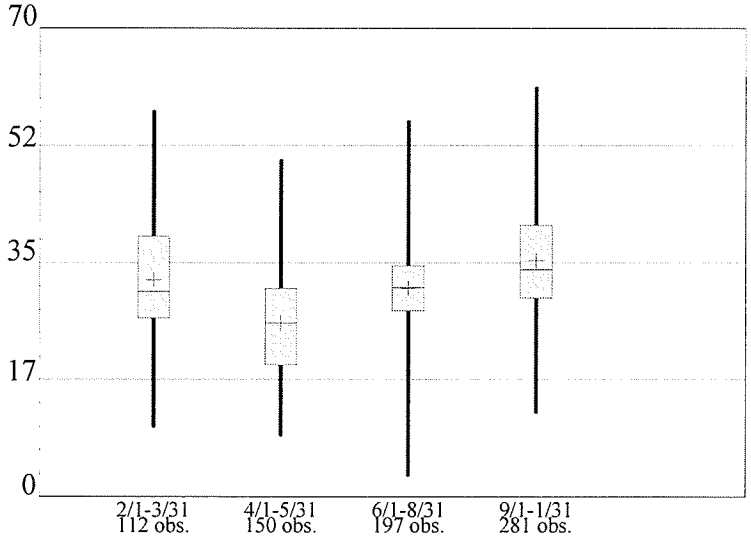

Figure A.12: Seasonality pattern of Dissolved Magnesium (mg/l) depicting the seasonal pattern of the constituent amongst all three monitoring stations

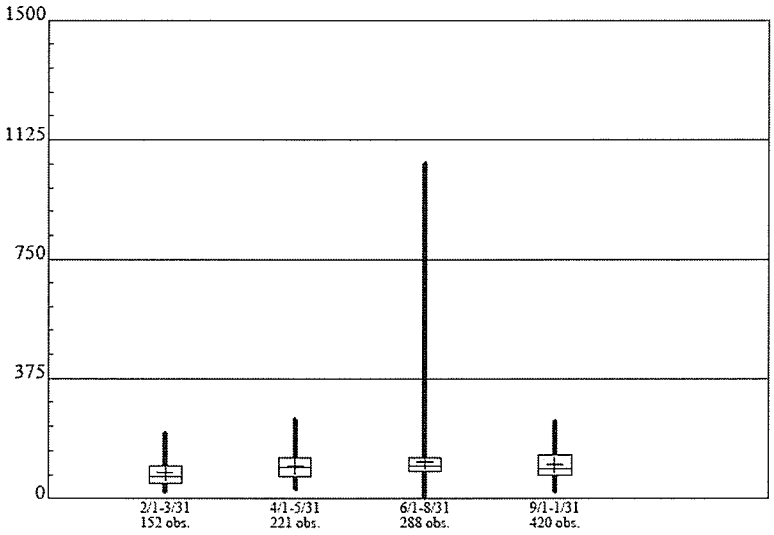

Figure A.13: Seasonality pattern of Dissolved Sulphate (mg/l) depicting the seasonal pattern of the constituent amongst all three monitoring stations

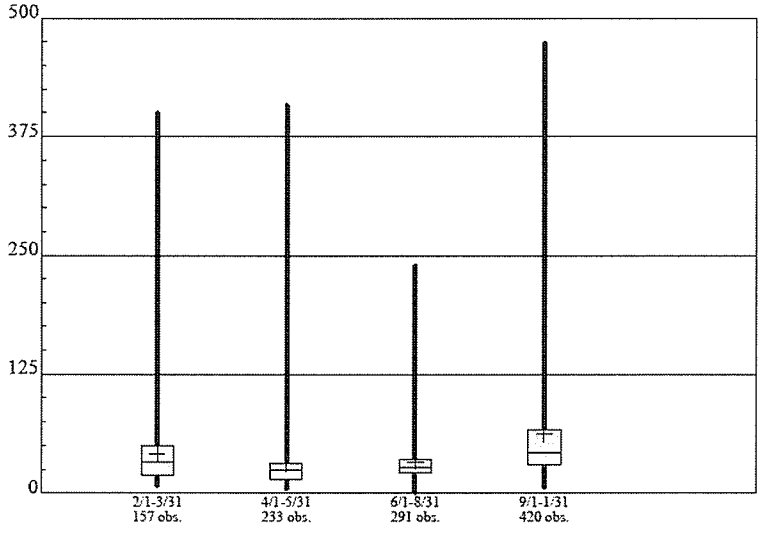

Figure A.14: Seasonality pattern of Dissolved Chloride (mg/l) depicting the seasonal pattern of the constituent amongst all three monitoring stations

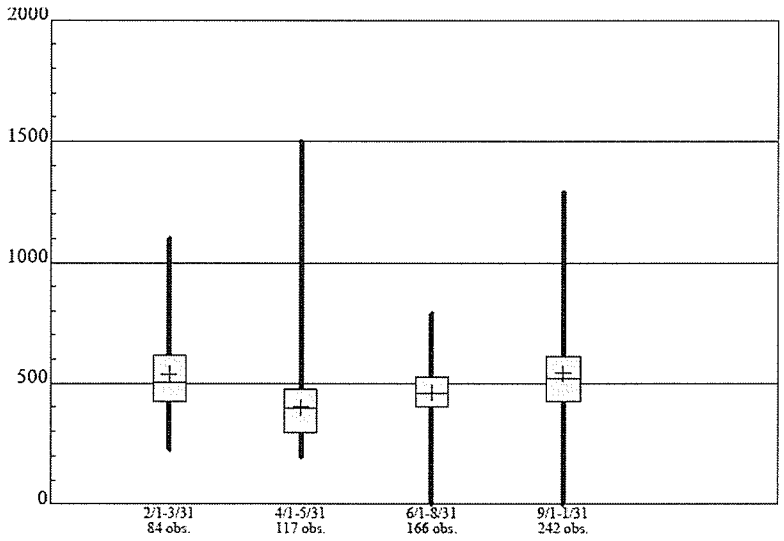

Figure A.15: Seasonality pattern of Total Dissolved Solids (mg/l) depicting the seasonal pattern of the constituent amongst all three monitoring stations

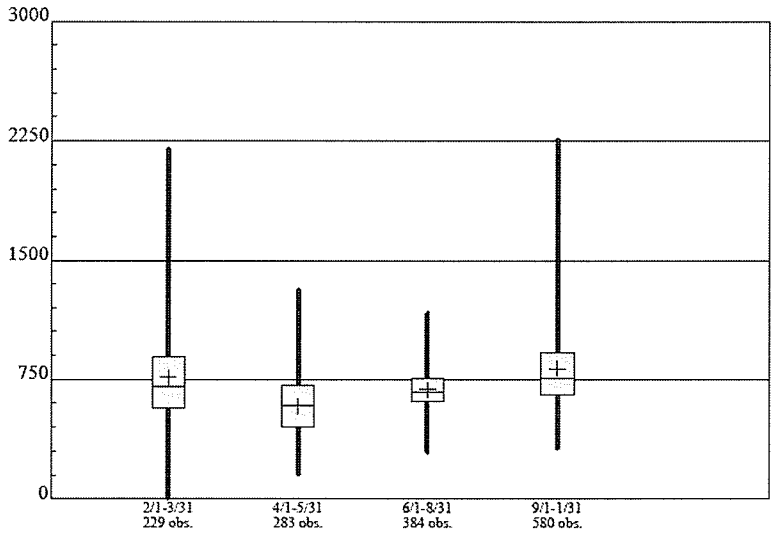

Figure A.16: Seasonality pattern of Specific Conductance (μS/cm) depicting the seasonal pattern of the constituent amongst all three monitoring stations

A.3 Non-Parametric Trend Results

The following figures depict the long term temporal trend of each constituent at each monitoring station. These were calculated using the Mann-Kendall Test and Sen's slope.

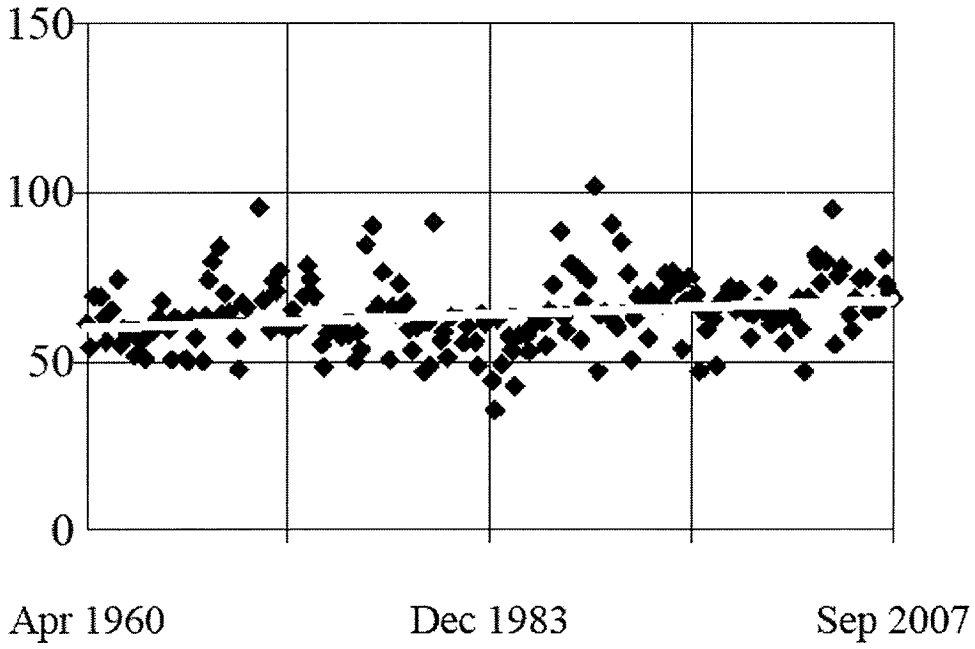

Figure A.17: Long term temporal trend of dissolved calcium (mg/l) at the Emerson monitoring station

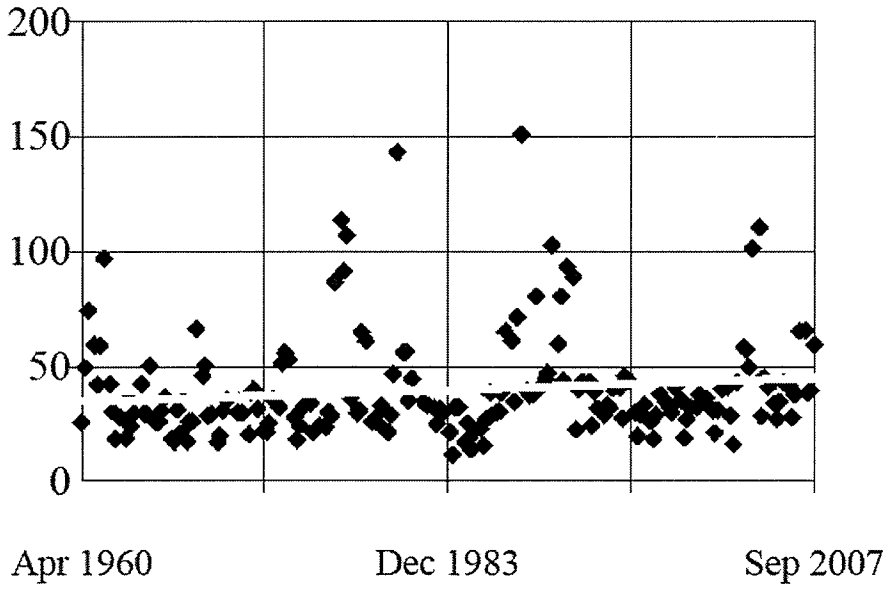

Figure A.18: Long term temporal trend of dissolved sodium (mg/l) at Emerson

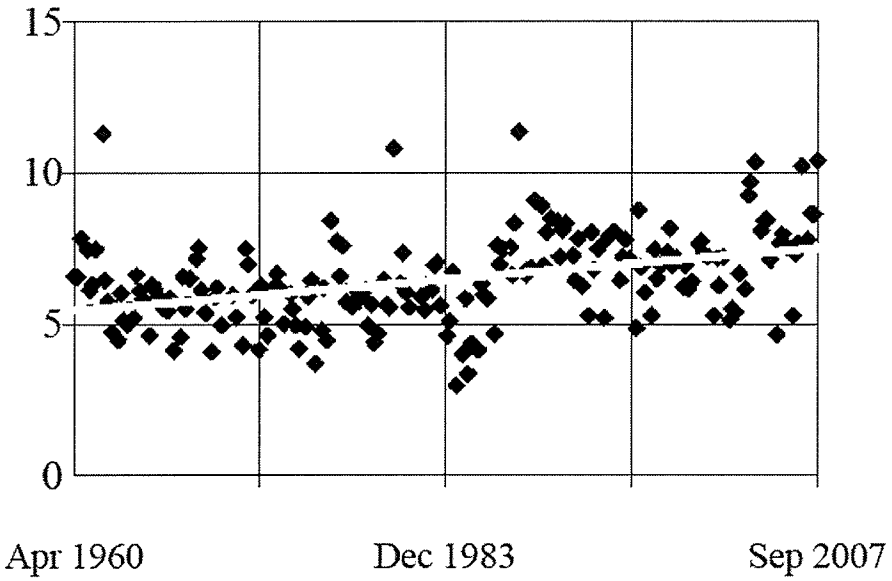

Figure A.19: Long term temporal trend of dissolved potassium (mg/l) at Emerson

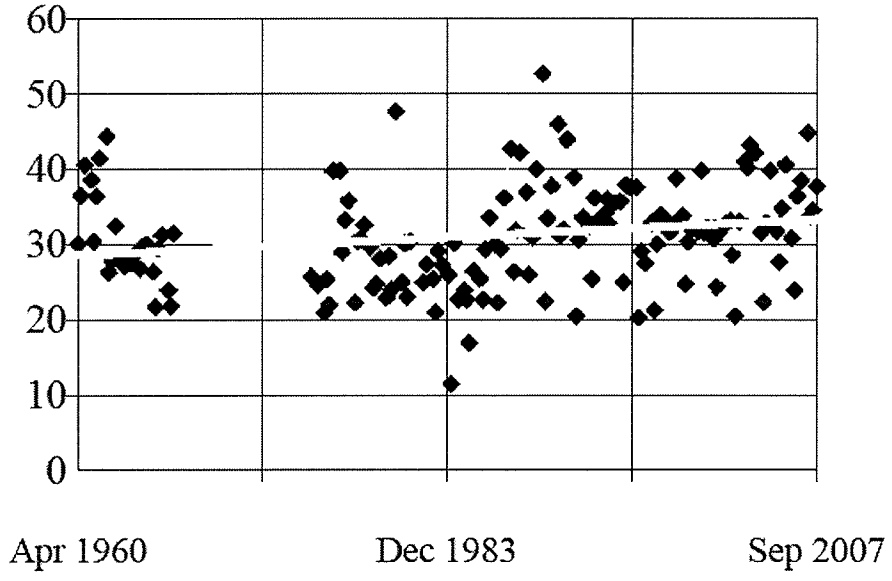

Figure A.20: Long term temporal trend of dissolved magnesium (mg/l) at Emerson

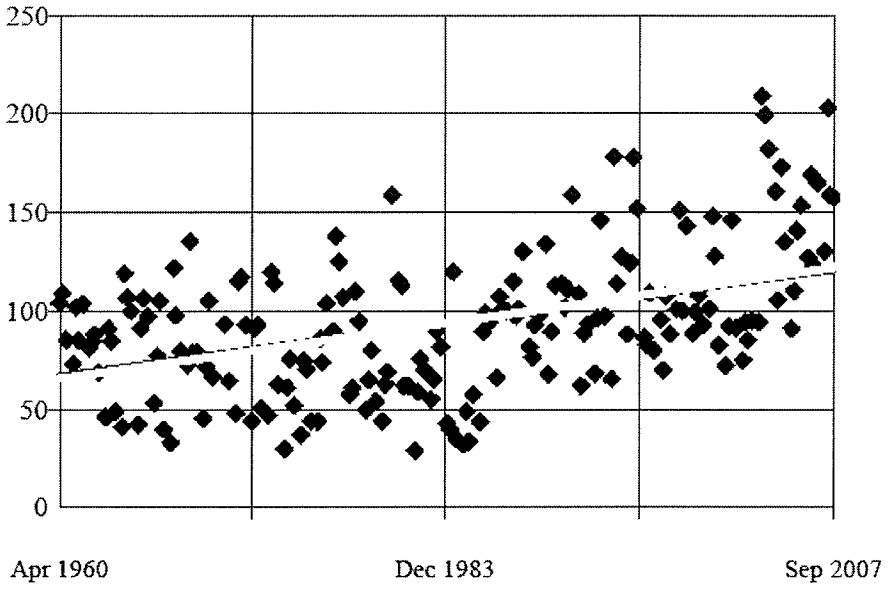

Figure A.21: Long term temporal trend of dissolved sulphate (mg/l) at Emerson

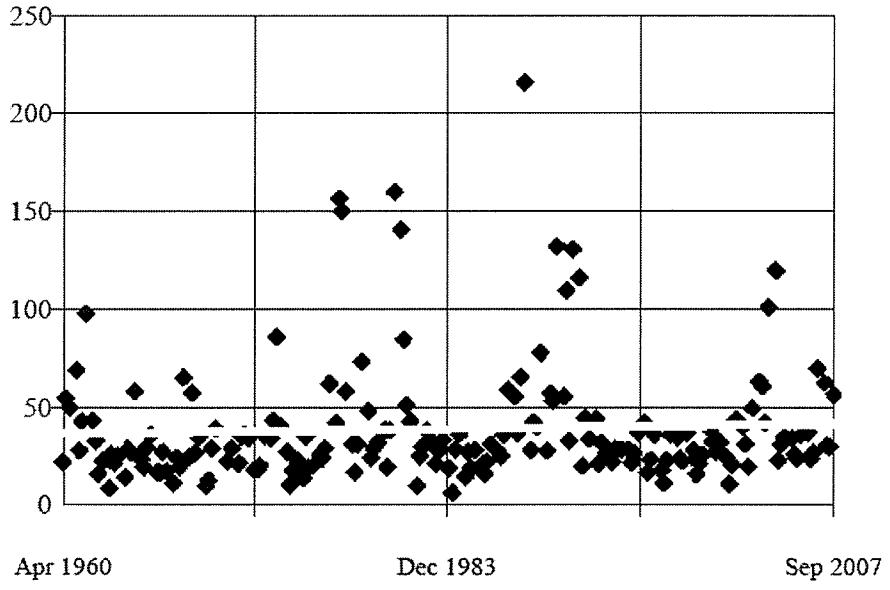

Figure A.22: Long term temporal trend of dissolved chloride (mg/l) at Emerson

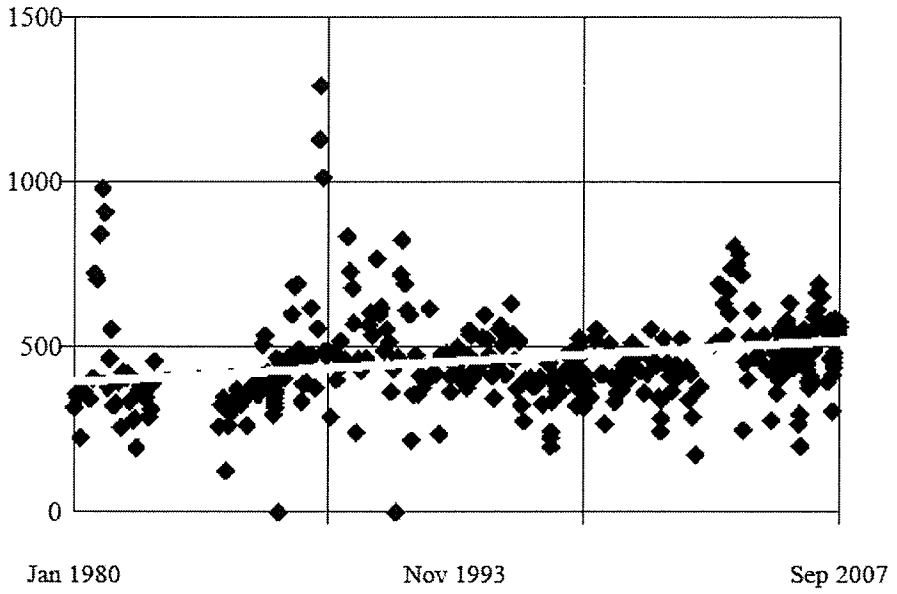

Figure A.23: Long term temporal trend of total dissolved solids (mg/l) at Emerson

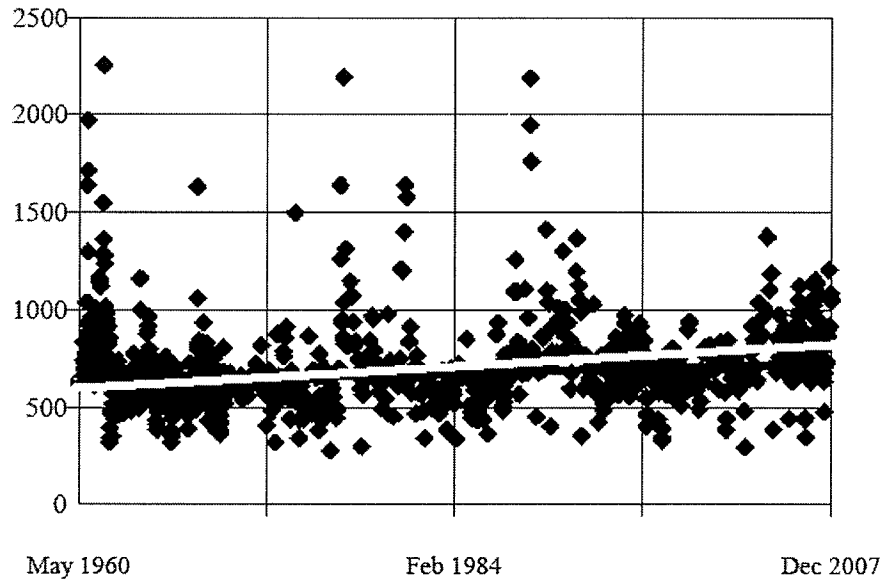

Figure A.24: Long term temporal trend of specific conductance (μS/cm) at Emerson

A.3.1 South Floodway at St. Norbert Monitoring Station

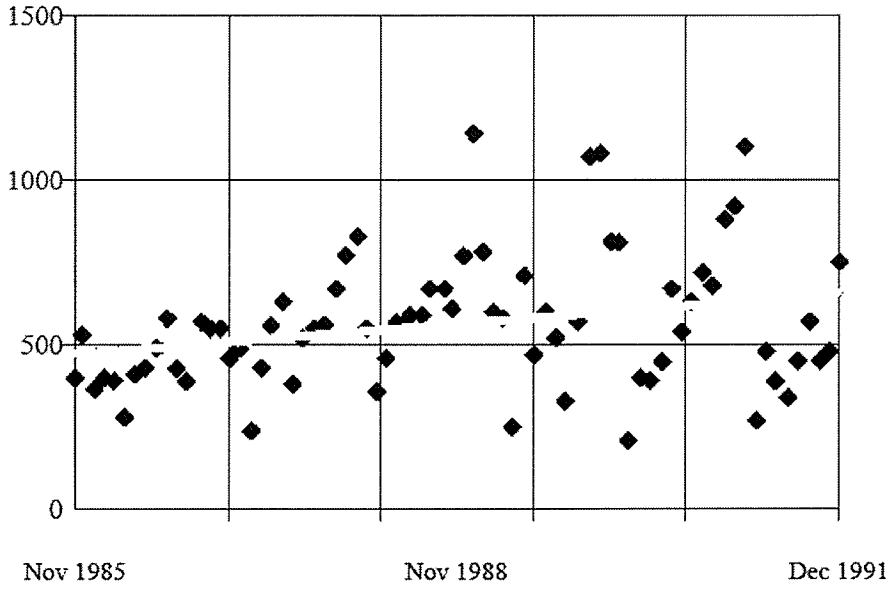

Figure A.25: Long term temporal trend of total dissolved solids (mg/l) at South Floodway

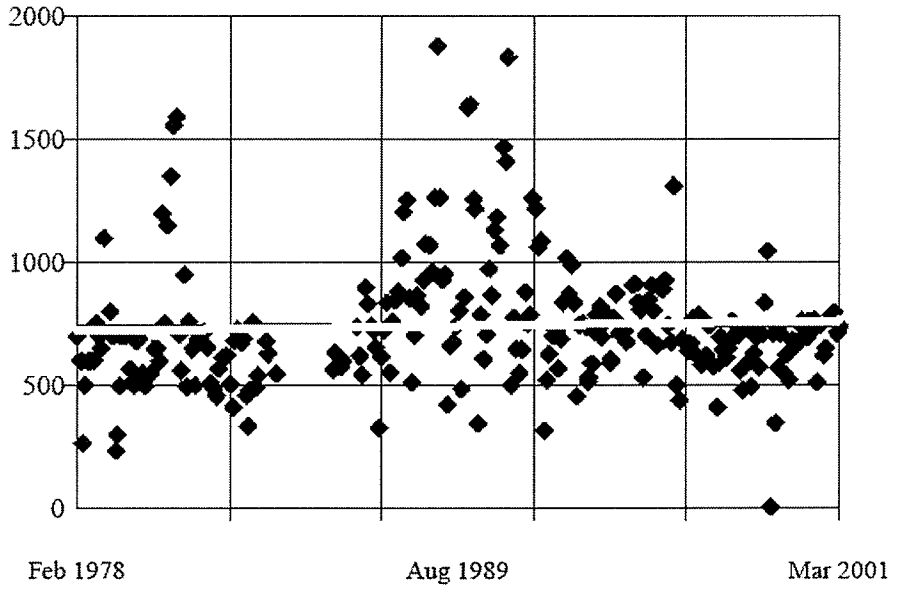

Figure A.26: Long term temporal trend of specific conductance (μS/cm) at South Floodway

A.3.2 Selkirk Monitoring Station

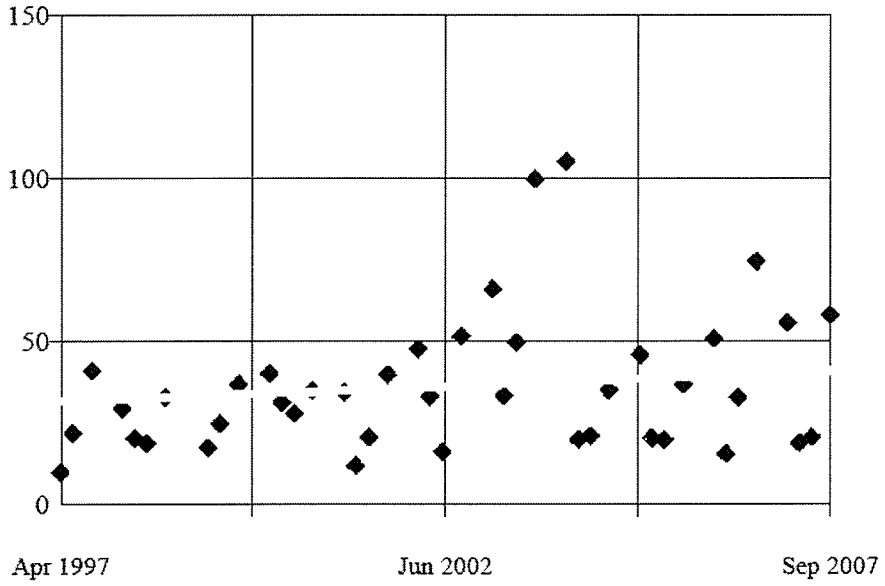

Figure A.27: Long term temporal trend of dissolved chloride (mg/l) at Selkirk

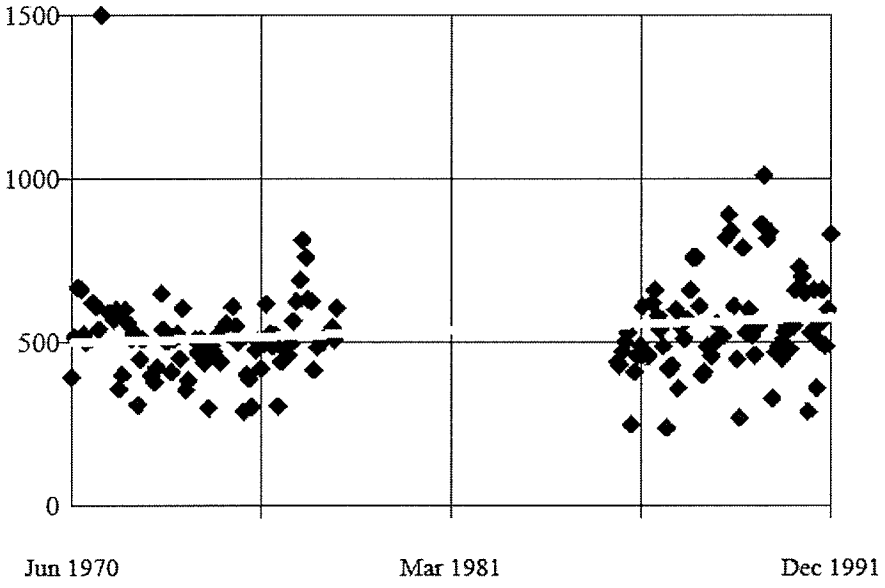

Figure A.28: Long term temporal trend of total dissolved solids (mg/l) at Selkirk

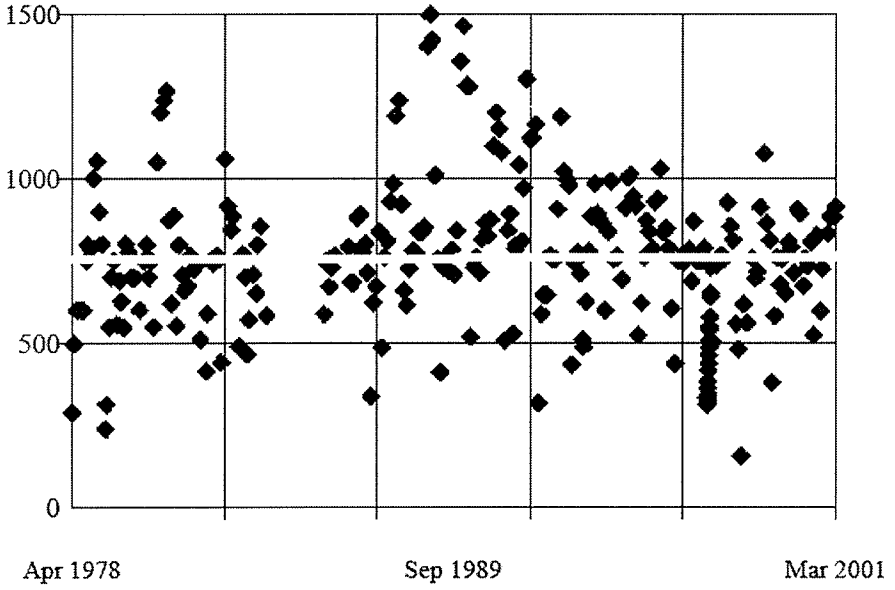

Figure A.29: Long term temporal trend of specific conductance (μS/cm) at Selkirk

A.4 Parametric Trend Results

The following figures depict the raw data of the constituents being used with QWTREND. The figures below pertain only to the Emerson Monitoring Station. The upper plots are the data points while the lower plots depict the number of data points by month.

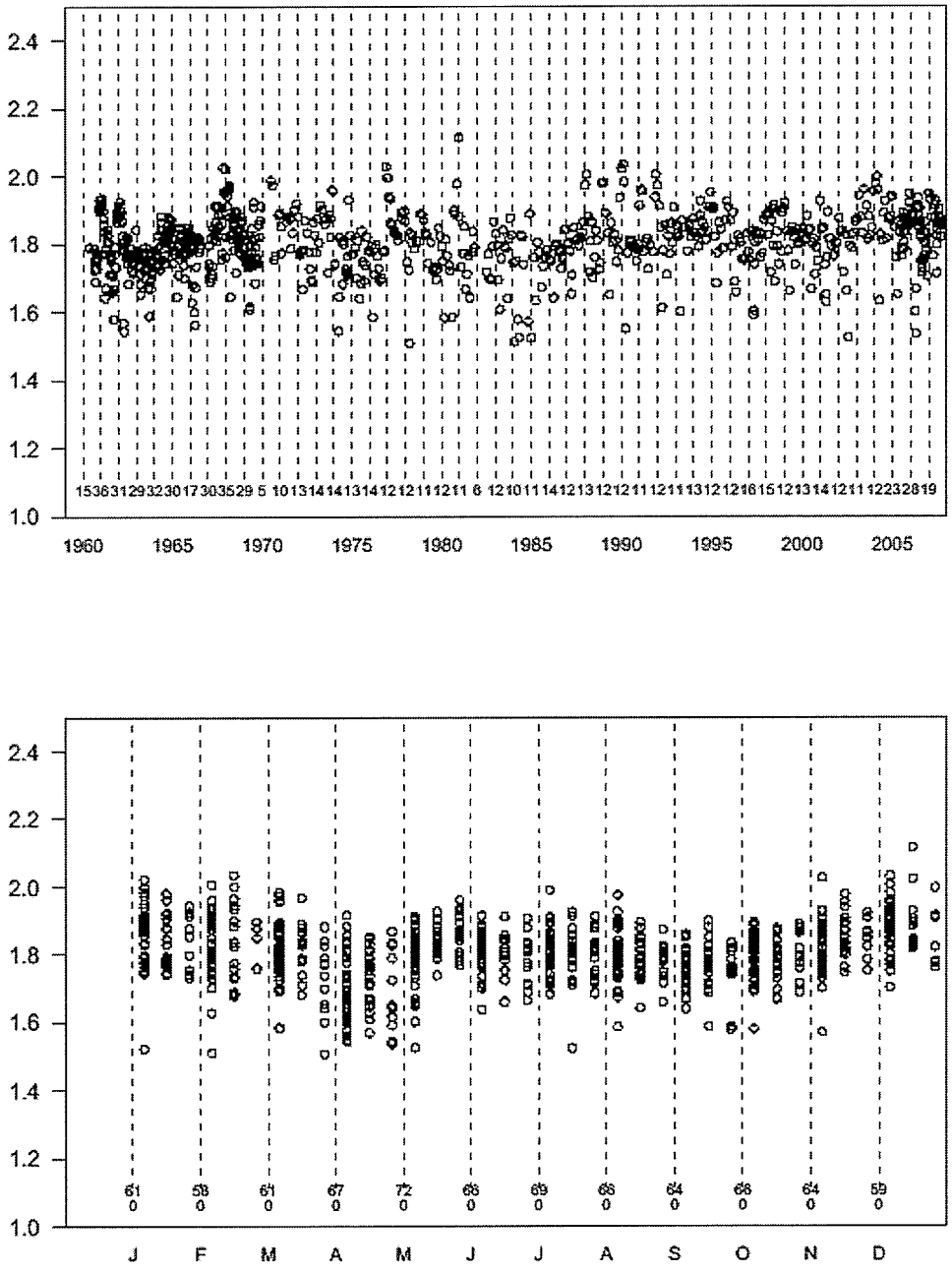

Figure A.30: Dissolved Calcium at Emerson ($\log_{10}$ mg/l)

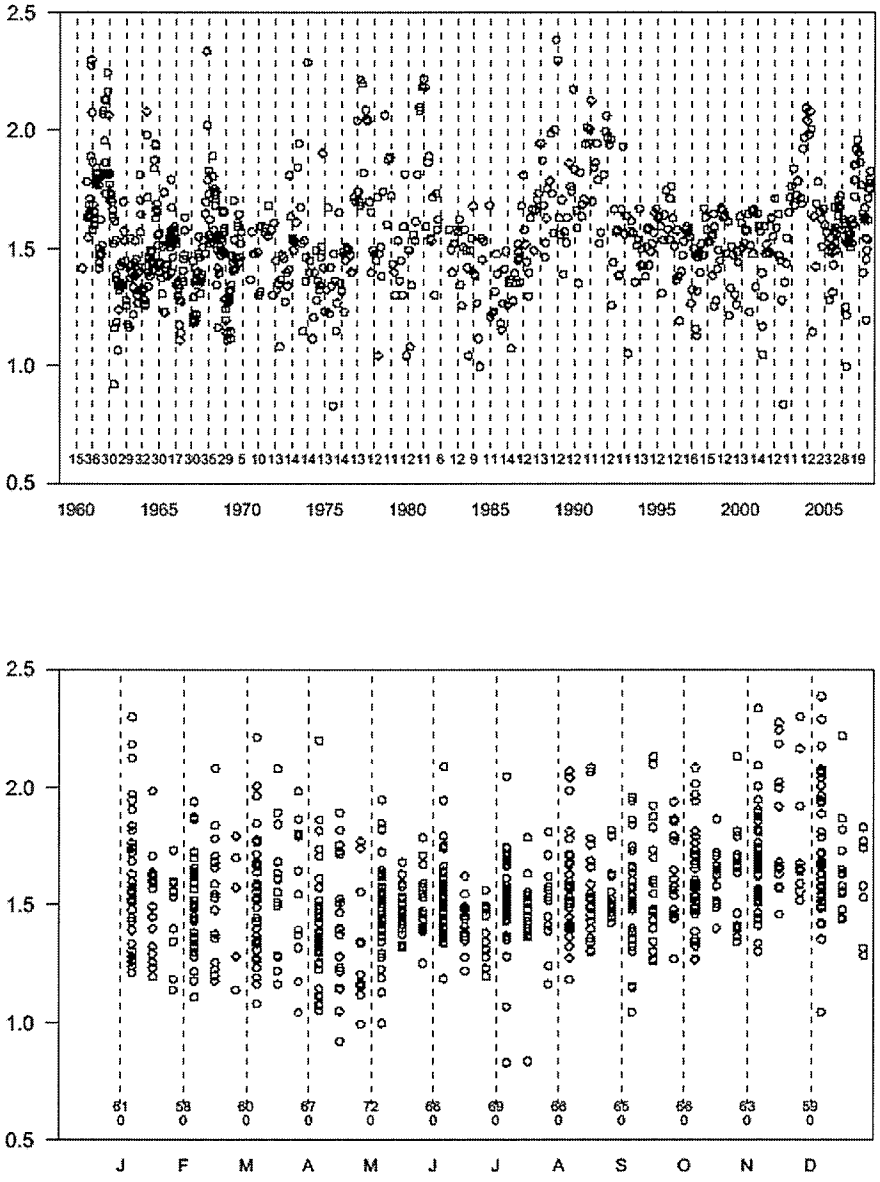

Figure A.31: Dissolved Sodium at Emerson ($\log_{10}$ mg/l)

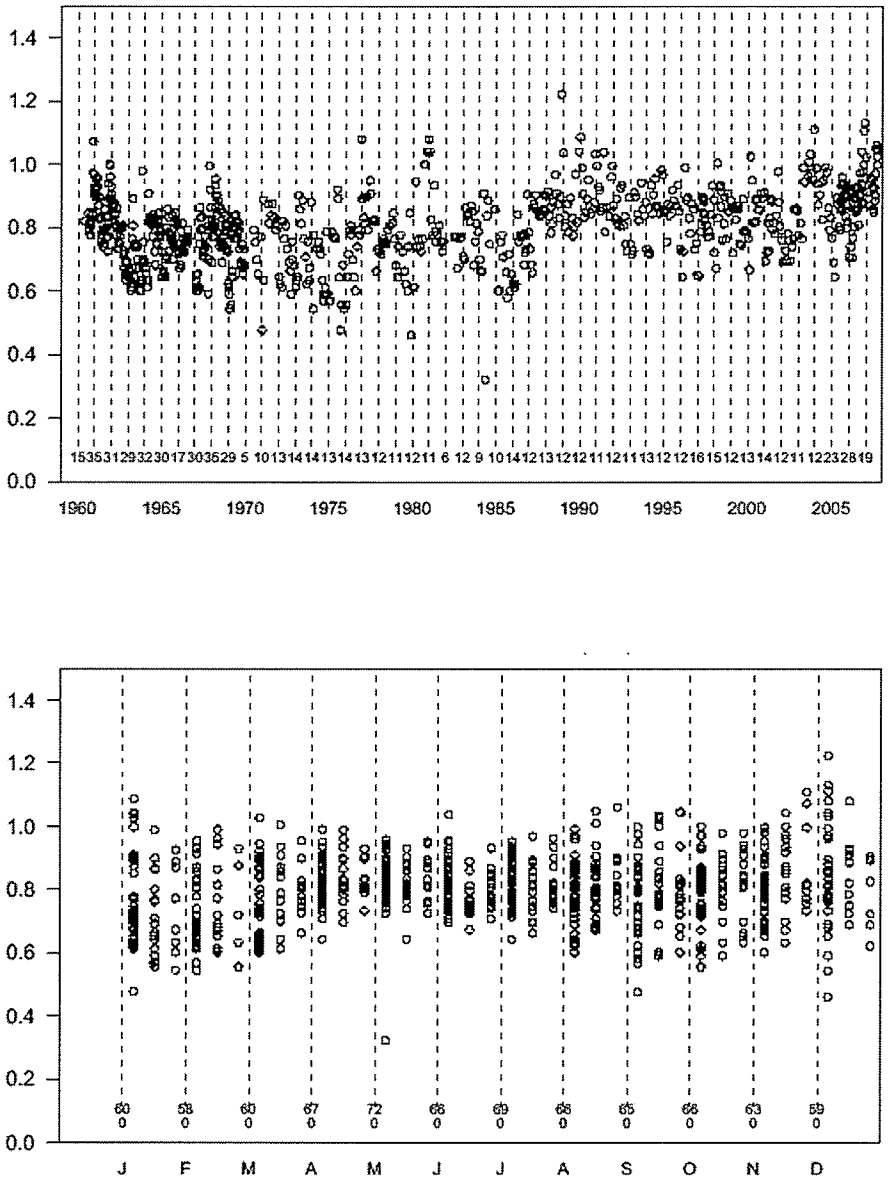

Figure A.32: Dissolved Potassium at Emerson ($\log_{10}$ mg/l)

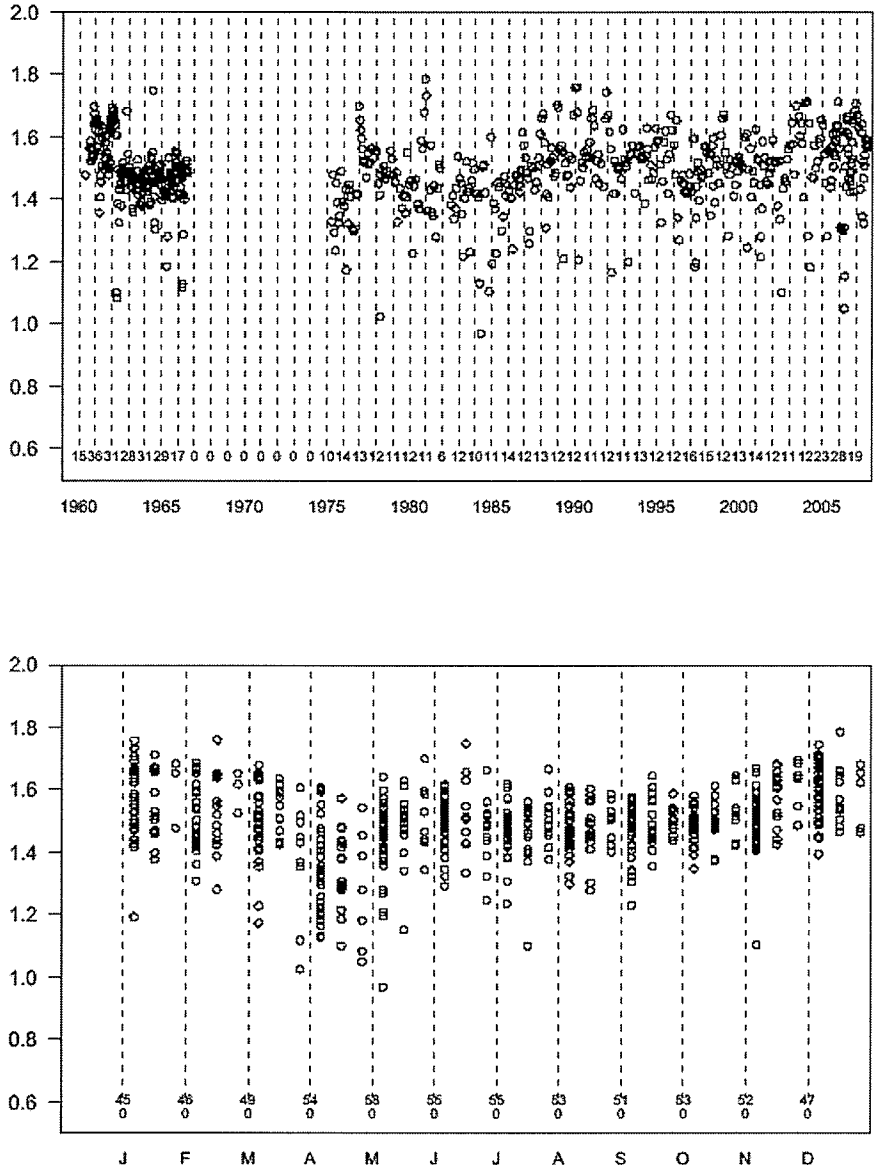

Figure A.33: Dissolved Magnesium at Emerson ($\log_{10}$ mg/l)

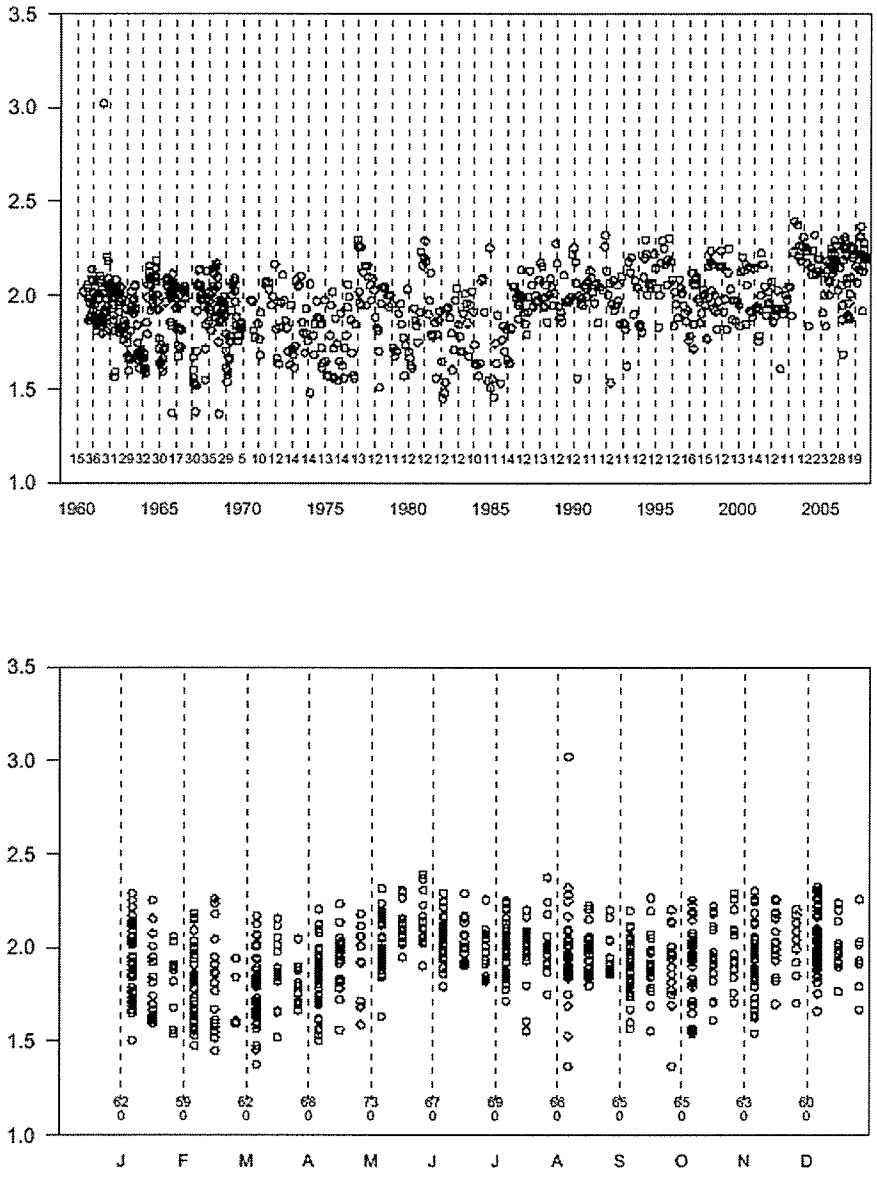

Figure A.34: Dissolved Sulphate at Emerson ($\log_{10}$ mg/l)

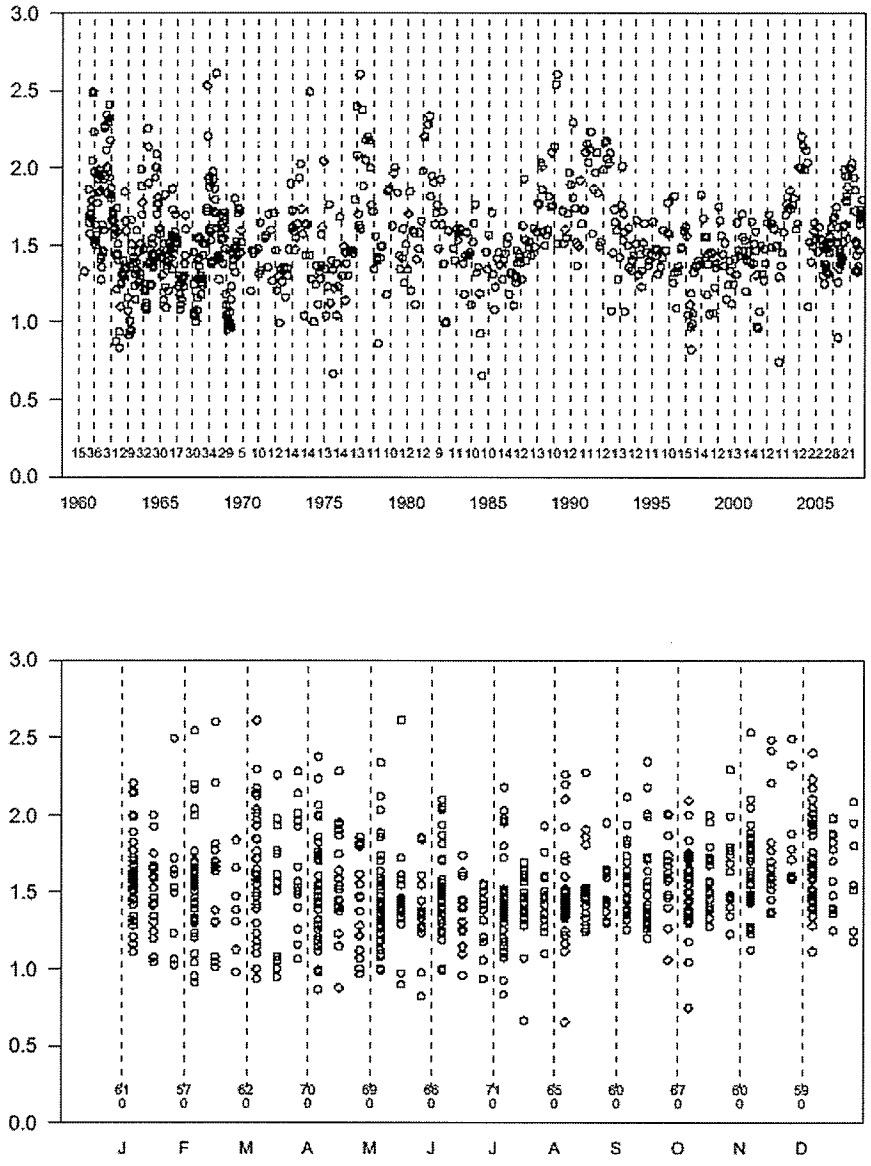

Figure A.35: Dissolved Chloride at Emerson ($\log_{10}$ mg/l)

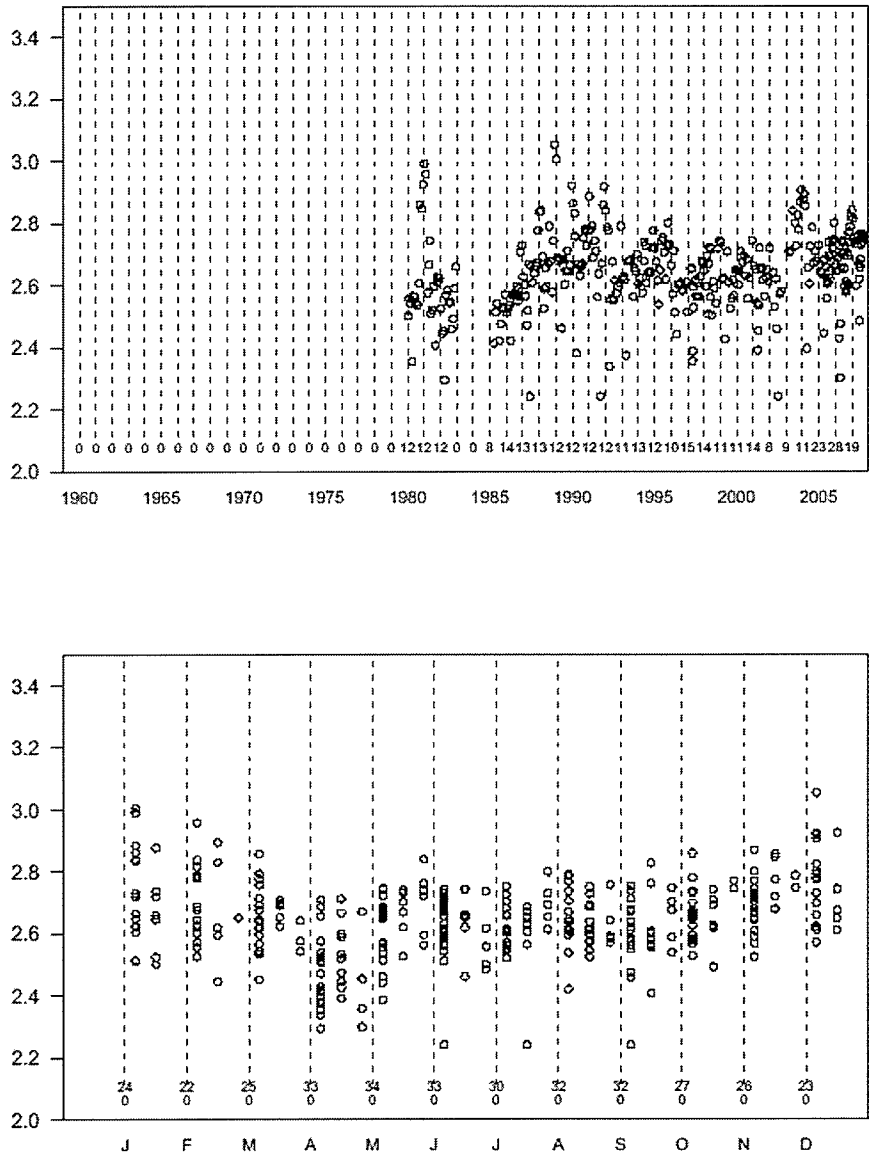

Figure A.36: Total Dissolved Solids at Emerson ($\log_{10}$ mg/l)

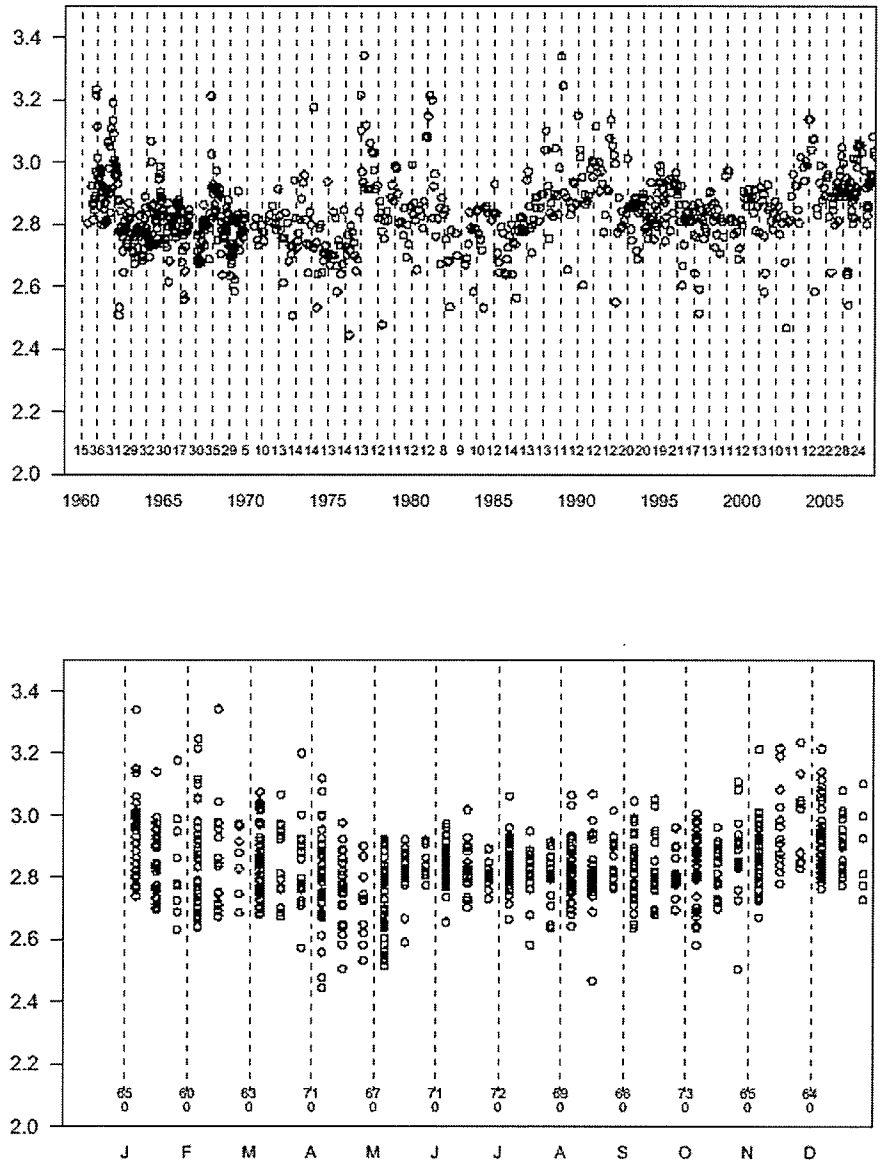

Figure A.37: Specific Conductance at Emerson ($\log_{10}$ USIE/cm)

A.5 Flow Adjustment Plots

The following sequence of plots (Figures A.38–A.83) show the streamflow related anomaly (plus trend); the seasonally adjusted and de-trended data and annual streamflow anomalies; the seasonally adjusted and flow adjusted data (with flat trend line); and the residual plots for the following constituents: dissolved calcium, dissolved sodium, dissolved potassium, dissolved magnesium, dissolved sulphate, dissolved chloride, total dissolved solids and specific conductance. These provide a baseline for further examinations of trends as discussed in the text.

A.5.1 Emerson Monitoring Station

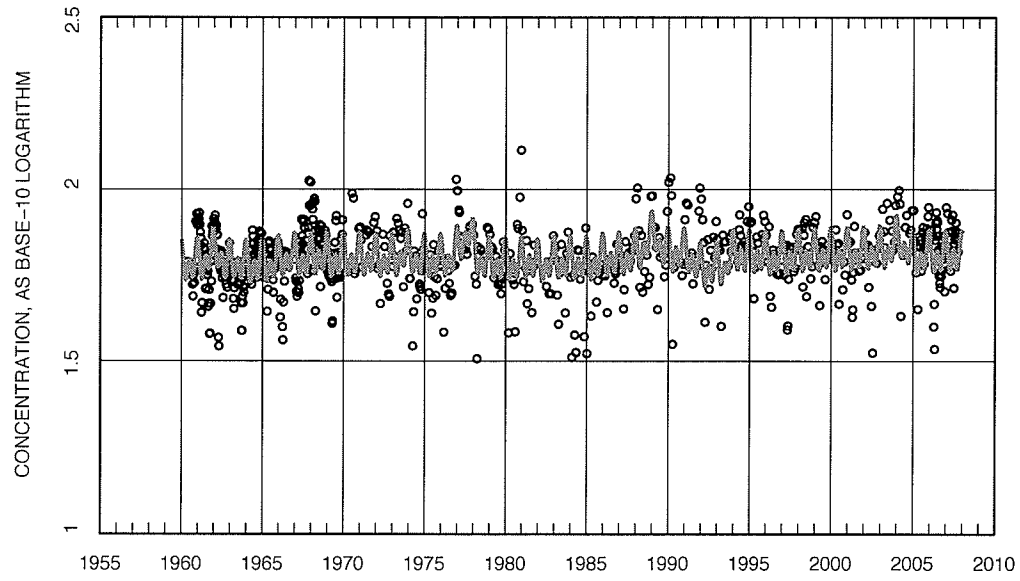

Figure A.38: Dissolved Calcium concentrations (points) and streamflow related anomaly + trend (line)

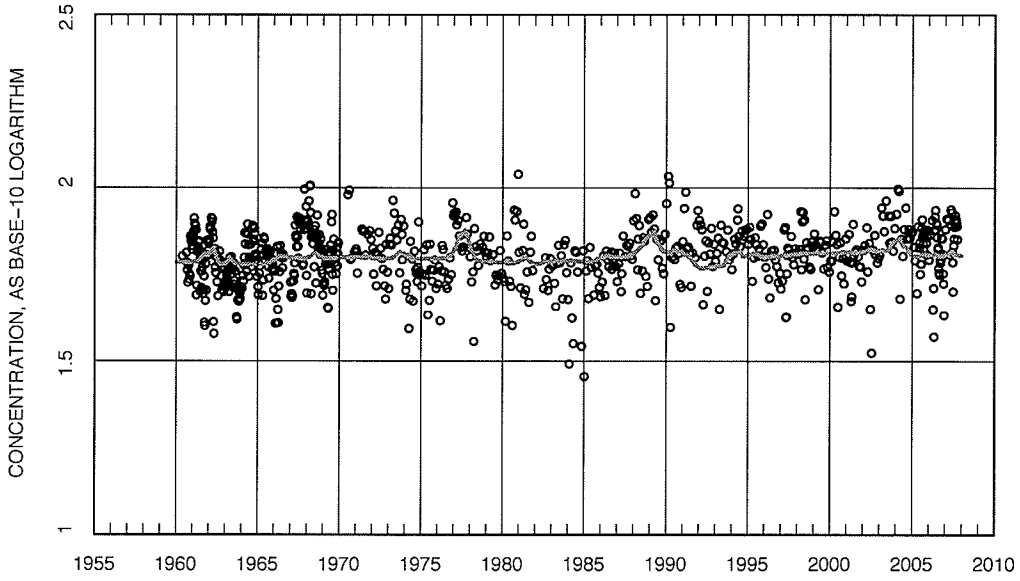

Figure A.39: Dissolved Calcium Flow Adjustments — Seasonally adjusted and detrended data (points) and annual streamflow-related anomaly (line).

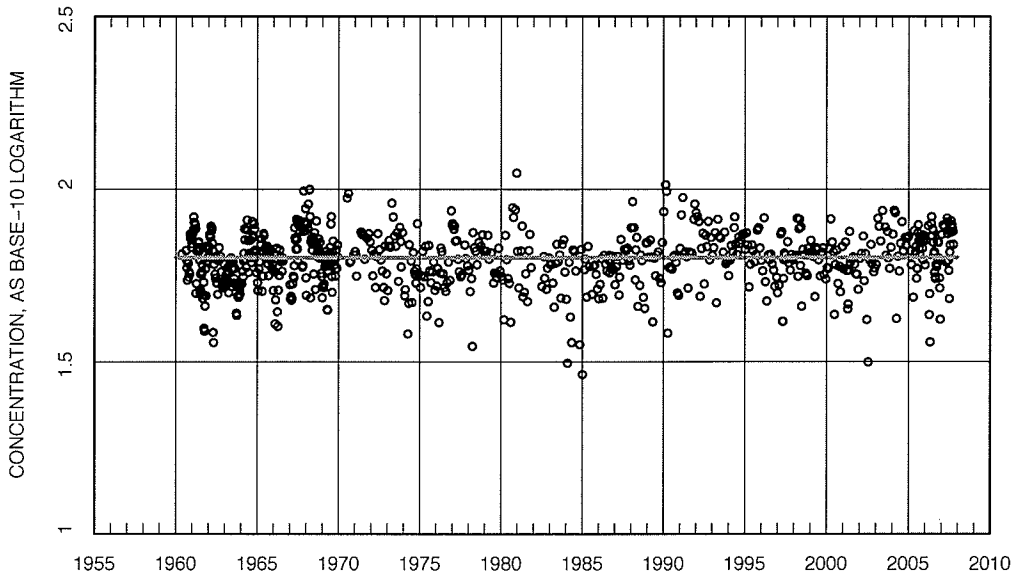

Figure A.40: Dissolved Calcium Flow Adjustments — Seasonally adjusted and flow adjusted data (points) and no-trend (line).

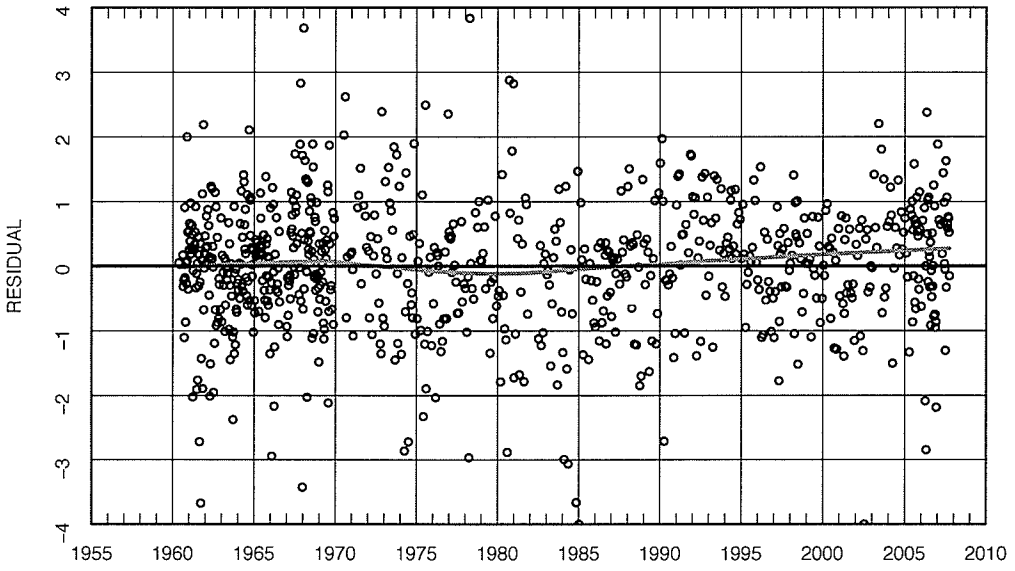

Figure A.41: Dissolved Calcium Flow Adjustments — Parametric no-trend model residuals (points) and lowess smooth line with $F = 0.5$.

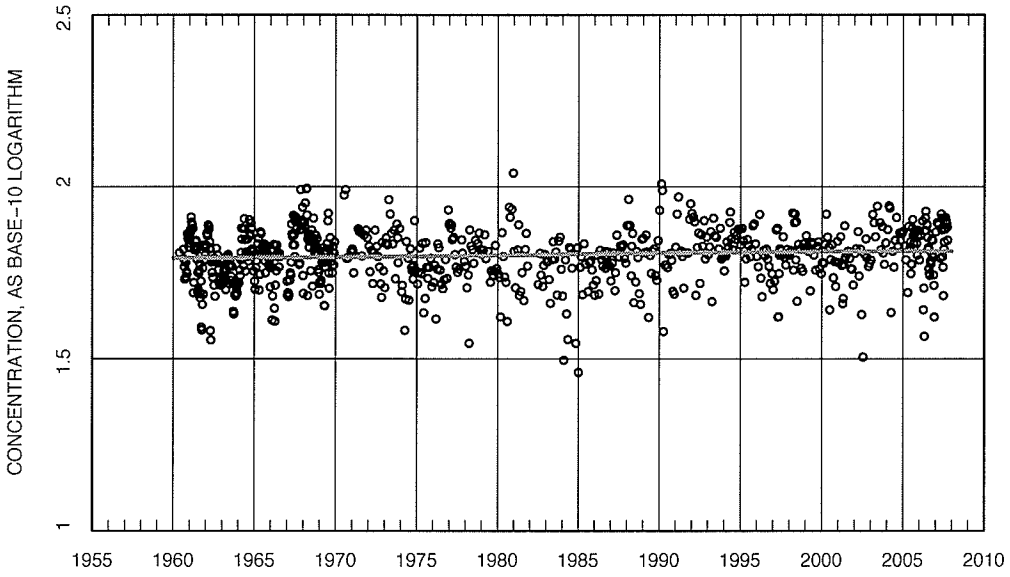

Figure A.42: Dissolved Calcium Flow Adjustments — Seasonally adjusted and flow adjusted data (points) and single trend (line).

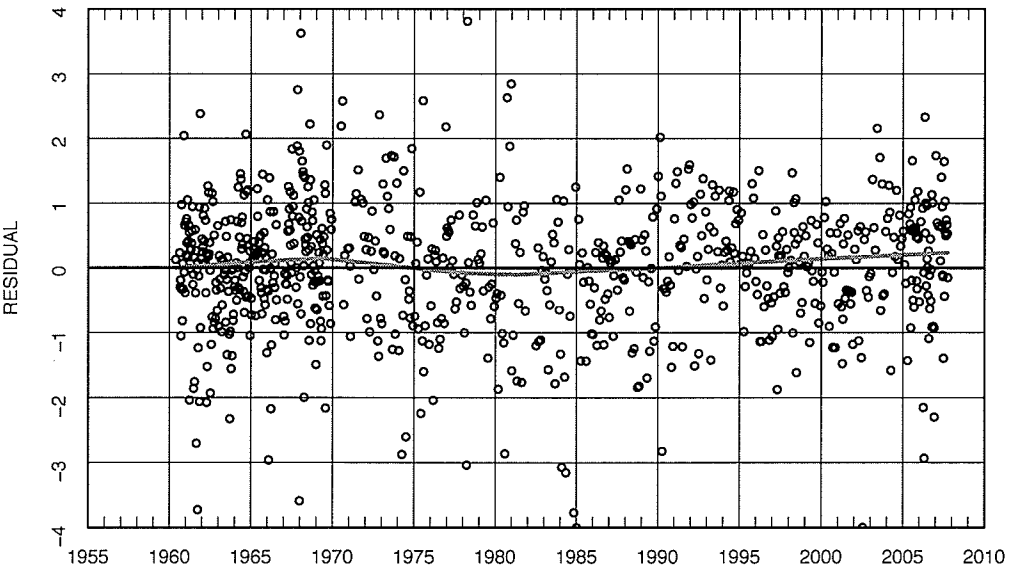

Figure A.43: Dissolved Calcium Flow Adjustments — Parametric single trend model residuals (points) and lowess smooth line with $F = 0.5$.

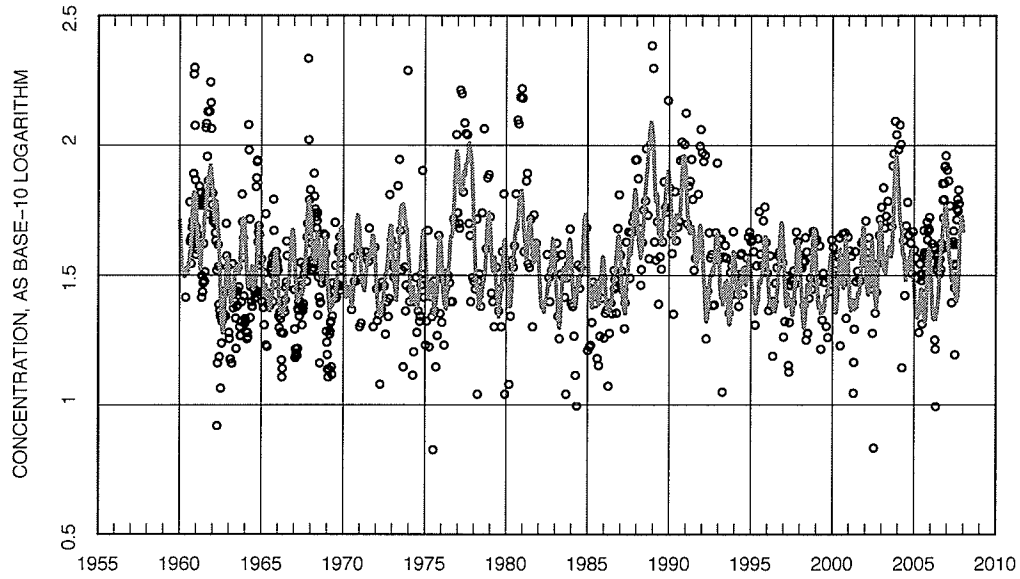

Figure A.44: Dissolved Sodium concentrations (points) and streamflow related anomaly + trend (line)

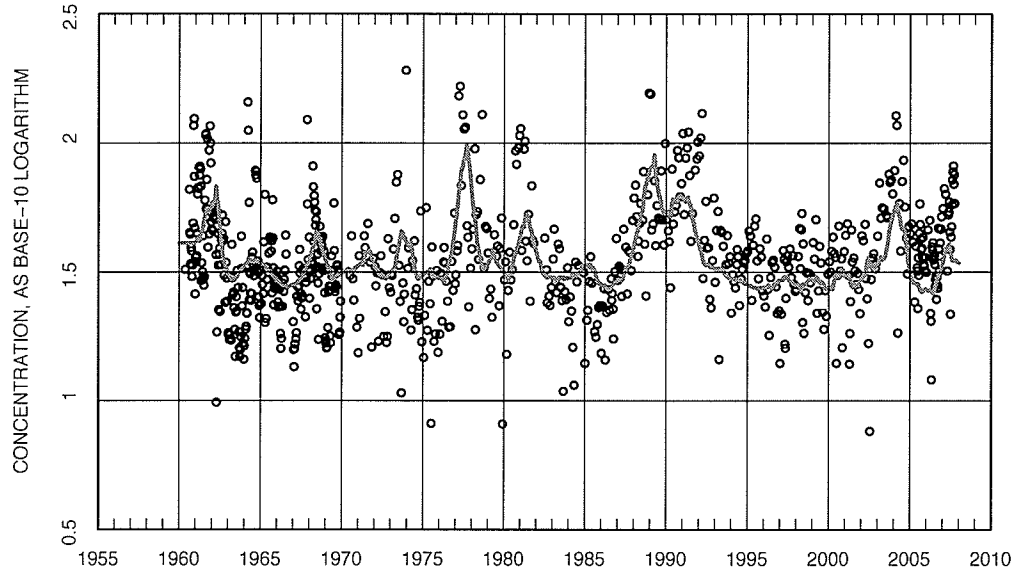

Figure A.45: Dissolved Sodium Flow Adjustments — Seasonally adjusted and detrended data (points) and annual streamflow-related anomaly (line).

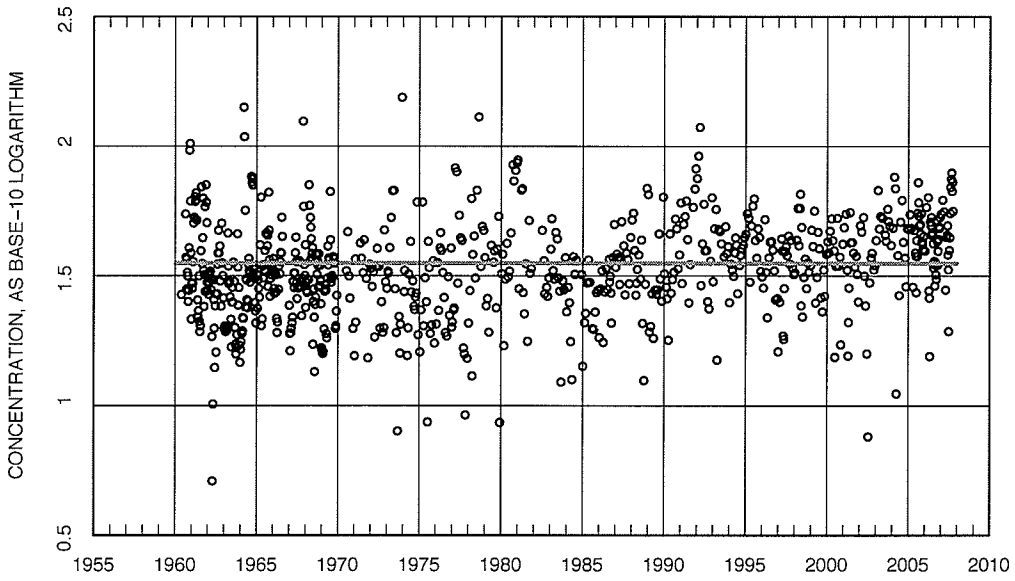

Figure A.46: Dissolved Sodium Flow Adjustments — Seasonally adjusted and flow adjusted data (points) and no-trend (line).

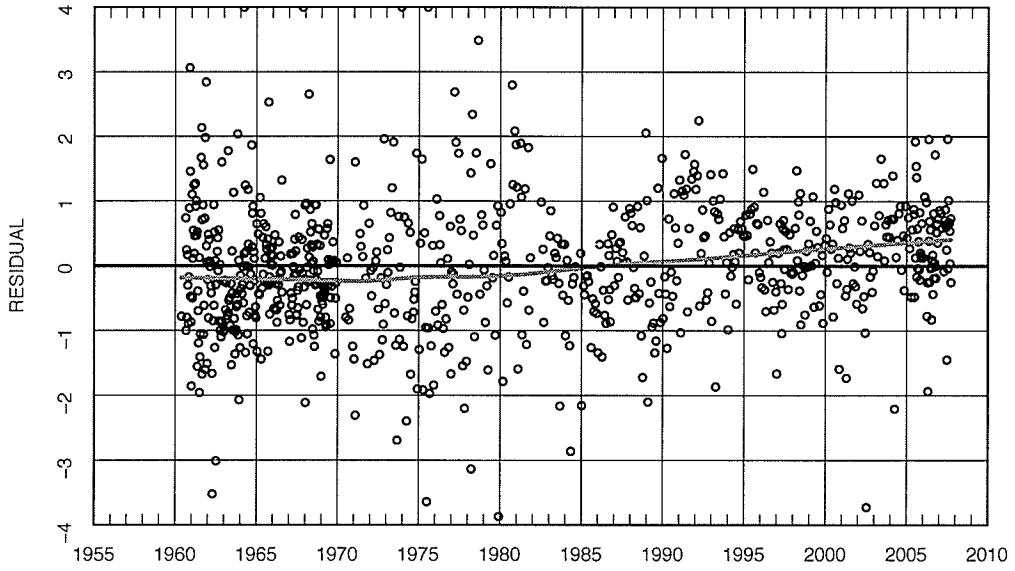

Figure A.47: Dissolved Sodium Flow Adjustments — Parametric no-trend model residuals (points) and lowess smooth line with $F = 0.5$.

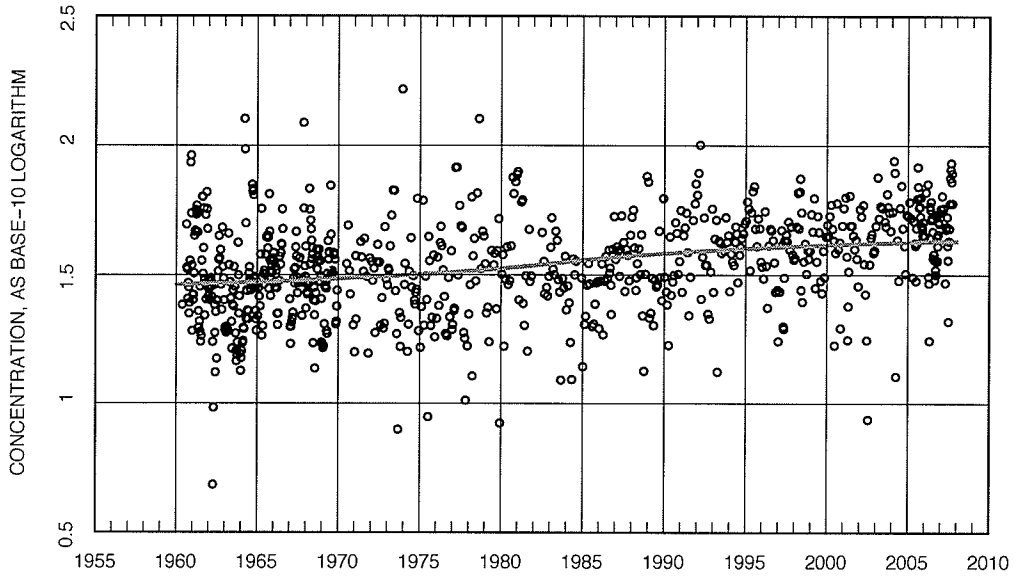

Figure A.48: Dissolved Sodium Flow Adjustments — Seasonally adjusted and flow adjusted data (points) and single trend (line).

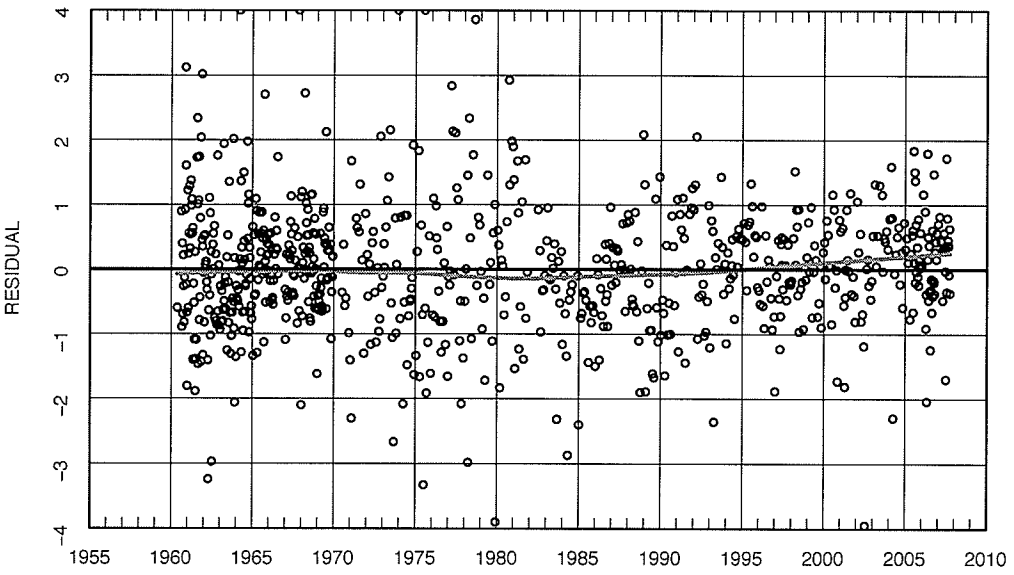

Figure A.49: Dissolved Sodium Flow Adjustments — Parametric single trend model residuals (points) and lowess smooth line with $F = 0.5$.

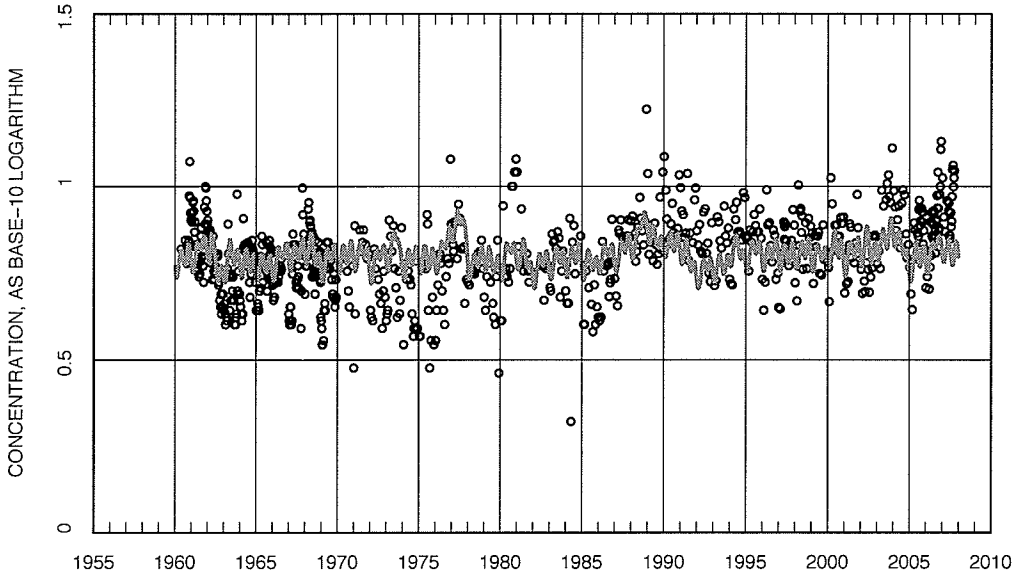

Figure A.50: Dissolved Potassium concentrations (points) and streamflow related anomaly + trend (line)

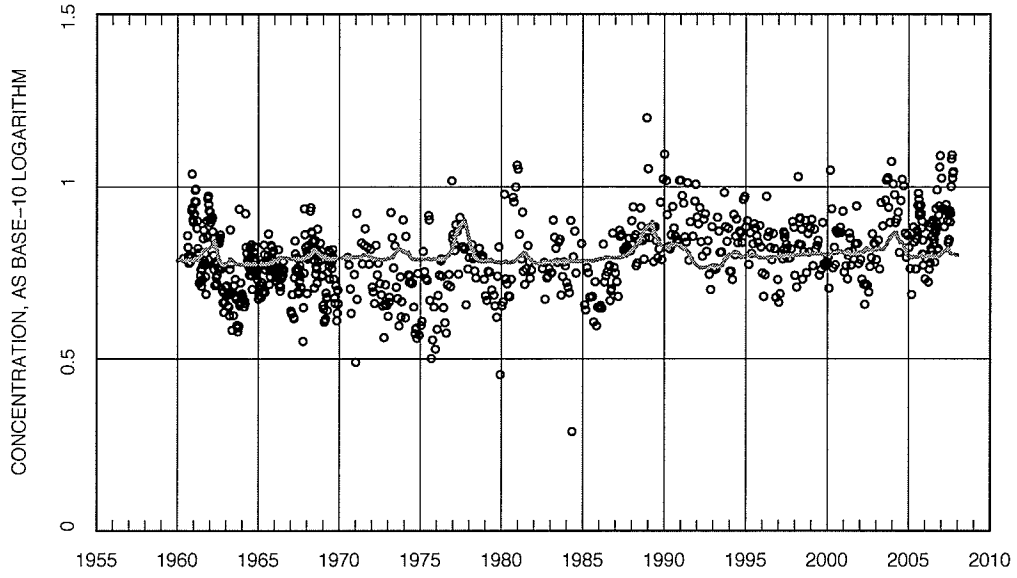

Figure A.51: Dissolved Potassium Flow Adjustments — Seasonally adjusted and de-trended data (points) and annual streamflow-related anomaly (line).

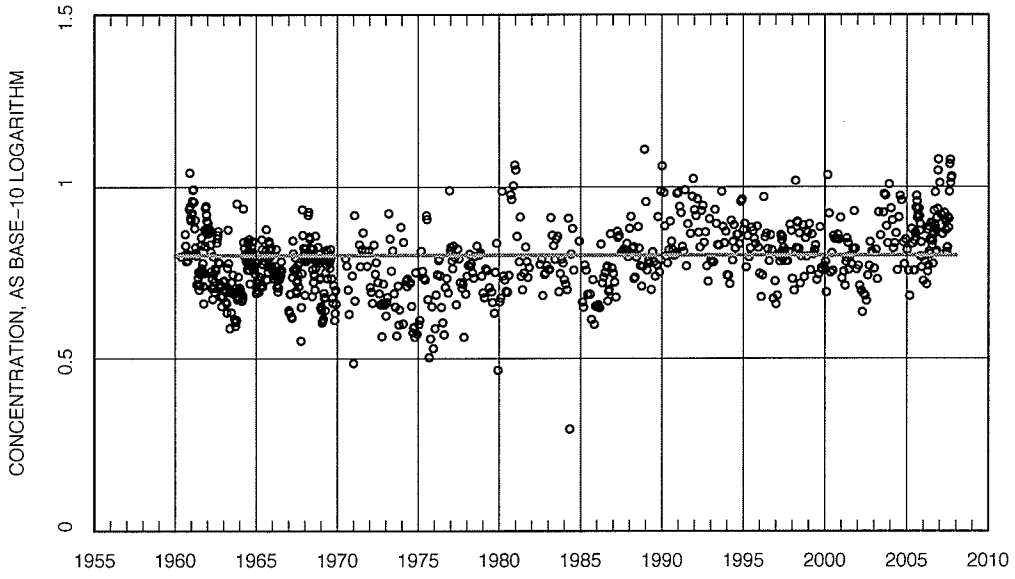

Figure A.52: Dissolved Potassium Flow Adjustments — Seasonally adjusted and flow adjusted data (points) and no-trend (line).

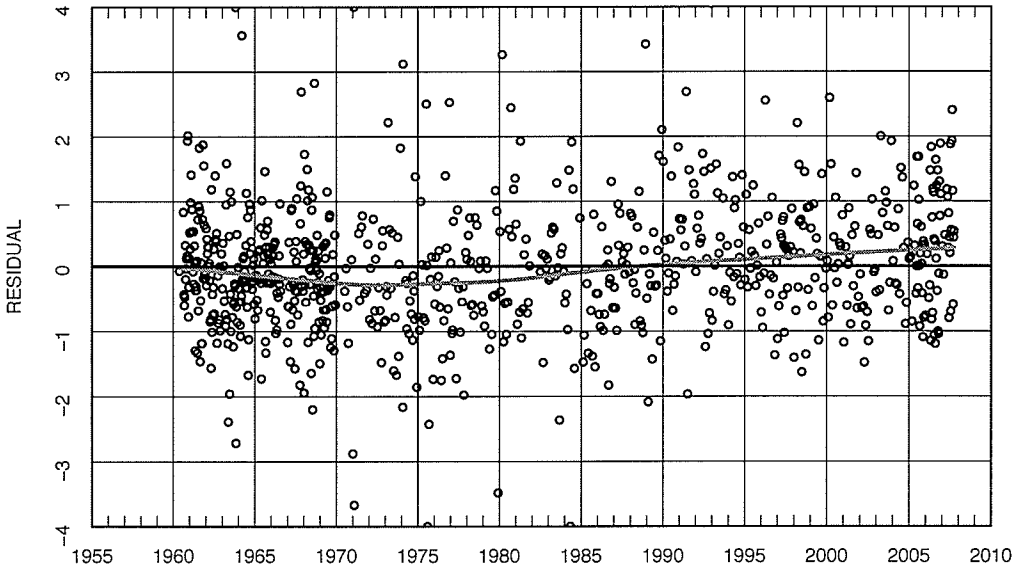

Figure A.53: Dissolved Potassium Flow Adjustments — Parametric no-trend model residuals (points) and lowess smooth line with $F = 0.5$.

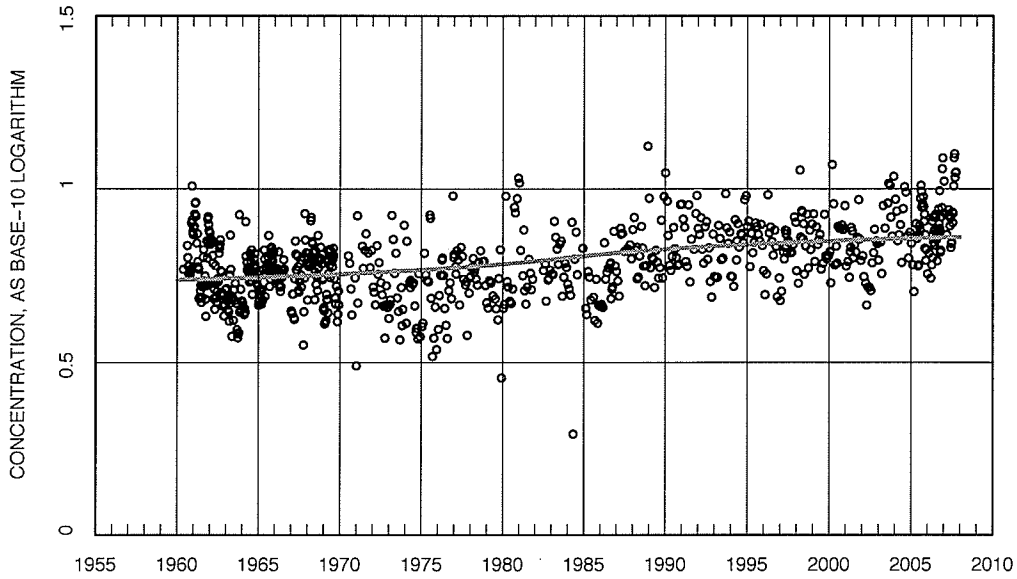

Figure A.54: Dissolved Potassium Flow Adjustments — Seasonally adjusted and flow adjusted data (points) and single trend (line).

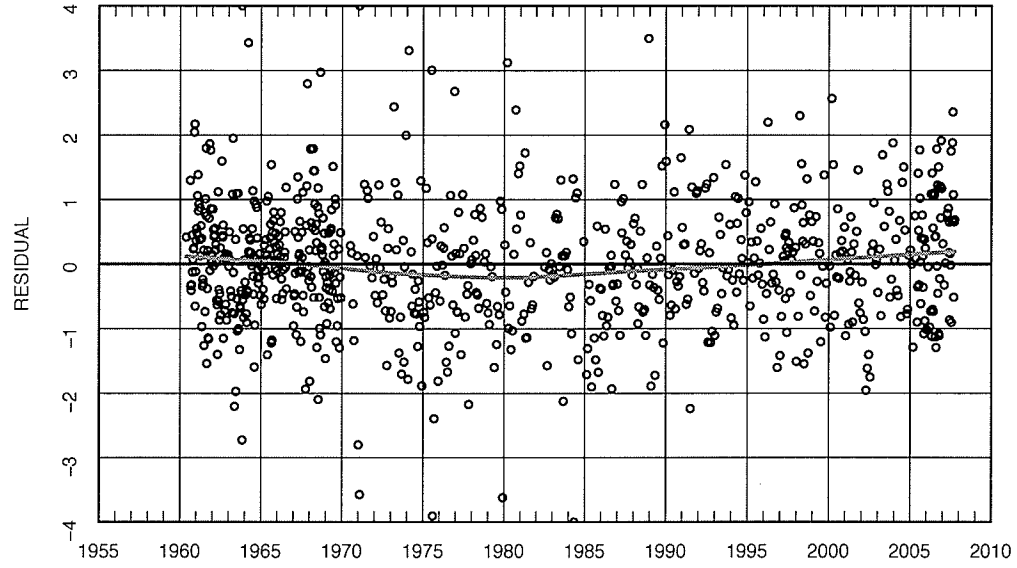

Figure A.55: Dissolved Potassium Flow Adjustments — Parametric single trend model residuals (points) and lowess smooth line with $F = 0.5$.

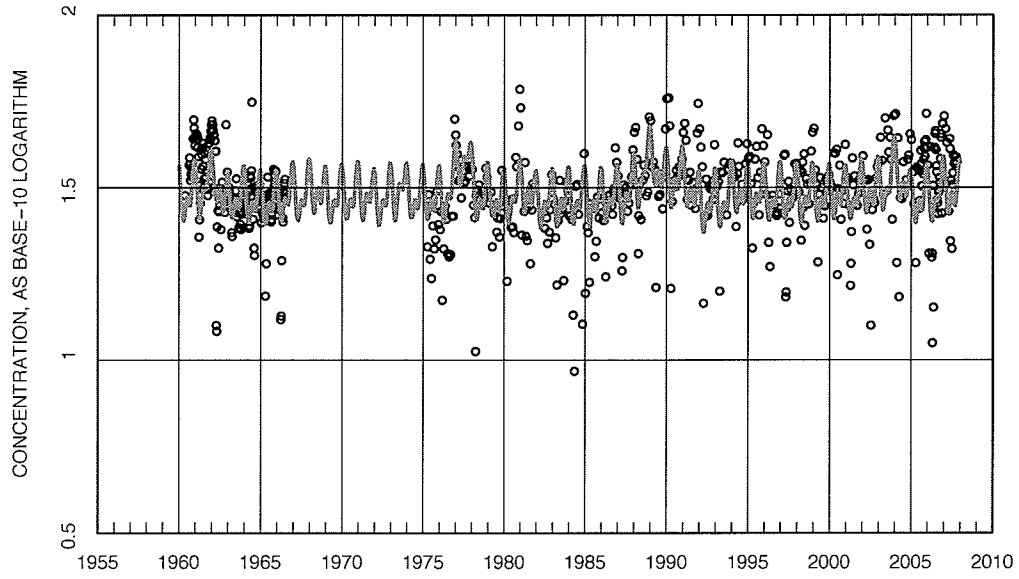

Figure A.56: Dissolved Magnesium concentrations (points) and streamflow related anomaly + trend (line)

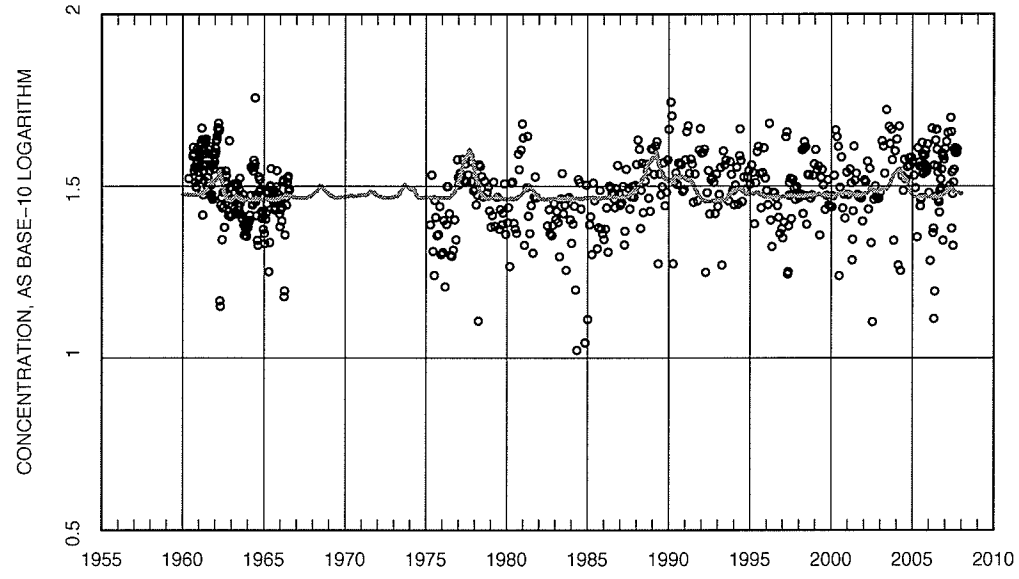

Figure A.57: Dissolved Magnesium Flow Adjustments — Seasonally adjusted and de-trended data (points) and annual streamflow-related anomaly (line).

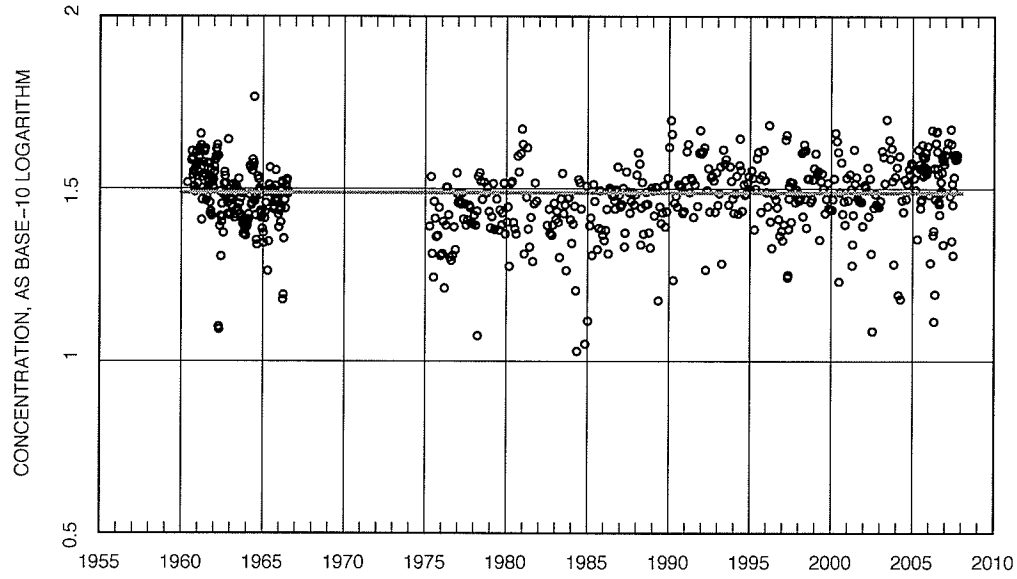

Figure A.58: Dissolved Magnesium Flow Adjustments — Seasonally adjusted and flow adjusted data (points) and no-trend (line).

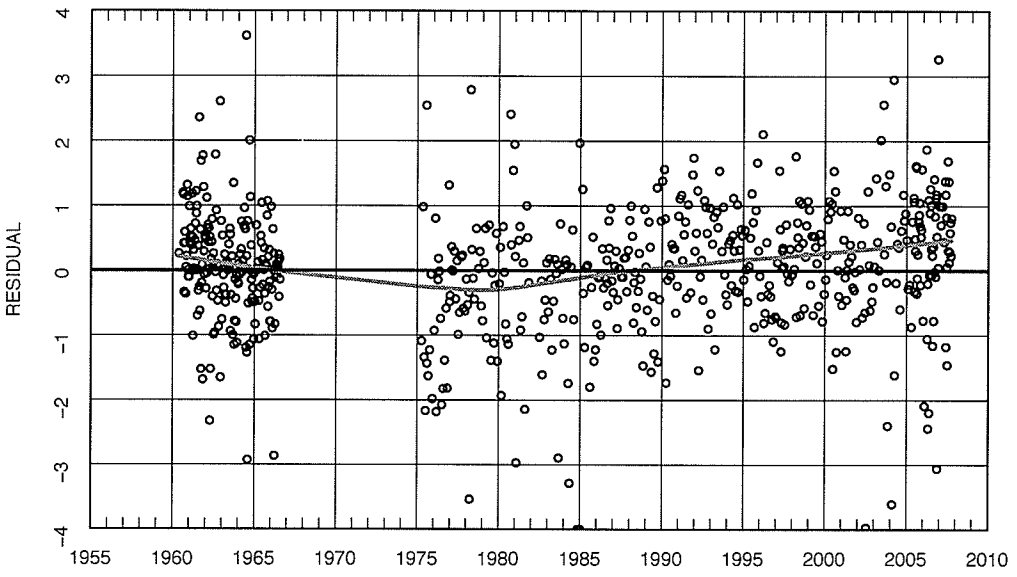

Figure A.59: Dissolved Magnesium Flow Adjustments — Parametric no-trend model residuals (points) and lowess smooth line with $F = 0.5$.

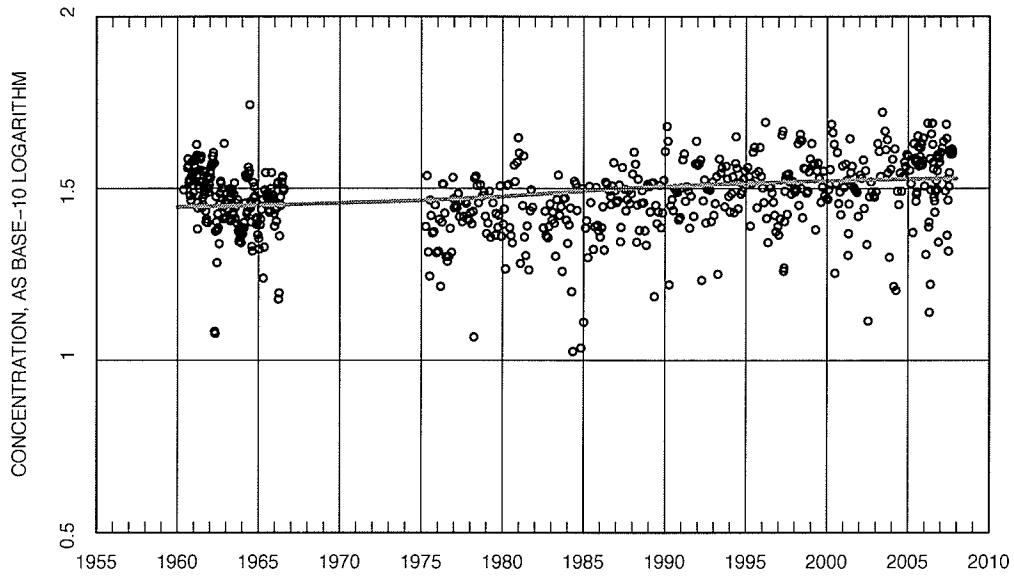

Figure A.60: Dissolved Magnesium Flow Adjustments — Seasonally adjusted and flow adjusted data (points) and single trend (line).

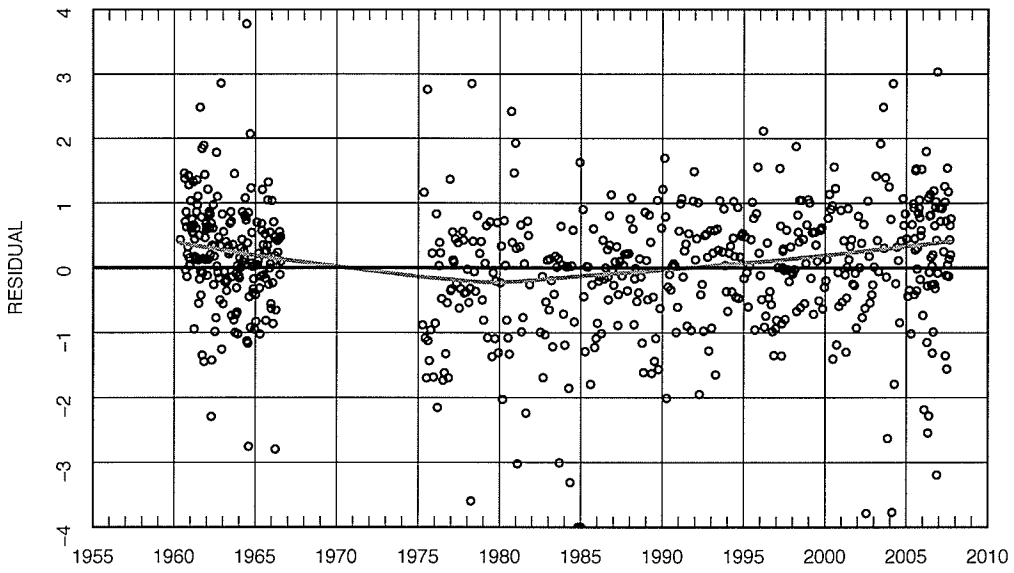

Figure A.61: Dissolved Magnesium Flow Adjustments — Parametric single trend model residuals (points) and lowess smooth line with $F = 0.5$.

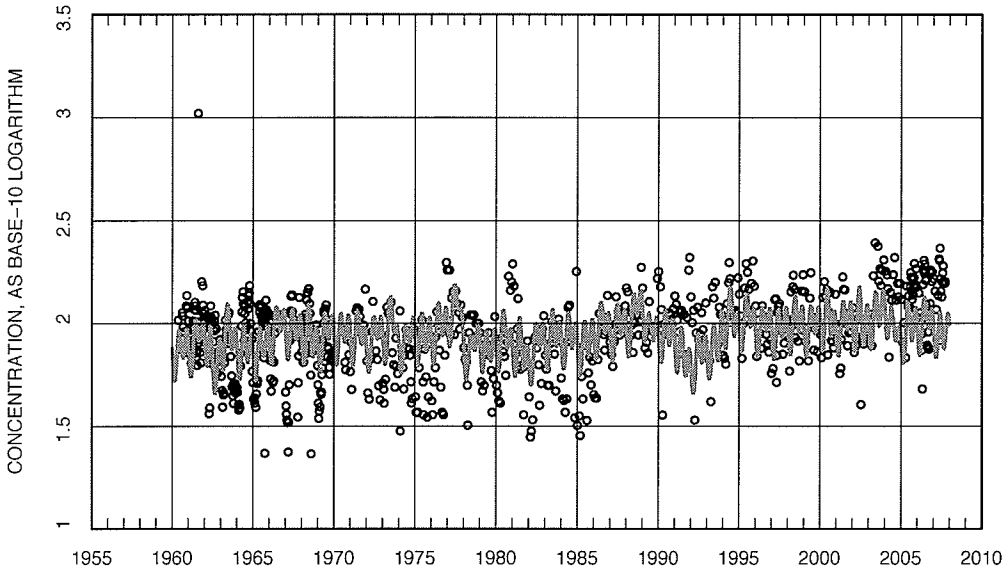

Figure A.62: Dissolved Sulphate concentrations (points) and streamflow related anomaly + trend (line)

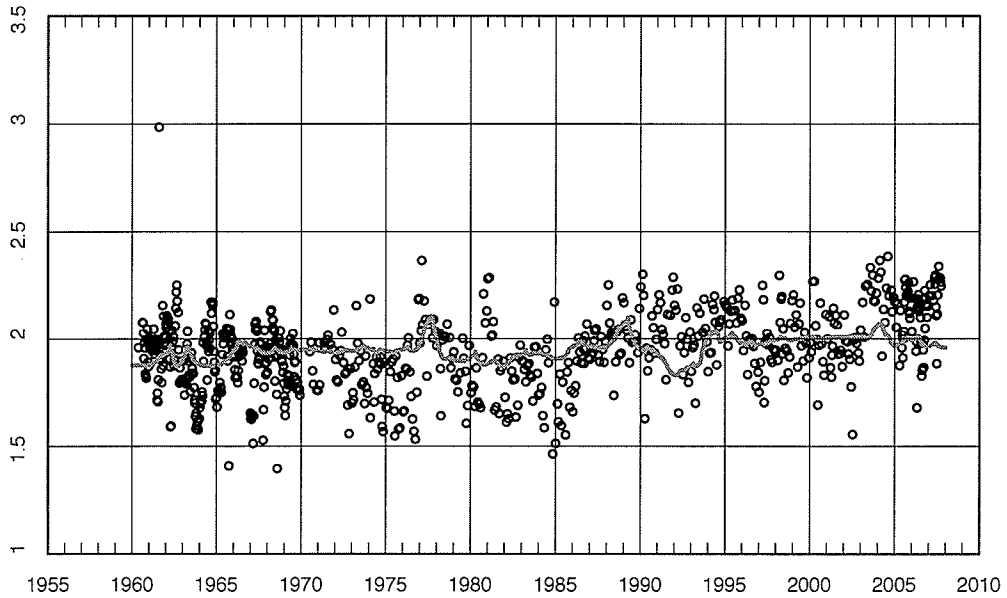

Figure A.63: Dissolved Sulphate Flow Adjustments — Seasonally adjusted and de-trended data (points) and annual streamflow-related anomaly (line).

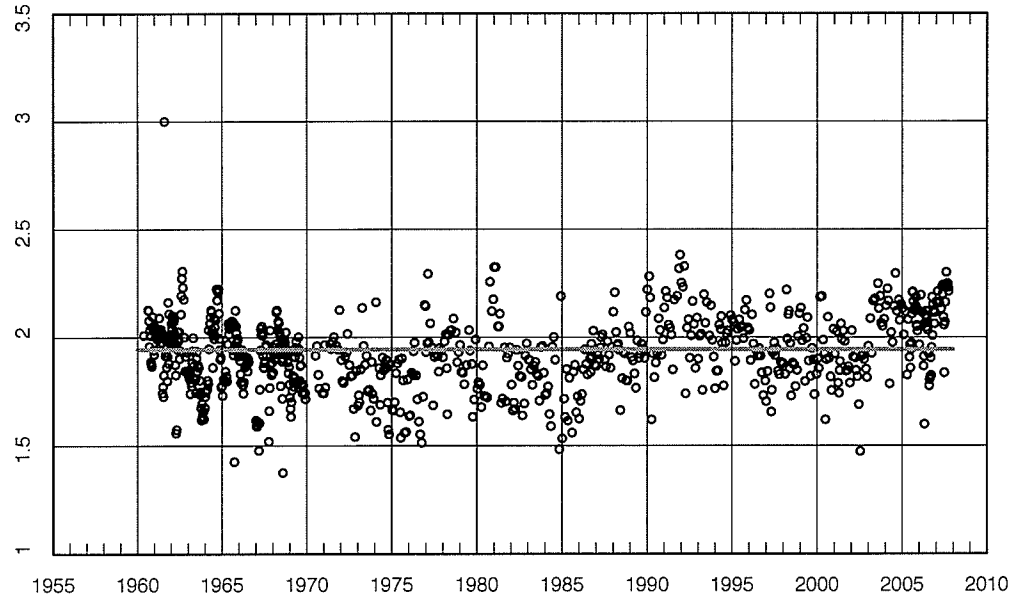

Figure A.64: Dissolved Sulphate Flow Adjustments — Seasonally adjusted and flow adjusted data (points) and no-trend (line).

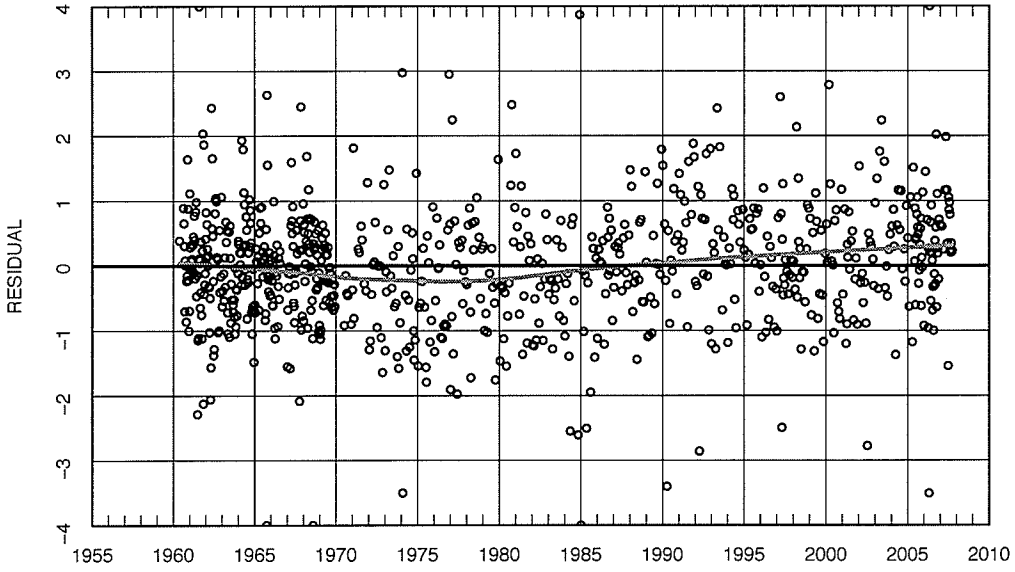

Figure A.65: Dissolved Sulphate Flow Adjustments — Parametric no-trend model residuals (points) and lowess smooth line with $F = 0.5$.

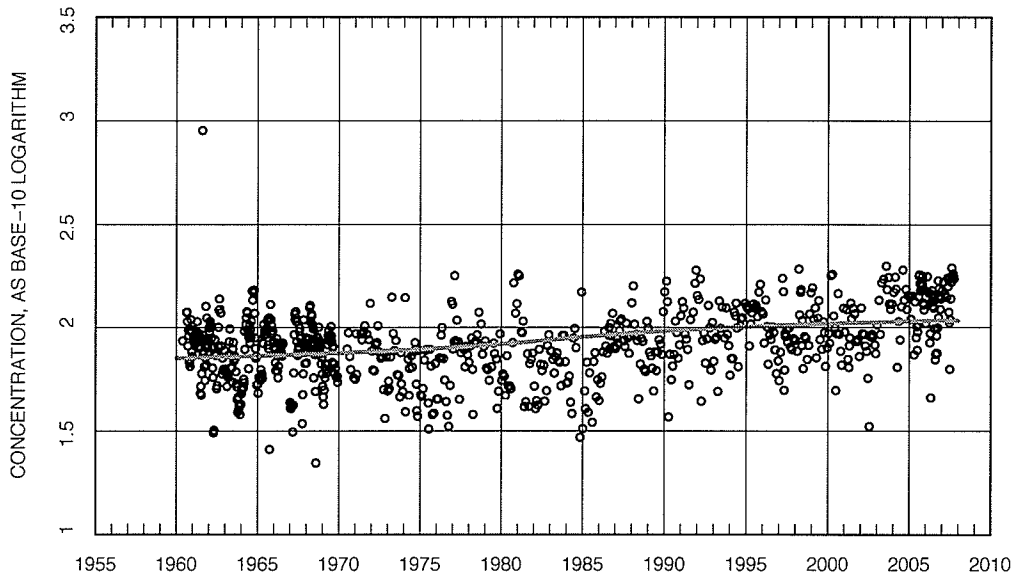

Figure A.66: Dissolved Sulphate Flow Adjustments — Seasonally adjusted and flow adjusted data (points) and single trend (line).

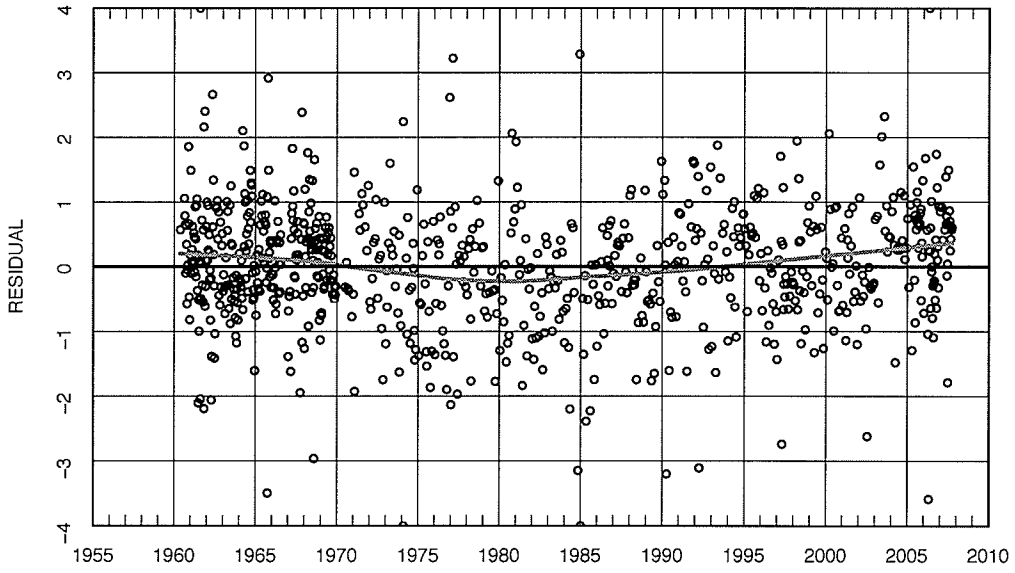

Figure A.67: Dissolved Sulphate Flow Adjustments — Parametric single trend model residuals (points) and lowess smooth line with $F = 0.5$.

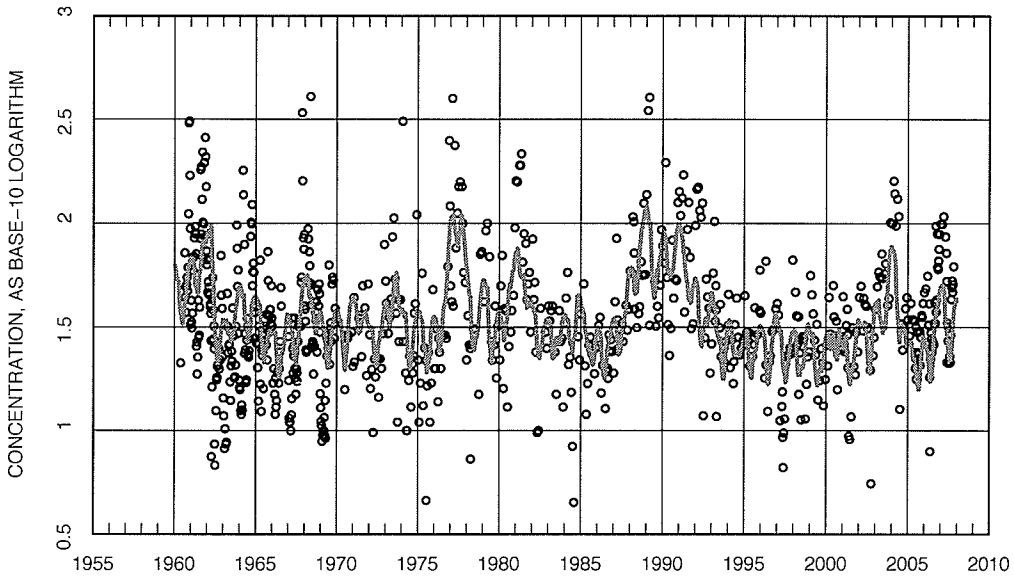

Figure A.68: Dissolved Chloride concentrations (points) and streamflow related anomaly + trend (line)

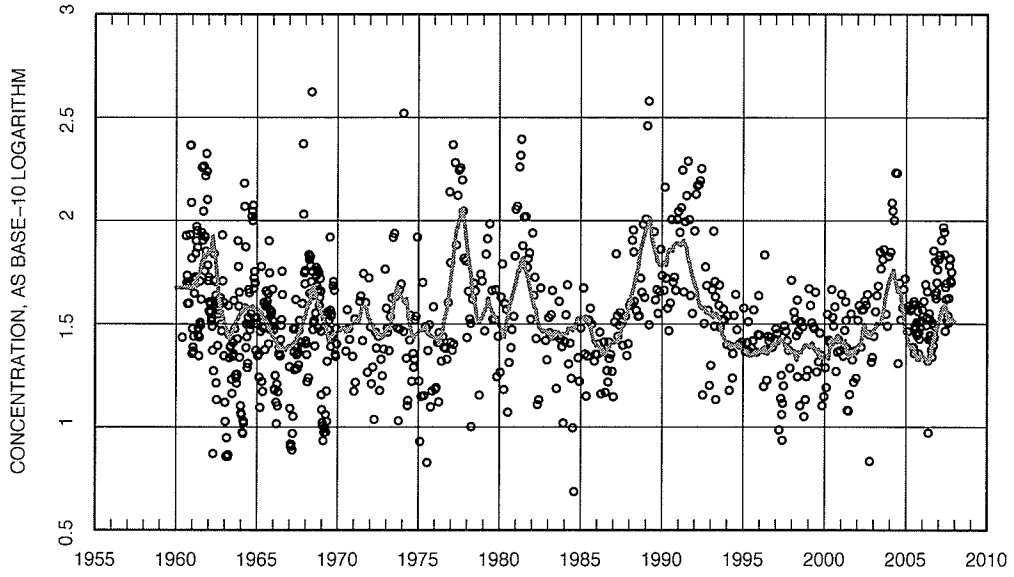

Figure A.69: Dissolved Chloride Flow Adjustments — Seasonally adjusted and detrended data (points) and annual streamflow-related anomaly (line).

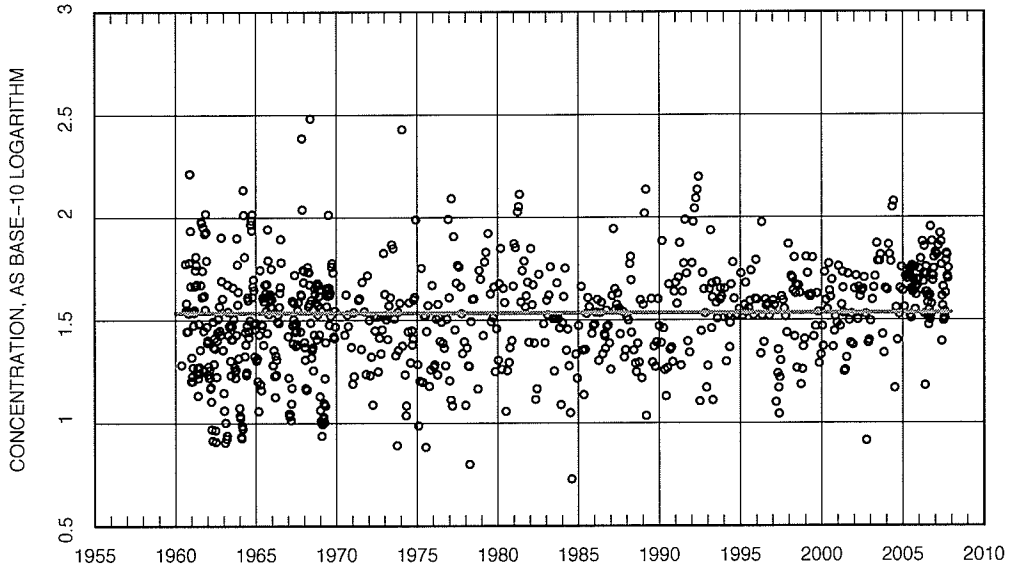

Figure A.70: Dissolved Chloride Flow Adjustments — Seasonally adjusted and flow adjusted data (points) and no-trend (line).

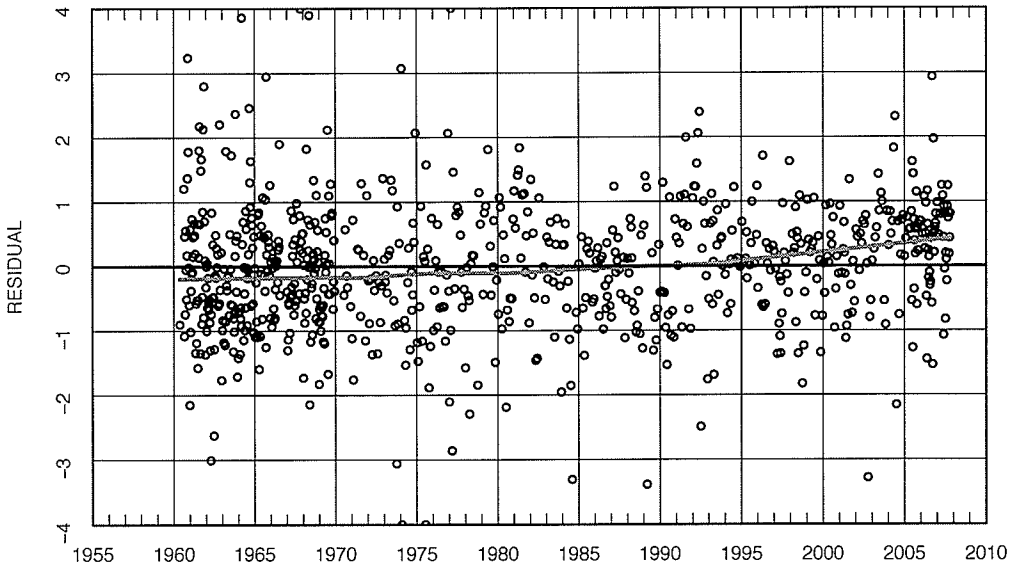

Figure A.71: Dissolved Chloride Flow Adjustments — Parametric no-trend model residuals (points) and lowess smooth line with $F = 0.5$.

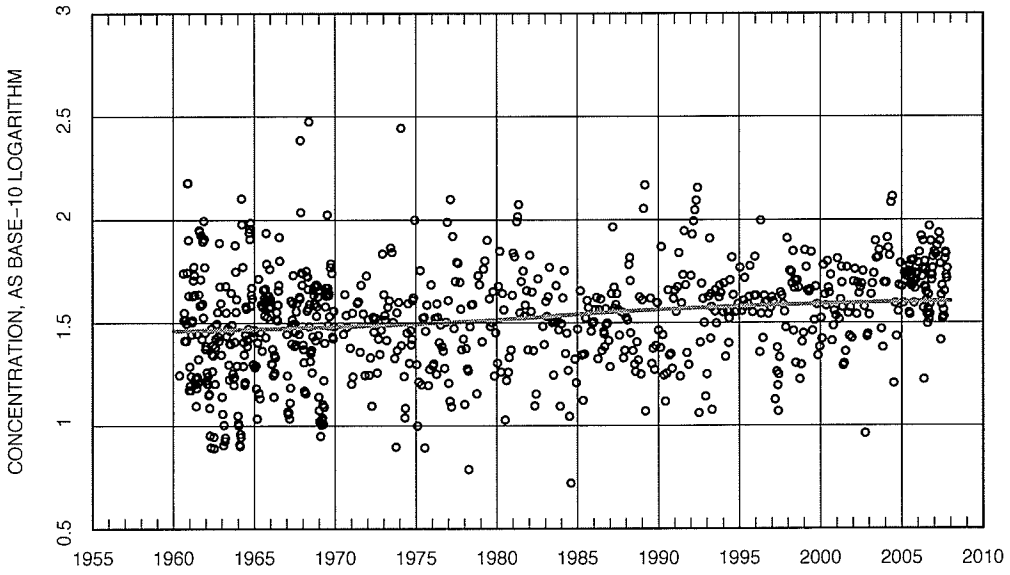

Figure A.72: Dissolved Chloride Flow Adjustments — Seasonally adjusted and flow adjusted data (points) and single trend (line).

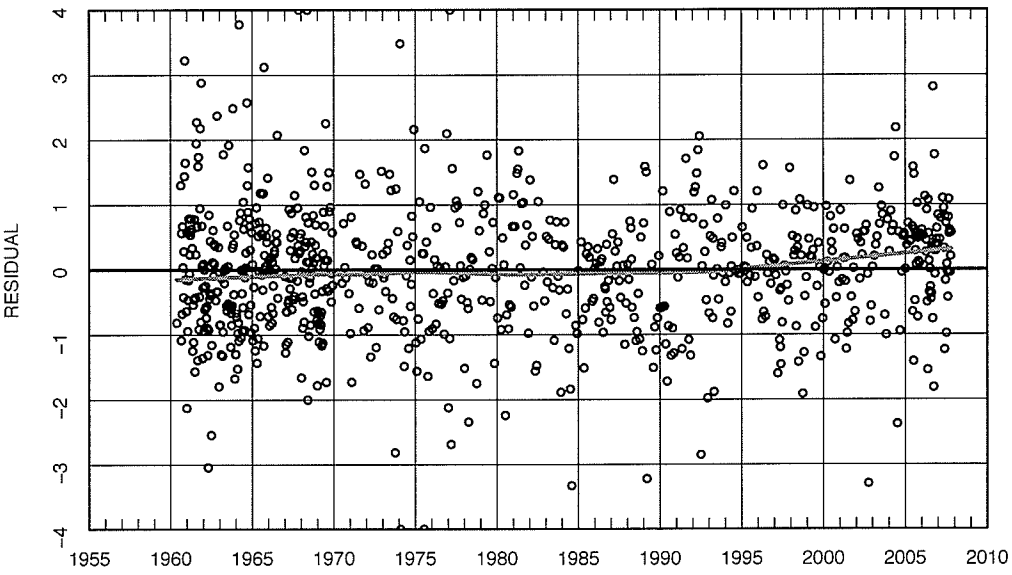

Figure A.73: Dissolved Chloride Flow Adjustments — Parametric single trend model residuals (points) and lowess smooth line with $F = 0.5$.

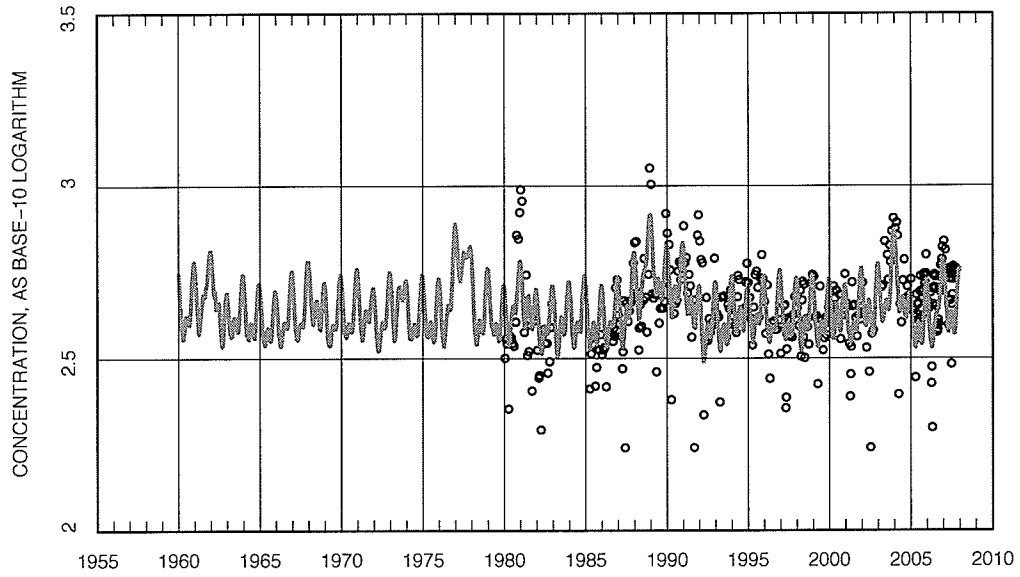

Figure A.74: Total Dissolved Solids concentrations (points) and streamflow related anomaly + trend (line)

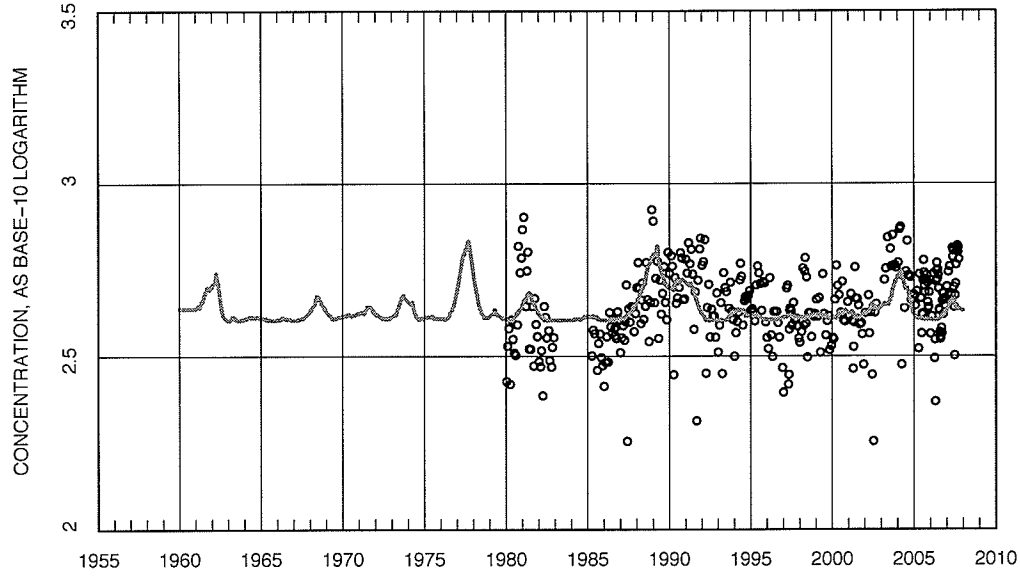

Figure A.75: Total Dissolved Solids Flow Adjustments — Seasonally adjusted and de-trended data (points) and annual streamflow-related anomaly (line).

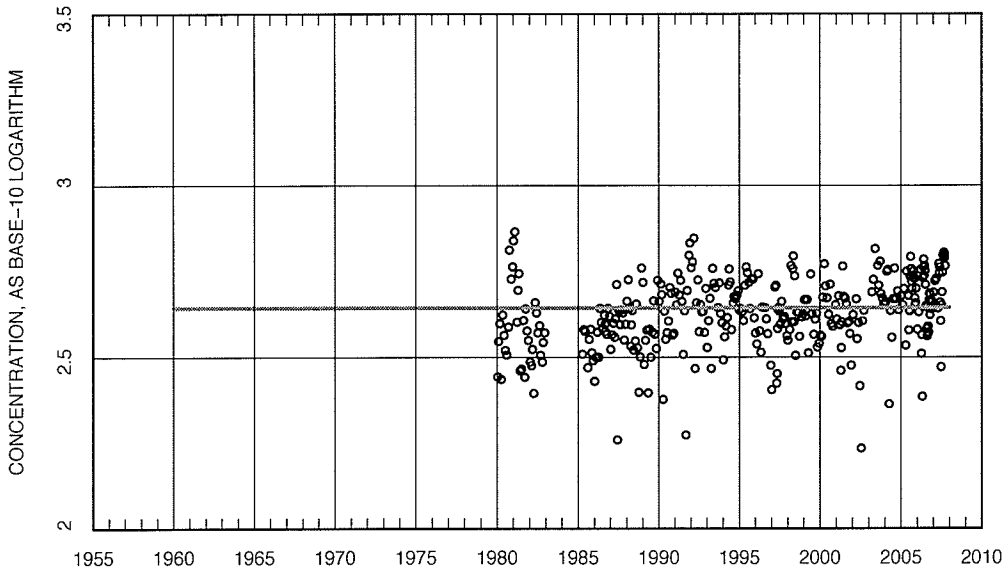

Figure A.76: Total Dissolved Solids Flow Adjustments — Seasonally adjusted and flow adjusted data (points) and no-trend (line).

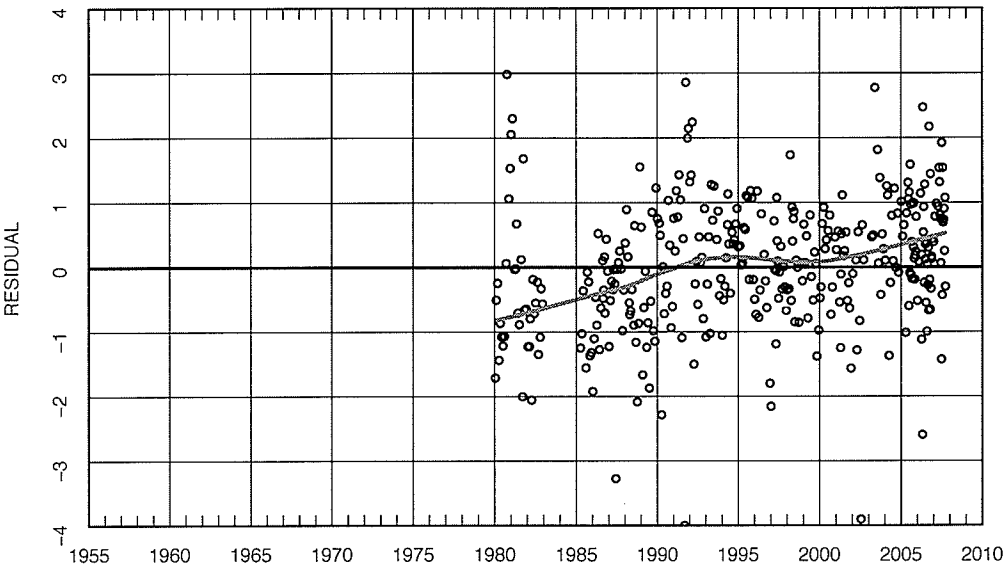

Figure A.77: Total Dissolved Solids Flow Adjustments — Parametric no-trend model residuals (points) and lowess smooth line with $F = 0.5$.

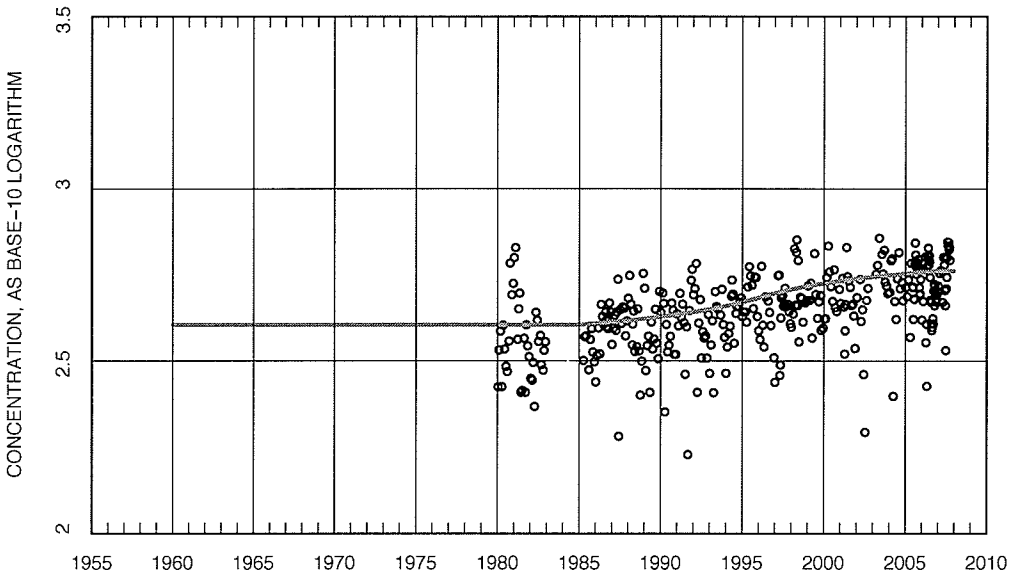

Figure A.78: Total Dissolved Solids Flow Adjustments — Seasonally adjusted and flow adjusted data (points) and single trend (line).

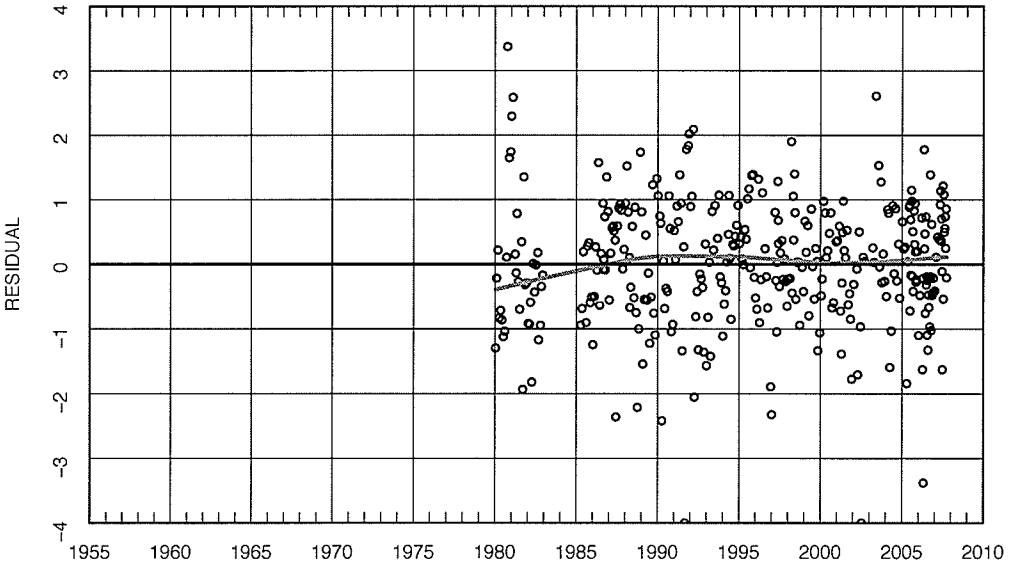

Figure A.79: Total Dissolved Solids Flow Adjustments — Parametric single trend model residuals (points) and lowess smooth line with $F = 0.5$.

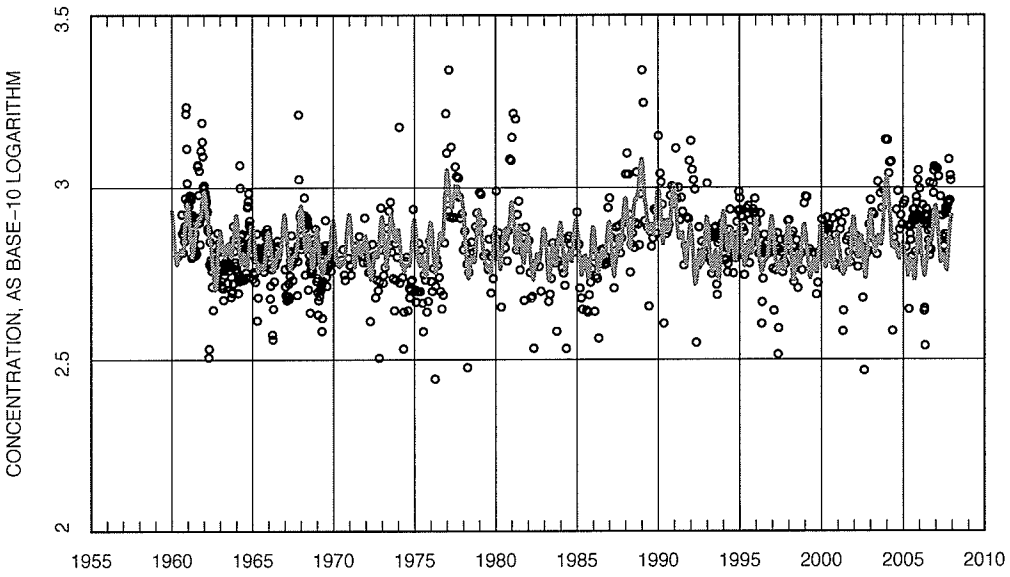

Figure A.80: Specific Conductance concentrations (points) and streamflow related anomaly + trend (line)

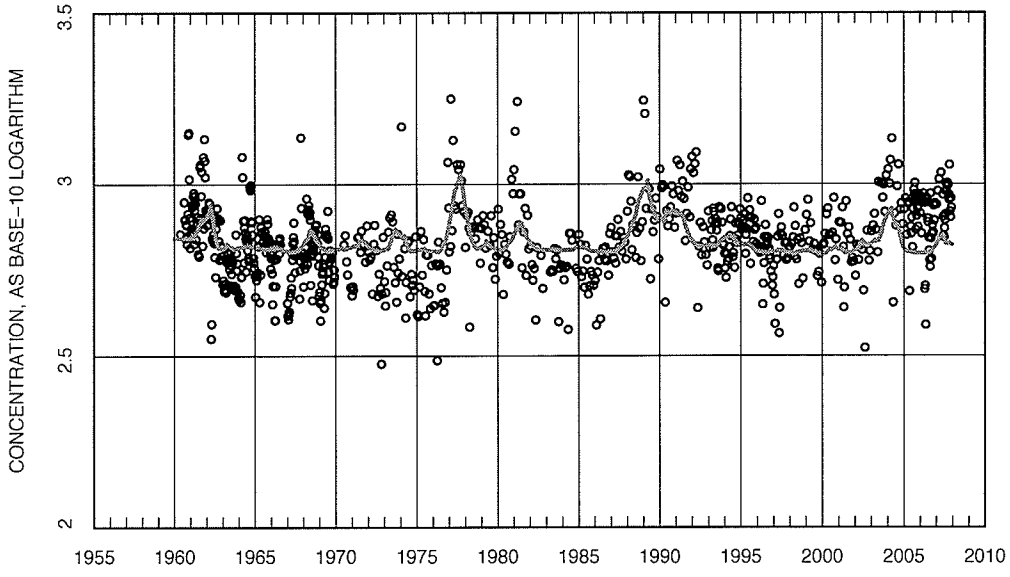

Figure A.81: Specific Conductance Flow Adjustments — Seasonally adjusted and de-trended data (points) and annual streamflow-related anomaly (line).

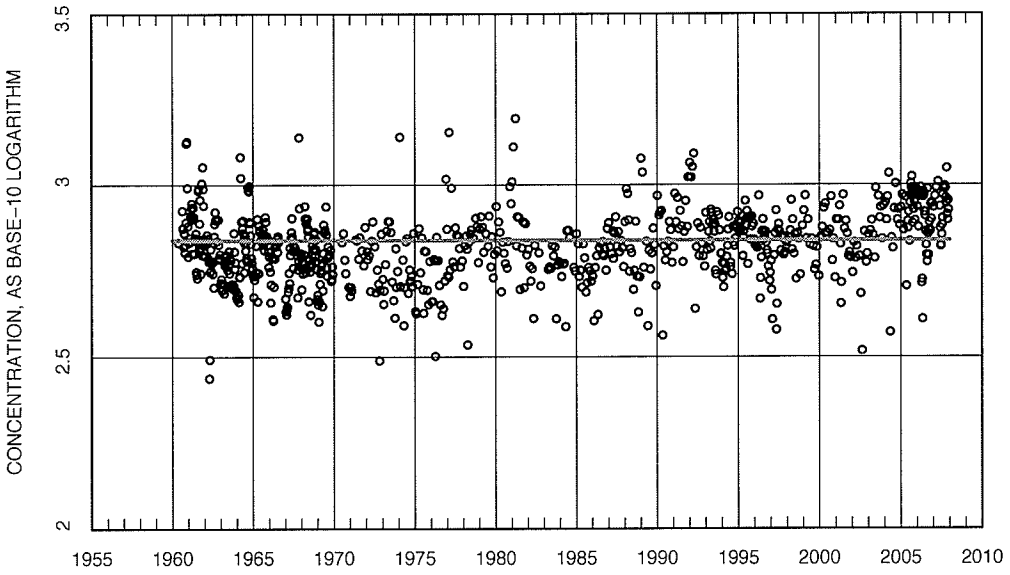

Figure A.82: Specific Conductance Flow Adjustments — Seasonally adjusted and flow adjusted data (points) and no-trend (line).

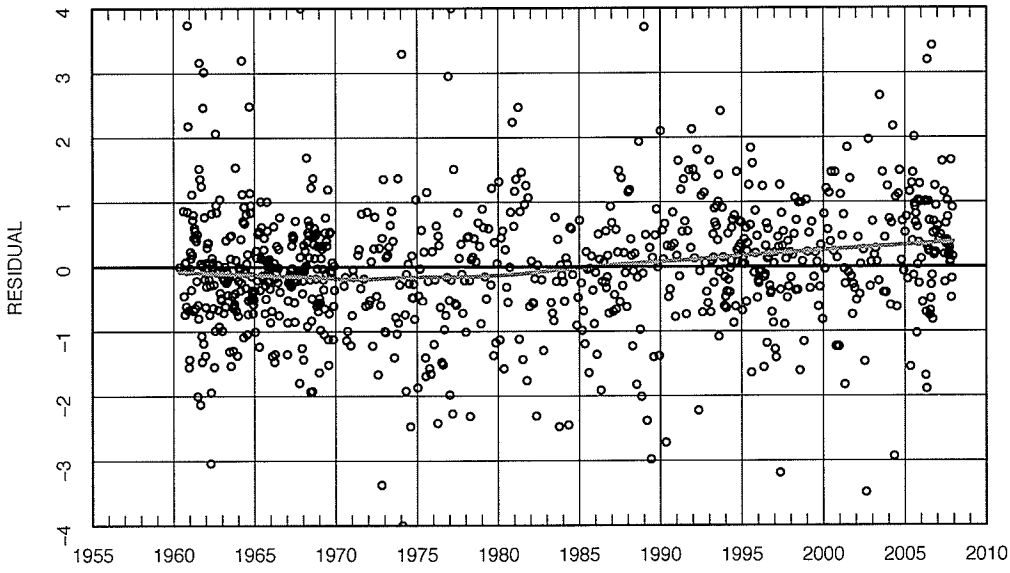

Figure A.83: Specific Conductance Flow Adjustments — Parametric no-trend model residuals (points) and lowess smooth line with $F = 0.5$.

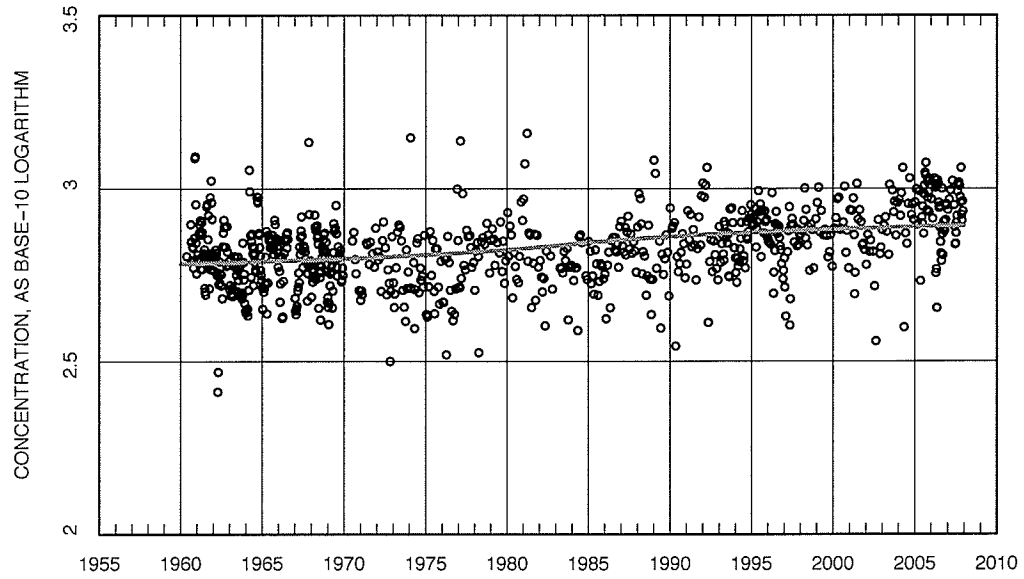

Figure A.84: Specific Conductance Flow Adjustments — Seasonally adjusted and flow adjusted data (points) and single trend (line).

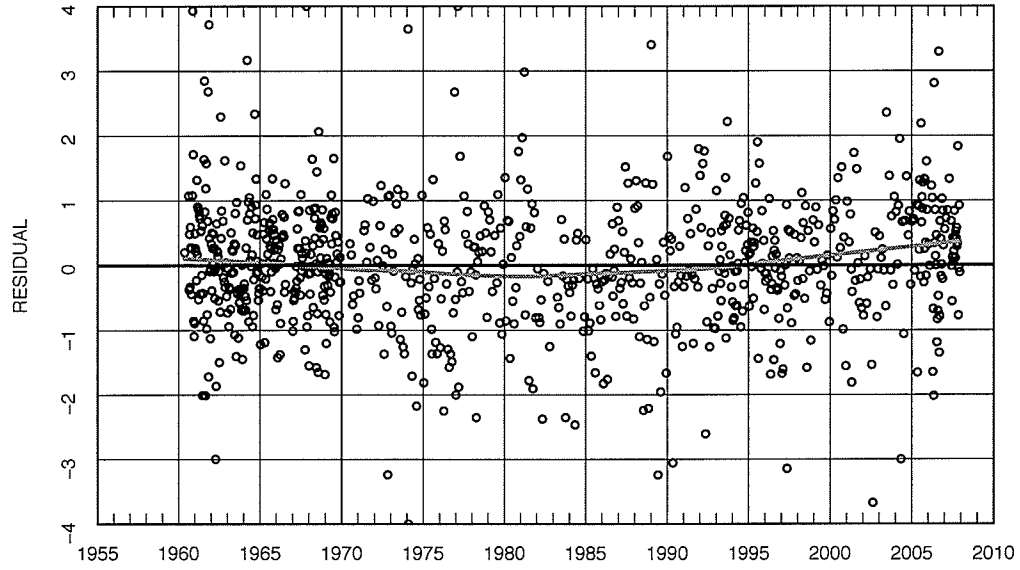

Figure A.85: Specific Conductance Flow Adjustments — Parametric single trend model residuals (points) and lowess smooth line with $F = 0.5$.

A.5.2 South Floodway at St. Norbert Monitoring Station

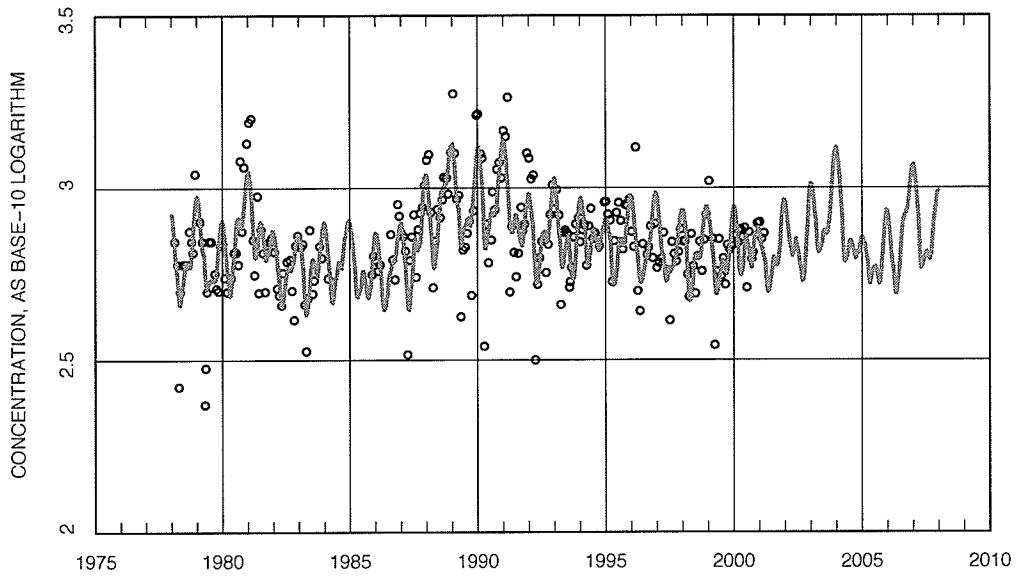

Figure A.86: Specific Conductance concentrations (points) and streamflow related anomaly + trend (line)

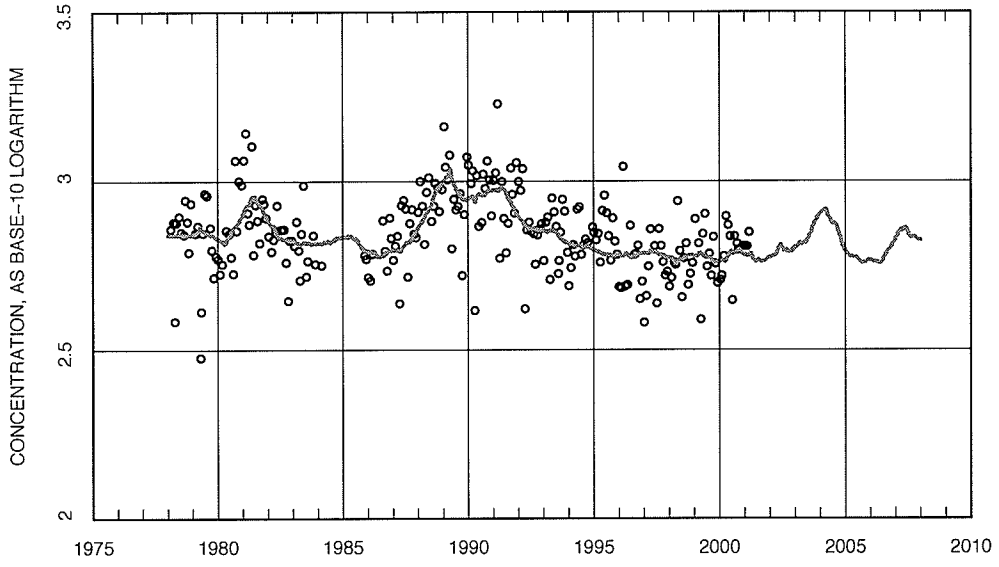

Figure A.87: Specific Conductance Flow Adjustments — Seasonally adjusted and de-trended data (points) and annual streamflow-related anomaly (line).

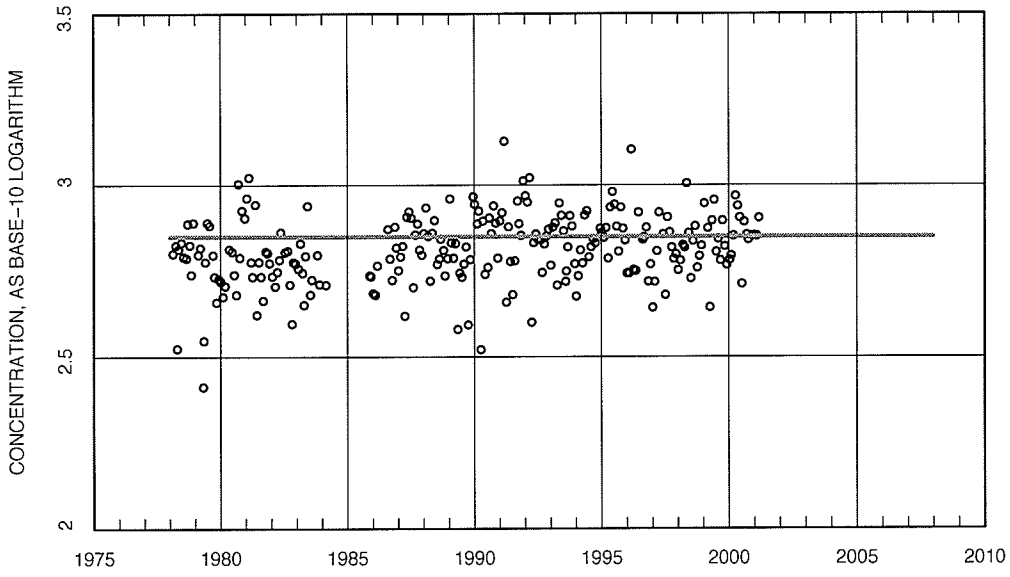

Figure A.88: Specific Conductance Flow Adjustments — Seasonally adjusted and flow adjusted data (points) and trend (line).

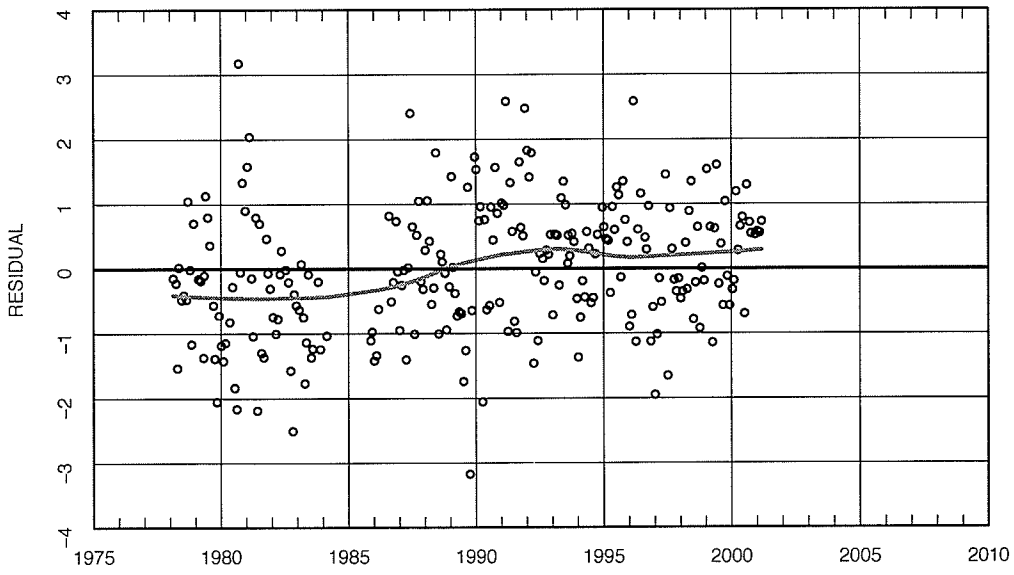

Figure A.89: Specific Conductance Flow Adjustments — Parametric no-trend model residuals (points) and lowess smooth line with $F = 0.5$.

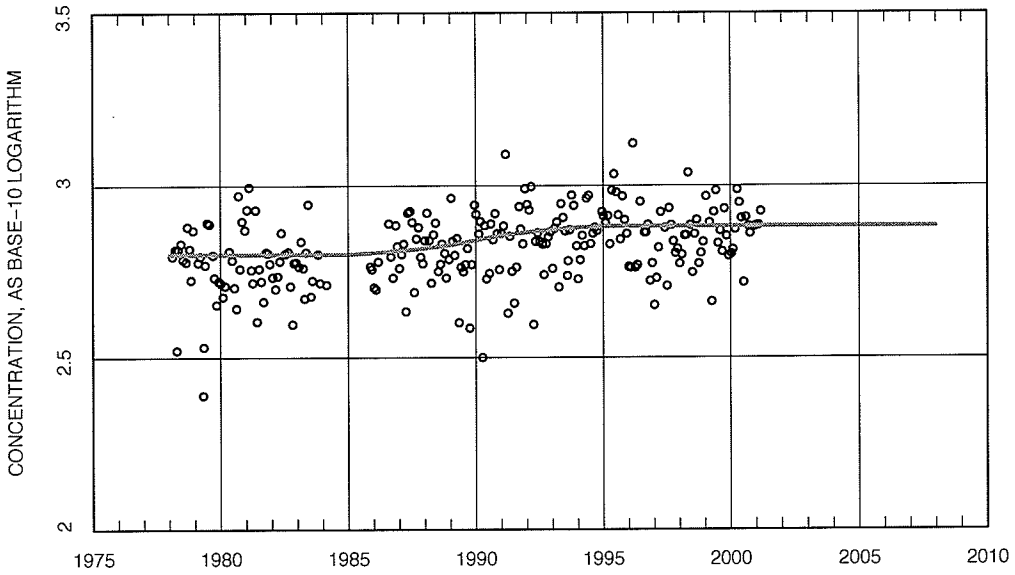

Figure A.90: Specific Conductance Flow Adjustments — Seasonally adjusted and flow adjusted data (points) and single trend (line).

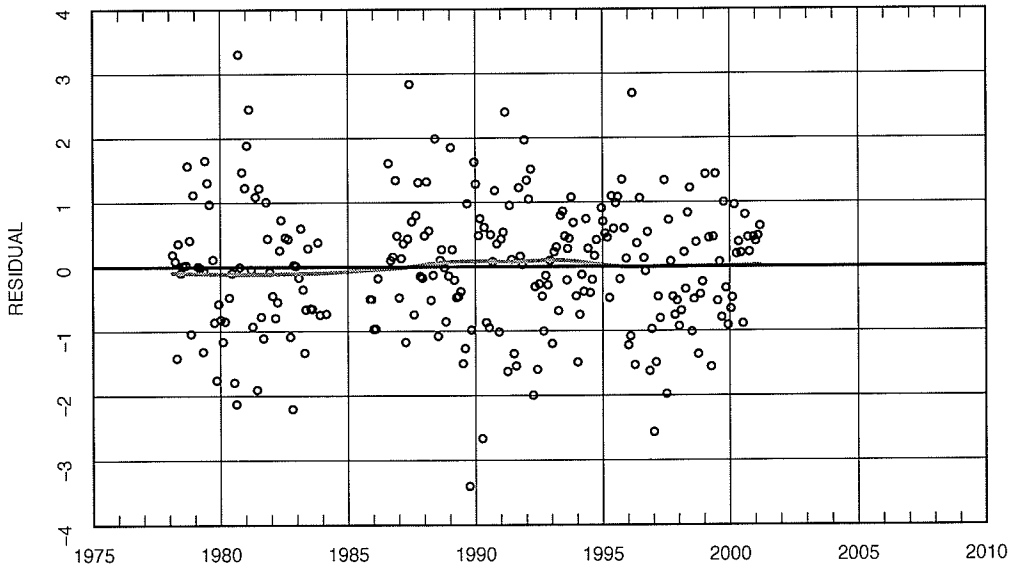

Figure A.91: Specific Conductance Flow Adjustments — Parametric single trend model residuals (points) and lowess smooth line with $F = 0.5$.

A.5.3 Selkirk Monitoring Station

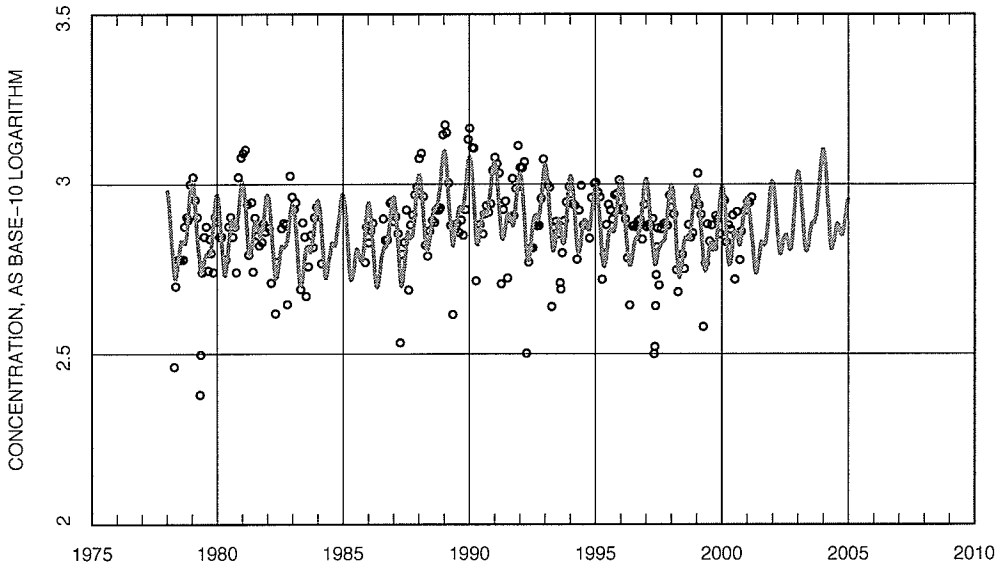

Figure A.92: Specific Conductance concentrations (points) and streamflow related anomaly + trend (line)

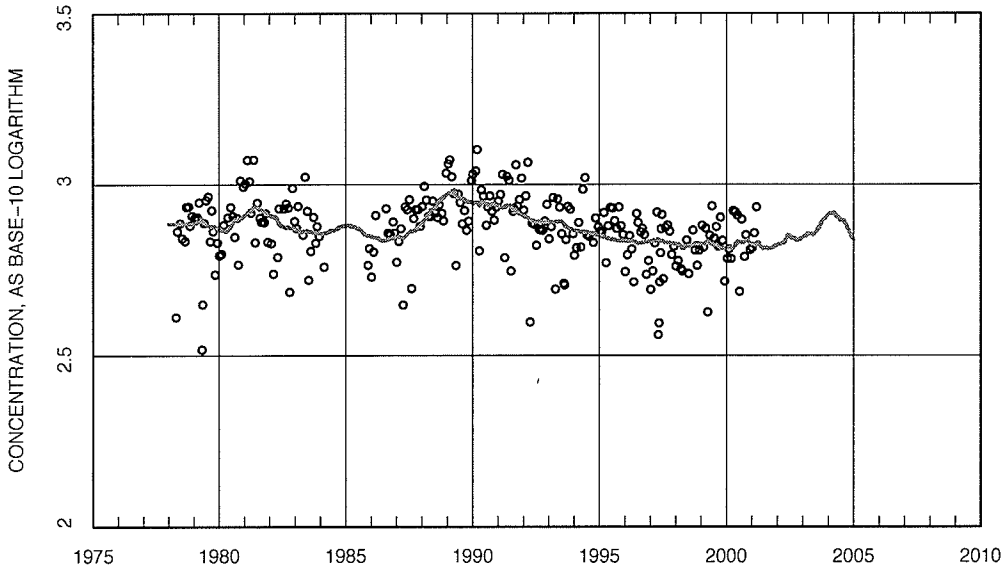

Figure A.93: Specific Conductance Flow Adjustments — Seasonally adjusted and de-trended data (points) and annual streamflow-related anomaly (line).

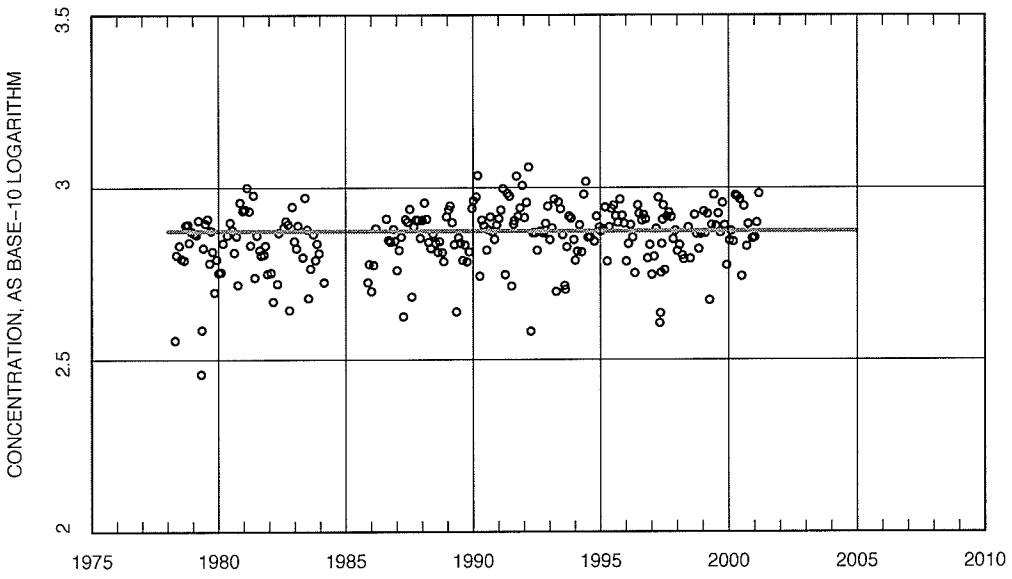

Figure A.94: Specific Conductance Flow Adjustments — Seasonally adjusted and flow adjusted data (points) and trend (line).

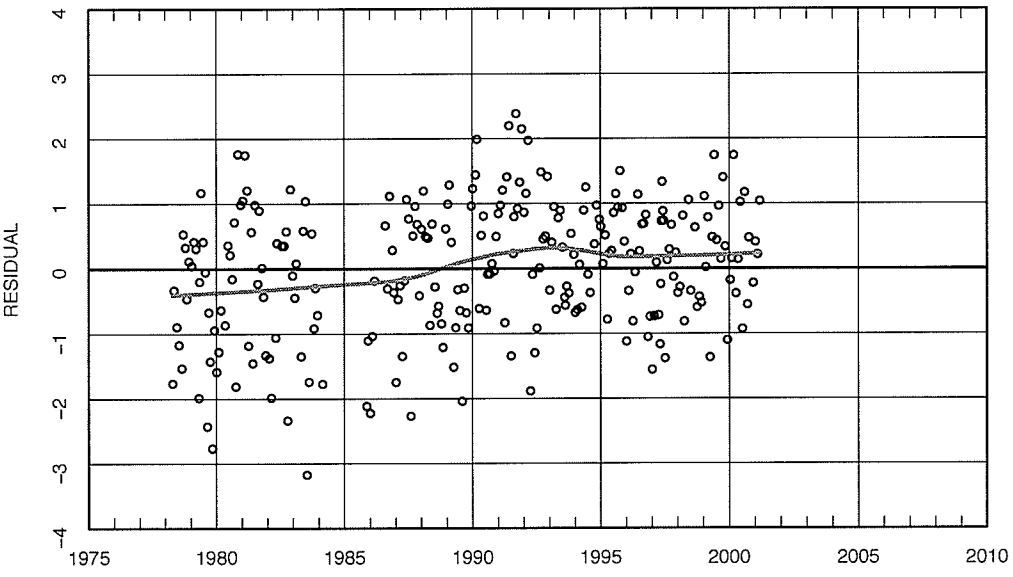

Figure A.95: Specific Conductance Flow Adjustments — Parametric no-trend model residuals (points) and lowess smooth line with $F = 0.5$.

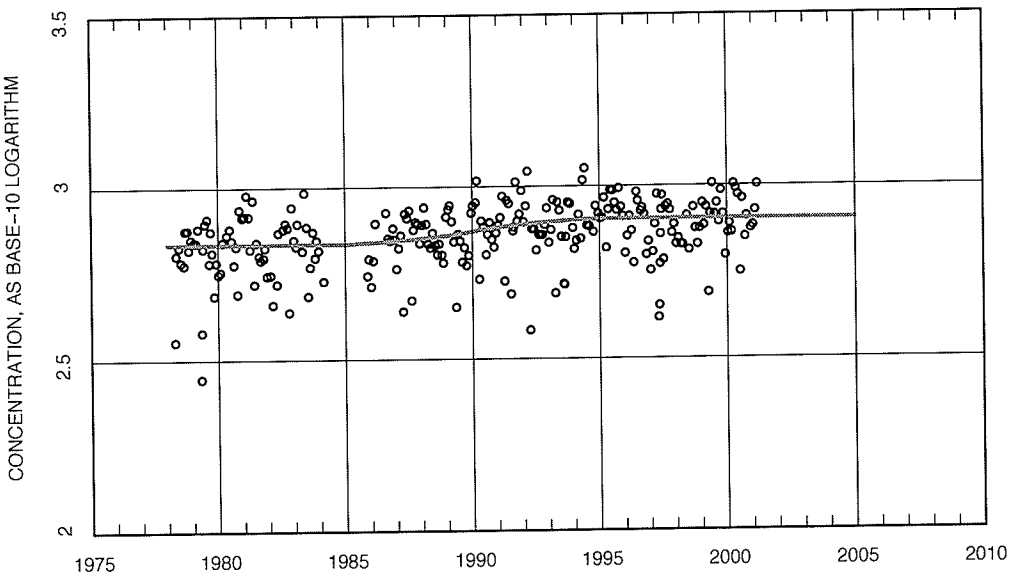

Figure A.96: Specific Conductance Flow Adjustments — Seasonally adjusted and flow adjusted data (points) and single trend (line).

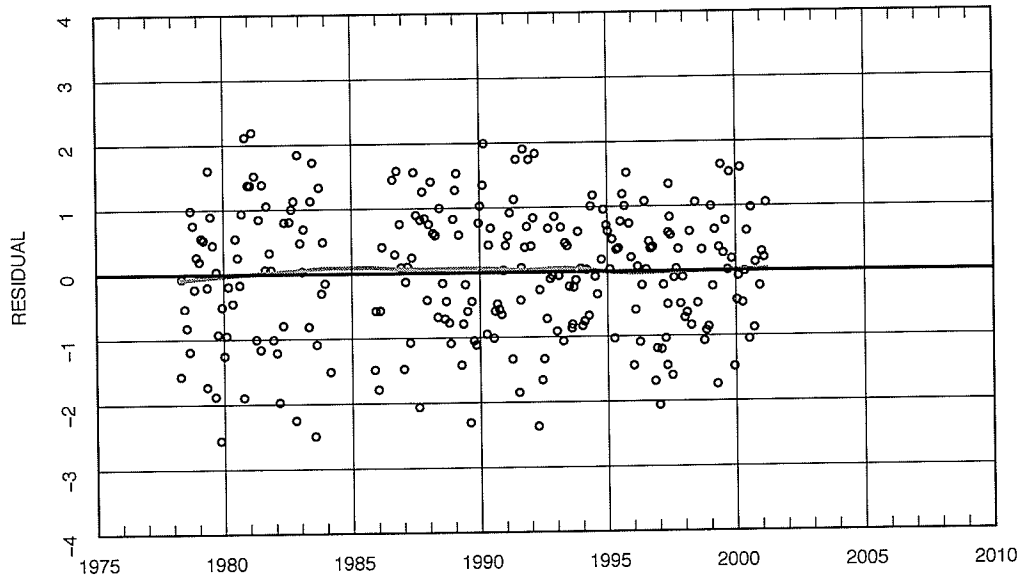

Figure A.97: Specific Conductance Flow Adjustments — Parametric single trend model residuals (points) and lowess smooth line with $F = 0.5$.